SYNTHESIS AND POSTMODIFICATION OF FUNCTIONALLY RELEVANT ORGANICALLY MODIFIED SILICA PARTICLES

by

Eric Brozek

A dissertation submitted to the faculty of
The University of Utah
in partial fulfillment of the requirements for the degree of

Doctor of Philosophy

Department of Chemistry

The University of Utah

May 2013

The University of Utah Graduate School

STATEMENT OF DISSERTATION APPROVAL

The dissertation of **Eric Brozek**

has been approved by the following supervisory committee members:

Ilya Zharov	, Chair	**11/13/2012** Date Approved
Jon Rainier	, Member	**11/13/2012** Date Approved
Peter Stang	, Member	**11/13/2013** Date Approved
Michael Bartl	, Member	**11/13/2013** Date Approved
Patrick Kiser	, Member	Date Approved

and by **Henry White**, Chair of the Department of **Chemistry**

and by Donna M. White, Interim Dean of The Graduate School.

ABSTRACT

This thesis describes the synthesis and properties of organically modified silica (ORMOSIL) particles with possible applications in the field of drug delivery. Nanoparticle drug delivery methods take advantage of the unique physical properties of nanoscale architecture to deliver a large payload of drug to a targeted site. They are highly porous, contain many organic functionalities for covalent attachment, and their surfaces can be functionalized. A particle-based approach allows for the delivery of a large and localized payload in a single package.

Initial study focused on the generation of submicron organically modified silica particles containing boron. This involved the synthesis of vinyl-enriched silica particles and the postmodification of the vinyl functionalities throughout the particle body. Hydroboration and bromination of the vinyl functionalities showed for the first time that the organic functionalities of ORMOSIL particles could be significantly modified.

Next, new organically modified silica particle types were developed. These new particle types incorporated unique organic functionalities that may undergo additional functionalization. Organic functionalities included alkenyl-,

cyano-, mercapto-, and isocyanto- throughout the particle body. The different organic functionalities were then modified to demonstrate their reactivity.

Finally, a particle containing nuclei suitable for neutron capture therapy, a fluorescent tag, and targeting ligand was synthesized. Boron was the active nuclei, fluorescein was the fluorescent label, useful for in vitro studies, and folic acid is a broad field targeting ligand, useful in targeting a variety of cancer types. The particle containing the three unique motifs underwent early stages of in vitro studies against the OVCAR-3 cell line.

This thesis has considerably advanced the field of ORMOSIL chemistry through the development and modification of new ORMOSIL products. While initial efforts were geared toward the development of an ORMOSIL suitable for drug delivery, the variety of products formed that possess unique characteristics make these materials useful far beyond drug scaffolding. Additional work that is currently being pursued in the Zharov research lab includes the development of highly porous OMROSIL particles for MRI imaging, ORMOSIL hybrids that are degradable under acidic conditions, and the use of ORMOSIL particles as a stationary phase for solid phase extraction.

For Dad. Thank you.

TABLE OF CONTENTS

LIST OF ABBREVIATIONS

APTES	3-(Aminopropyl)triethoxysilane
APTMS	3-(Aminopropyl)trimethoxysilane
VTMS	Vinyltrimethoxysilane
VTES	Vinyltriethoxysilane
ATMS	Allyltrimethoxysilane
ATES	Allyltriethoxysilane
FITC	Flourescein Isothiocyanate
FA	Folic Acid
SEM	Scanning Electron Microscopy
BNCT	Boron Neutron Capture Therapy
NCT	Neutron Capture Therapy
TEM	Transmission Electron Microscopy
NMR	Nuclear Magnetic Resonance
SSNMR	Solid State NMR
IR	Infrared
UV	Ultraviolet
TGA	Thermogravimetric analysis
nm	Nanometer
µm	Micrometer

DLS	Dynamic light scattering
EtOH	Ethanol
MeOH	Methanol
Et_2O	Diethyl ether
THF	Tetrahydrofuran
ACN	Acetonitrile
RB	Round Bottom
ºC	Degrees Celsius
NaOH	Sodium Hydroxide
DMSO	Dimethyl Sulfoxide
mg, g	Milligram, gram
TEOS	Tetraethylorhosilicate
3-MPTMS	3-(mercaptopropyl)trimethoxysilane
3-MPTES	3-(mercaptopropyl)triethoxysilane
2-CPTMS	2-(cyanopropyl)trimethoxysilane
2-CPTES	2-(cyanopropyl)triethoxysilane
3-ICPTES	3-(isocyanatopropyl)triethoxysilane
ICP	Inductively Coupled Plasma
THF-BH_3	Tetrahydrofuran-borohydride complex
HCl	Hydrochloric acid
BTC	Benzothonium Chloride
NaCl	Sodium Chloride
mM, M	Millimolar, molar
mmol, mol	Millimole, mole

Et_3N	Triethylamine
LAH	Lithium aluminum hydride
RT	Room temperature
TLC	Thin layer chromatography
ORMOSIL	Organically Modified Silica
℃	Degree Celsius
PAMAM	Poly(amidoamine) dendrimer
µg, mg, g	Microgram, milligram, gram
µM, mM, M	Micromolar, millimolar, molar
µmol, mmol, mol	Micromole, millimole, mol

ACKNOWLEDGMENTS

I would first like to thank my P.I., Ilya Zharov. Without his support, both financially and mentally, this work never would have come together. I appreciate the freedom he offered me in the laboratory as it has greatly affected my growth as a scientist. I also appreciate the push he would give when times were looking grim. I am proud to call him both mentor and friend.

Additionally, I would like to thank my coworkers both inside and outside of the Zharov research group. They have all been friends and colleagues and provided me with support which kept me moving toward this final goal.

I would also like to thank Dr. Kevin Czerwinski from the University of Wisconsin Stevens Point. I thank him for providing my first real opportunity to fall in love with chemistry and instill in me a sense of responsibility and passion for the work.

Very special thanks to my loving wife, Sarah, who has truly seen me through the best and worst of times. I cannot think of a more important individual who has looked over me through this journey. I thank her for being the rock when times looked their worst.

Finally, and most importantly, I want to thank my father, who passed away in November 2009 from pulmonary fibrosis. He remains the best man I have ever met to this day and it was his support that is shaping me into the man I am still trying to become. Grace and peace Dad!

CHAPTER 1

INTRODUCTION

Silica nanoparticles are unique materials with applications in various fields such as chromatography[1] and drug delivery.[2] This stems from the ability to readily control the size and shape of the particles and the ability to easily functionalize the surface of silica with a variety of organic and inorganic materials, and incorporate such materials into the core of the particles. The resulting hybrid structures often possess unique properties while eliminating weaknesses.

A number of methods exist to prepare silica hybrid nanoparticles. The most widely studied and continually evolving method involves the modification of the silanols found on the silica surface.[3] This can involve modification to alter the surface hydrophilicity or growth of polymer shells responsive to external stimuli. Additionally, materials may be incorporated throughout the particle body. This can be achieved by noncovalent inclusion during the nanoparticle formation, or by condensing a mixture of silica precursors.[3] Porous silica particles can be generated in the presence of different templates.[3]

Less common hybrid silica particles are called ORMOSILs, an acronym for Organically Modified Silica.[4] They are formed when an organically modified silica

precursor is used as the only silica source. This generates a material that is organic in nature but retains silica particle properties. ORMOSIL particles are attractive because they contain reactive organic functionalities throughout the entire particle body. Their modifications could include a number of guest species (catalysts, drugs, solution-based contaminants) or conversion to a different organic functionality (alkene to dibromine, or alkene to diol). Thus, ORMOSIL particles have applications in a variety of fields, such as chromatography, catalysis, chemical clean-up, and drug delivery.

Unfortunately, ORMOSIL particle preparation is less developed compared to that for other hybrid silica materials. This may be because ORMOSIL nanoparticles are much more difficult to synthesize than traditional Stöber particles.

The goal of this work was to explore in detail the preparation of novel ORMOSIL nanoparticles and study their properties. This includes the discovery of new ORMOSIL particle types through new reaction conditions to induce particle formation from different silica precursors. The study also includes the exploration of the chemical modification of the organic functional groups found inside the nanoparticles. Additionally, we aimed to synthesize a prototype ORMOSIL particle to demonstrate the applications of these materials in drug delivery. This study significantly expands ORMOSIL chemistry by generating new materials and learning what additional modifications are possible.

In this chapter, we provide background and history of hybrid silica nanoparticles, as well as their applications. In subsequent chapters, we will

discuss in detail our experimental efforts and will discuss results and potential implications of the study.

1.1 Particle Formation

The synthesis and growth of silica particles typically involves a series of hydrolysis and condensation steps under aqueous conditions. These processes are catalyzed by either an acid (i.e., HCl) or a base (i.e., NH_4OH). The chemical reactions shown in Scheme 1.1 are commonly observed for the initiation and growth of a silica particle.[5] Condensation leads to dimerization, trimerization, and eventually, to individual clusters of growing silica which form the desired silica colloidal particles. While the products formed vary greatly depending on the conditions, the steps used to form the desired product have many similarities. First, the silica precursor undergoes hydrolysis and condensation with other silica monomers. Dimers then hydrolyze and condense to form trimers or cyclic structures and so on as polymerization continues to form larger silica networks. However, the types of products that are formed are often determined by the pH of the solution and conditions used. High pH conditions typically yield individual nanoparticles resistant to aggregation due to electrostatic repulsions.[6] Low pH conditions yield gels because individual particle growth is inhibited by nuclei reacting with one another instead of preferentially reacting with the silica monomer.[7] The difference between the acid- and base-catalyzed methods has to do with the nature of the growing nuclei. Under the alkali conditions, the silanol species is more likely to be deprotonated and thus, the growing nuclei

become increasingly negatively charged. The negatively charged species repel each other due to electrostatic repulsion. This repulsion results in a higher concentration of individual particles undergoing growth. Since the growing nuclei preferentially react with the silica monomer, well-defined particles are the final product. Under the acidic conditions, the growing nuclei possess no substantial charge. Because of the small repulsion between the growing nuclei, the individual clusters react with each other to produce extended polymer chains. Therefore, the common products of the acid catalyzed method are three-dimensional gels.[6] A schematic of the possible silica products as a function of reaction conditions is shown in Figure 1.1. In general, the methods developed for pure silica particle and gel synthesis are also valid for silica hybrid materials (i.e., co-condensation, organosilica particle formation, etc.). Thus, it is important to discuss the chemistry of the particle growth.

1.2 Stöber Method for Silica Particle Synthesis

While there are many methods that may be used to synthesize silica colloids,[8-16] the most popular and widely developed method is the so-called Stöber process (Scheme 1.2).[17] The method was first published in 1968 and involves the addition of tetraethylorthosilicate (TEOS) to a solution of ethanol, water, and ammonium hydroxide with rapid stirring. As the TEOS is added to the solution, the mixture quickly becomes opalescent and increasingly opaque as the sizes of the particles increases. After the particles are formed, they are isolated by centrifugation and washed to remove the ammonium hydroxide and silica

precursor. This relatively simple process can be used to synthesize particles of a desired diameter by altering the concentration of NH_4OH. Because NH_4OH increases the solubility of the silica intermediates, in particular of the growing clusters, particles can be grown to a larger diameter by increasing the NH_4OH concentration. Alternatively, particles of smaller diameter can be synthesized by using less NH_4OH. Additionally, the temperature of the solution during the particle formation affects the final particle sizes.[18,19,20] As the temperature of the solution increases, the surface energy of the particles decreases. Particle growth minimizes the interfacial tension in solution. Thus, particles decrease in diameter as the temperature of the solution increases. Using the Stöber method or a slight variation in the conditions, monodisperse particles have been synthesized between ~50 nm[21] and over 2 μm[22] in diameter.

1.3 Encapsulation of Fluorophores in Silica Particles

One example of hybrid silica materials includes the encapsulation of fluorescent dyes. The interest in incorporation of such dyes inside silica nanoparticles stems from the fact that fluorophores easily undergo photo or chemical bleaching in solution, thus limiting their useful fluorescence lifetime. Additionally, their fluorescence quantum yield can be low. This can be particularly problematic for confocal microscopy experiments. Silica particles can help to circumvent these issues altogether. If a fluorescent species is isolated within a silica particle body, the silica body can protect the fluorophore and thus reduce quenching and improve the fluorescence lifetime. Another benefit to the

encapsulation of the fluorescent dye is the increase in its quantum yield.[23,24] This is due to the synergistic effect that occurs when multiple of the same fluorescent species are housed together in a solid material.

There are two common methods used to generate fluorescent silica particles. The first method involves the generation of silica particles through a reverse phase microemulsion. To the emulsion, TEOS and the fluorophore are added. As the reagents enter the cavity of the micelle, the TEOS polymerizes and forms the particle with the fluorescent dye trapped within the particle body. The particle size is controlled by the size of the initial micelles in the emulsion. One possible disadvantage to this method involves the leakage of the dye out of the silica. To help circumvent this issue, a cationic dye, such as ruthenium(II) chloride hexahydrate, can be used.[25,26,27] A cationic dye electrostatically interacts with the negatively charged silica species and leaching from the silica is greatly reduced.

The second and more conventional method is to covalently bind the dye to the silica particle. This involves covalently attaching the dye to a silica precursor such as 3-aminopropyltriethoxysilane. This precursor can then be co-condensed with TEOS in the emulsion-mediated method or under the standard Stöber conditions. The resulting particle contains the dye throughout the body.[28] Alternatively, the dye can be covalently attached to presynthesized silica particles.[29,30,31] This reduces the process to a simple surface modification method, but comes at the cost of a lower level of protection offered to the dye. Additional protection may be introduced if a layer of silica is grown on top of the

fluorescent silica nanoparticle. Despite the increased particle size, a fresh silica surface is available for further surface modification. These highly fluorescent particles were found to be useful for a variety of biologically relevant applications. For example, if the surfaces of these particles are covalently modified with a targeting or recognition species, a complimentary target can be readily recognized. This has been useful for the determination of different cell lines and DNA.[32,33] Alternatively, fluorescent particles may also be used as an indirect means of determining ions in solution or to detect organic species. In this case, the guest interaction with the fluorophore of the particle induces a change in fluorescence. Thus, the change in fluorescent intensity is monitored. For example, TNT can cause quenching of silica-bound FITC dyes and fluorescence is lost in the presence of this molecule. Additionally, different metal ions have been detected using a method that monitors the change in fluorescence of the particle.[34] A schematic of the different kinds of dye-enriched products can be seen in Scheme 1.3. Overall, fluorescent silica particles can act as a very stable fluorophore that is resistant to bleaching, have high quantum yields when irradiated with UV light, and can be used in a variety of fields due to the ability to further tailor the surface depending on the need.

1.4 Core-Shell Silica Nanoparticles

Silica can also be used to protect other particles. For example, Quantum Dots (QD) can be protected by growing a layer of silica on the QD particle surface. QDs are strongly luminescent and their luminescent emission can be

controlled by their size. Additionally, they are highly resistant to photobleaching and do not require additional protection to maintain their luminescence.[35] These properties, combined with their small size, make them particularly attractive for biological imaging and sensing. However, they are highly toxic. QD toxicity is due to the generation of toxic reactive oxygen species or from the leaching of heavy metal ions.[36] However, since both of these cytotoxic properties involve interaction with the QD itself, toxicity can be greatly reduced by minimizing interaction with the QD surface. Not only does the silica layer reduce interaction with the QD surface, but it also introduces a surface that can be modified in a variety of ways. Growing a layer of silica on the surface of QDs usually involves either a modification of the Stöber method or the micelle-mediated reverse emulsion method.[3742] In either case, a ligand exchange must first be conducted on QDs in order to introduce a hydrophilic interface between the silica-layer and the QD. After the ligand exchange, the QDs can be transferred to the silica growth solution. Depending on the surface charge of the QDs, either a single QD will be in the core of the silica shell or multiple QDs will reside within. Silica-coated QDs have shown toxicity that was dramatically decreased or outright removed.[43] With the greatly reduced toxicity and the ability to further functionalize the surface, silica-coated QDs have been used as a cell imaging agent as they are able to undergo endocytosis.[42] With further modification of the silica shell, coated QDs have also been able to target and label different cancer cells.[44]

Other metallic nanoparticles gain several distinct advantages when coated with a layer of silica. A silica shell can help stabilize a colloidal solution of nanoparticles by preventing the particle surfaces from interacting, which can reduce particle aggregation. The silanols of the silica surface can also be functionalized with a variety of modified silanes such as fluorescent labels and targeting ligands. The silica layer also prevents interaction of the particle surface with healthy tissue, which can help to alleviate concerns about particle toxicity.[45] These added properties are particularly useful for iron oxide and gold nanoparticles as they may have useful drug and imaging properties. Iron oxide nanoparticles are seen as a potentially useful MRI contrast agent[46] while gold nanoparticles are seen as a possible low toxicity photothermal therapy drug.[47] Growing silica on the surface of metallic particles is similar to growing silica on the surface of QDs. The surface of the particles will typically need to undergo a ligand exchange to prepare for silica shell growth, followed by transfer to a silica growth solution where the shell is grown to the desired thickness. This method is common for presynthesized metallic particles. A silica shell may be grown on the surface of metallic nanoparticles during particle synthesis; however, this method required growth in situ using a microemulsion and is considerably more sensitive to changes in reactions conditions and as a result, is less common.[48]

1.5 Silica as a Template

Silica particles can also be used as a template for hollow nanostructures (Scheme 1.4). For example, if a cationic polymer is adhered to the silica surface,

an anionic polymer can next be adsorbed on top of the positively charged polymer. This process can be repeated until a thick polymer layer is formed. The polymer can then be chemically crosslinked.[49] The silica core can be etched out to yield a hollow polymeric capsule. Such capsules have been used for drug delivery and/or drug targeting.[50,51] The benefit to this method is the ability to control the size of the polymeric capsules by changing the size of the original silica core.

1.6 Preparation of Silica-Polymer Hybrids

Another approach to silica surface modification involves covalent attachment to the silanols on the silica surface. This is accomplished by the addition of an alkoxy silane, which forms a new silyl ether bond to the particle surface. A variety of organic moieties can be attached to the silica surface if the organic moiety is covalently bound to the alkoxysilane precursor. Particle properties can be altered through covalent modification of its surface. For example, hydrophobicity/hydrophilicity and surface charge can be easily tailored through a simple surface modification.[6]

Another important approach is the attachment of polymers to the silica particle surface.[52] Polymers on the surface of a silica particle may have a variety of functions. For example, if the polymer is stimuli responsive, the polymer brush may expand or contract upon stimulation or undergo a charge reversal. This can be useful as a type of gating mechanism for chemical separations.[53,54,55]

There are two common ways to anchor a polymer to the surface of a silica particle (Scheme 1.5).[56] The first method is called a "grafting too" approach. This involves the attachment of a presynthesized polymer directly to the surface of a silica particle. The benefit to this method is that the polymer can be fully characterized before its covalent attachment to the particle. The disadvantage of this method, however, is the limited grafting density that can be achieved. As the particle surface becomes covered with polymers, access to the silanols or other functional groups becomes sterically hindered.

The second method is called the "grafting from" approach. It involves the modification of the particle surface with polymerization initiators. The initiator species can then induce polymerization of a monomer which would grow a polymer brush from the surface one monomer at a time. One benefit of this method is the higher grafting density that can be achieved. The other benefit of this method is the control of the length of the polymer brush that stems from using living polymerization techniques. Additionally, because of the living polymerization conditions, block co-polymers can be formed by using different monomers. There are a number of living polymerization techniques that can be used, including Reversible Addition-Fragmentation chain Transfer polymerization (RAFT), Atom Transfer Radical Polymerization (ATRP), Nitroxide Mediated Polymerization (NMP), and Ring Opening Polymerization (ROP).[52] However, the disadvantage of this method is the difficulty in characterizing the polymers after they have been formed. Solution characterization techniques such as NMR and GPC can prove difficult or impossible when polymers are bound to a silica

surface. Furthermore, additional modification of the polymer brush can prove difficult to conduct and characterize when bound to the silica surface. In the end, the type of grafting technique used depends on the goals at hand and the level of characterization required.

1.7 Mesoporous Silica Nanoparticles

Mesoporous silica nanoparticles combine the properties of silica materials with a well-defined porous network throughout the body of the nanoparticle. These materials were first discovered by Mobile in 1992 and attracted attention as a new type of highly porous molecular sieve.[57,58] Typically, mesoporous silica materials are synthesized via the hydrolysis and condensation of a silica precursor (i.e., TEOS) in the presence of a micellar solution. As the micelles form and assemble in the solution, they act as a template for the silica precursor condensing around them. An illustration of how such materials can be formed is shown in Scheme 1.6. Mesoporous silica nanoparticles can be synthesized with various pore sizes, different organization of the porous network, and varying degrees of penetration throughout the particle body.[5969] The diameters of the pores are determined by the surfactant used to generate the template and by the reaction temperature. Victor-Lin and coworkers developed good synthetic methodology for the preparation of monodisperse particles containing the same levels of porosity as the bulk mesoporous silica.[70] By carefully controlling the interactions between the cationic surfactant (CTAB) and the growing anionic silica nuclei, they were able to limit the degree of assembly of the silica and thus

produce well-defined and highly porous particles. They were able to control this interaction and thus control the characteristics of the resulting products by introducing an organically modified silane along with their primary silica precursor (TEOS).[71] The development of these highly porous silica nanoparticles led to the renewed interest in silica chemistry.

Applications of the mesoporous silica nanoparticles are often related to drug delivery. Since mesoporous silica particles are highly porous and the surfaces are easily modified, they are ideal candidates for uptake and release of drug molecules. This can be accomplished by immersing the particles into a solution of drug molecules. The drug molecules enter the pores of the particles and the pores can be sealed off with a cleavable plug (Scheme 1.7). The drug molecules are trapped inside the particle and are only released upon cleavage of the plug. For example, vancomycin was successfully encapsulated within mesoporous silica particles utilizing a cleavable disulfide bridge. The surface of the silica particles was modified with an amine terminated disulfide ligand. After the drug had been loaded into the particle, a CdS nanocrystal functionalized with carboxcylic acid plugged the pores through amidation on the surface of the silica, sealing the drug within the pores.[72] The drug could be released after the cleavage of the disulfide bond and release of the CdS nanocrystal from the silica. Other plugs have also been used to seal mesoporous silica particles after particle loading, such as iron oxide particles that would open the pores in response to magnetic field.[73]

An additional advantage to the mesoporous particles is the ability to selectively modify the interior of the pores or the surface of the particle. Conventional silica surface modification can be conducted before the templating surfactant is removed. The surfactant thus protects the pore walls from functionalization. After the surface modification is complete, removal of the surfactant from the pores exposes the nanopore surface for additional modification.[74]

1.8 Co-Condensation Method for the Preparation of Silica Nanoparticles

Another method used to synthesize hybrid silica nanoparticles is the co-condensation of different silica species (Scheme 1.8). Instead of using TEOS as the only silica source, an organically modified silane is added to the solution. If the organic silane is condensed with TEOS, some of the properties of the organo-silane are introduced into the silica nanoparticles. This approach has been utilized to generate new particle types. Waters Corporation has taken advantage of the co-condensation method to generate a high-performance packing for their HPLC columns. They co-condensed TEOS with bis(triethoxysilyl)ethane. The bridge group that was introduced through the particle body of the silica particles added increased mechanical and chemical stability while greatly improving the materials' tolerance to high pH conditions.[75]

Other species have been incorporated into the co-condensed silica nanoparticles including complex structures. For example, fluorescent dyes[76,77,78] and anticancer agents[79] have been introduced throughout the body of a silica

particle. Co-condensation can also be conducted during the generation of mesoporous nanoparticles in order to increase the number of organic groups on the nanopores.[71] Placing the organo-silane throughout the particle body rather than limiting it to the surface helps to protect the organic functionality. For example, fluorescent dyes will be more resistant to chemical and photobleaching due to the protective nature of the particle body. In the case of the porous materials, functional groups may be present within the pores, thus increasing the amount of organic material on the total surface area. Thus, co-condensation of a silica-bound material with TEOS can yield particles with unique properties.

1.9 Preparation of ORMOSIL Nanoparticles

ORMOSIL nanoparticles are prepared by hydrolysis of a trialkoxysilanes. This method is not well developed due to the difficulty in particle preparation. Ottenbrite and coworkers were one of the first groups to develop ORMOSIL particles without the use of TEOS as a co-condensation agent.[80] They were able to generate a variety of particles containing hydrophobic organic groups (methyl, ethyl, vinyl, etc.) using aminopropyltriethoxysilane as a catalyst in an emulsion-mediated method. While the result was technically a co-condensation product, they showed that most of the products were comprised of the hydrophobic silica monomer. This method yielded well-defined spherical particles between 100-500 nm in diameter. Hay and coworkers expanded on this work by producing two unique methodologies to generate well-defined OMROSIL particles. Based on a study that used sodium silicate as a seed to grow silica particles,[81] they were

able to synthesize a variety of hydrophobic ORMOSILs.[82] The synthesis involved a variation of the Stöber method and used all of the same reagents. However, the important difference was the use of an organo-silane instead of TEOS. The sodium silicate solution added to the mixture induced particle growth by acting as a nucleation site for the organosilane nanoparticles (Scheme 1.9). Using this method, they were able to generate a family of particles smaller than 200 nm in diameter. While this method requires a seed source to generate the particles, the products themselves are comprised of mostly the organosilane rather than the seed source.

The second and more recent method the Hay group developed involved a micelle-mediated synthesis (Scheme 1.10).[83] This method utilized a cationic surfactant as a means to control the particle size. A micellar solution was prepared in an aqueous alkali solution and the organosilane was added to it. They were able to generate a family of ORMOSIL particles using this method, and to tune the size of the particle by manipulating the surfactant concentration.[84] This method is one of the only examples were ORMOSIL particles are prepared from a single organosilane.

1.10 ORMOSIL Nanoparticle Applications

ORMOSILs are unique because they combine the properties of both mesoporous silica and of organic species. ORMOSILs are partially porous due to the lack of the four siloxane bridges found in standard silica particles. This disrupts the compact nature of the silica matrix. Additionally, the steric bulk

introduced by the organic groups can add to the porosity. ORMOSILs also contain organic functional groups covalently bound to the silica network. These organic groups may undergo reactions much like any other organic moieties. For example, vinyl-thiol ORMOSIL particles were used to grow different metallic particles both on the surface and throughout the silica particle body.[85] The thiol and vinyl functionalities immobilize growing metallic particle nuclei and keep the particle in place as it grew. This can be advantageous as metallic nanoparticles tend to aggregate in solution. Keeping the particles immobilized inside the nanoparticles prevents metallic particle interactions and thus unwanted agglomeration. The other benefit to this method is the potential for the use as a catalyst.

Like other silica nanoparticles, ORMOSILs have applications in drug delivery. For example, a photosensitizer useful for photodynamic therapy was co-condensed with a vinyl silane precursor to generate a vinyl particle with covalently bound iodobenzyl-pyrosilane throughout the particle body. The resulting nanoparticles were monodisperse, could be synthesized in a very small size range (sub 20 nm), were water stable, and could be up taken directly into different cancer cells. Additionally, due to the organic functionality, there is opportunity to further tailor these particles with targeting agents.[86] Finally, ORMOSIL particles have also found use as a polymer binder to alter physical properties of polymer films.[87,88]

In many ways, ORMOSIL particle synthesis and applications are still in their infancy. Indeed, few publications involve the use of pure ORMOSIL

particles and most utilize a vinyl precursor since it behaves much like TEOS. However, as new methods are developed to generate new particle types, the applications for these unusual materials will surely grow.

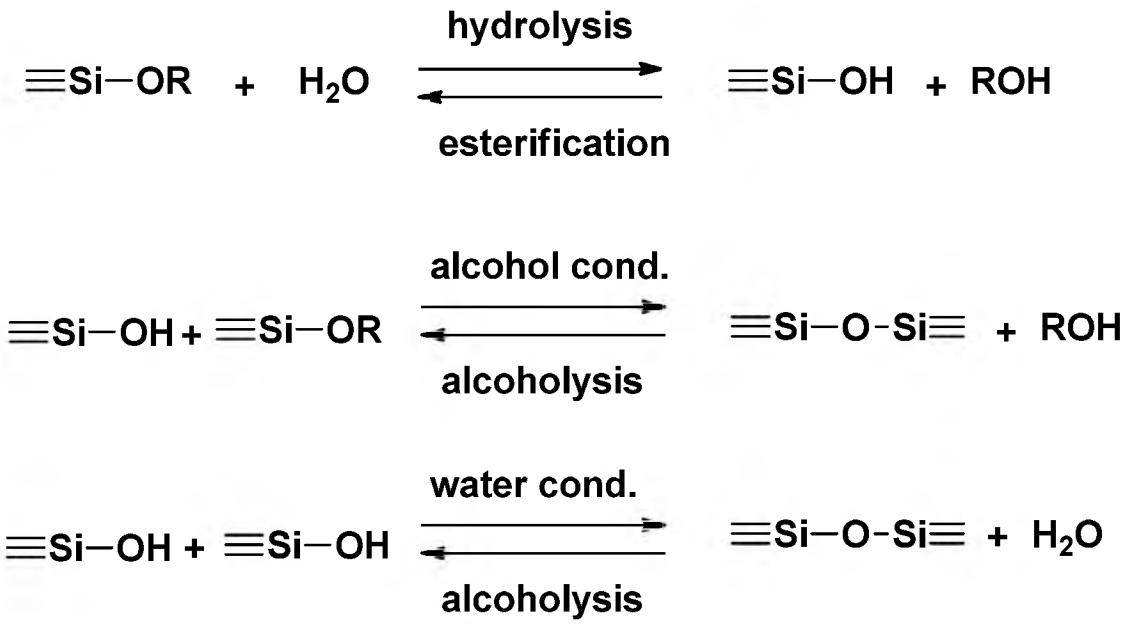

Scheme 1.1: Common reaction intermediates in sol-gel synthesis.

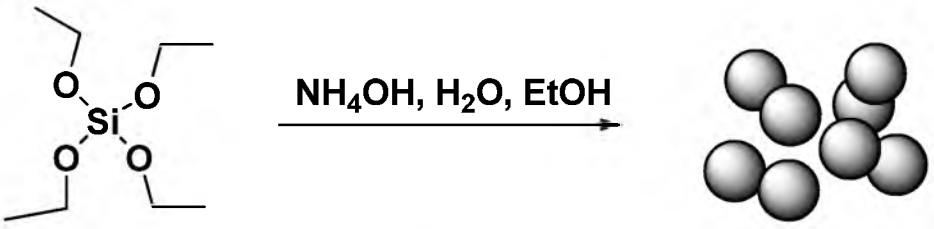

Scheme 1.2: Stöber particle synthesis.

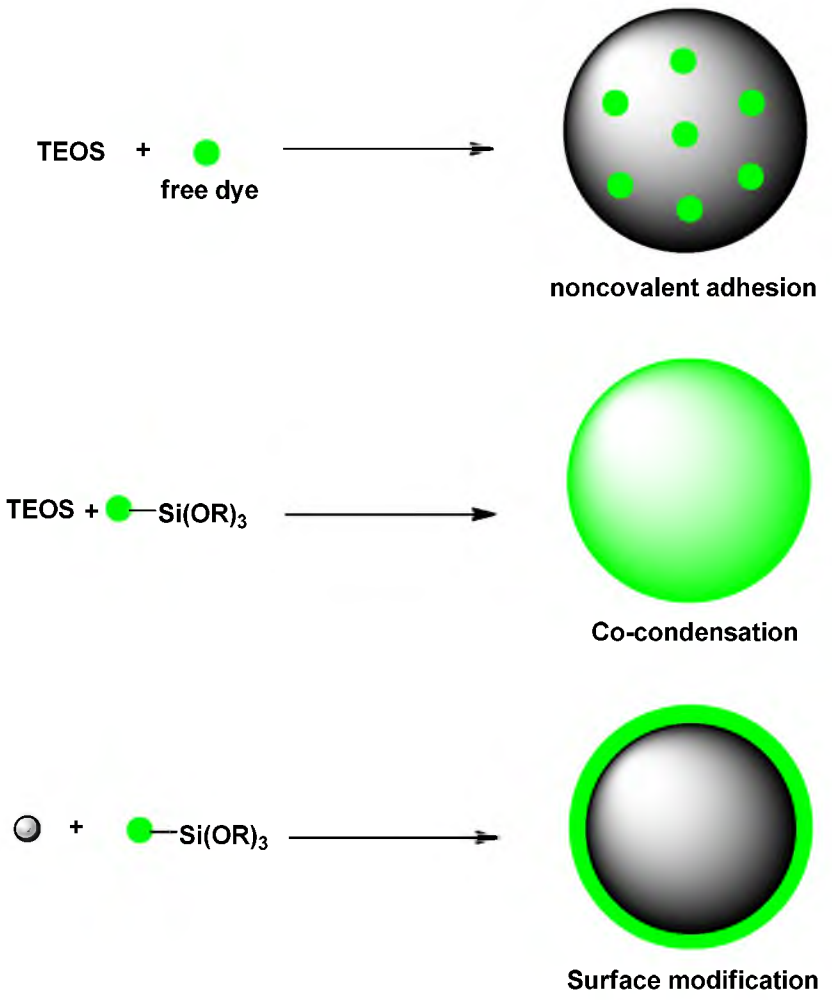

Scheme 1.3: Different methods of generating fluorescent silica particles.

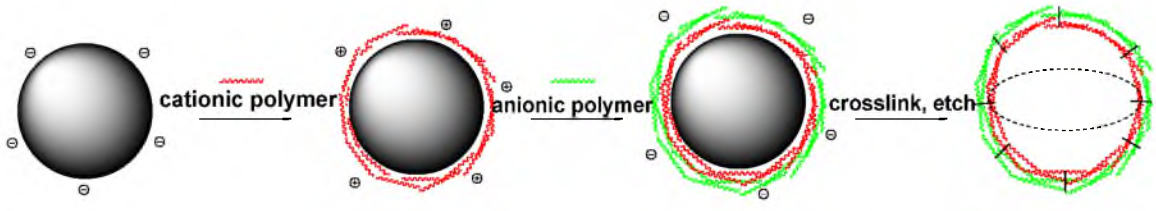

Scheme 1.4: Formation of polymer capsules using silica as a template

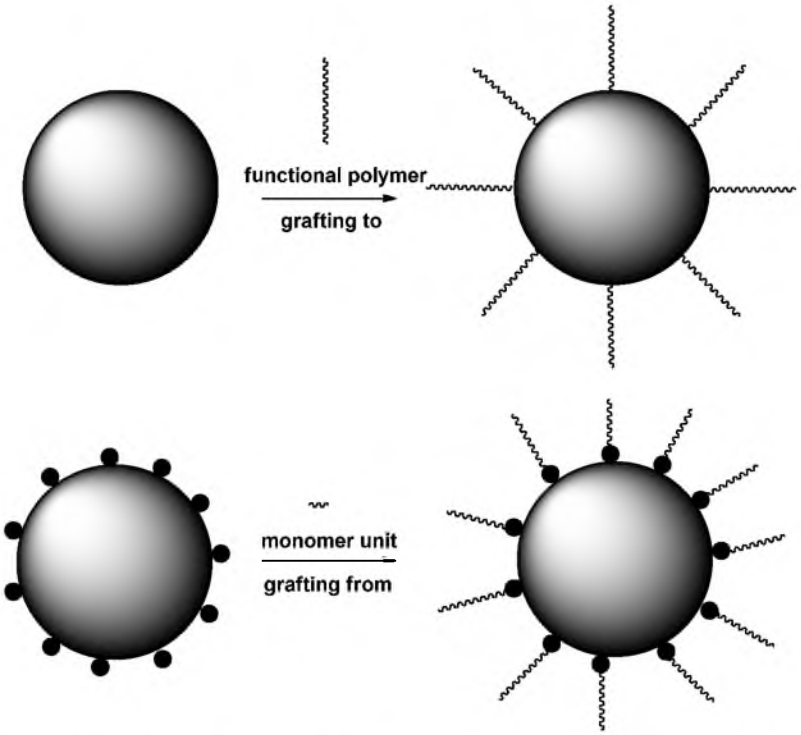

Scheme 1.5: Grafting to and grafting from polymer addition.

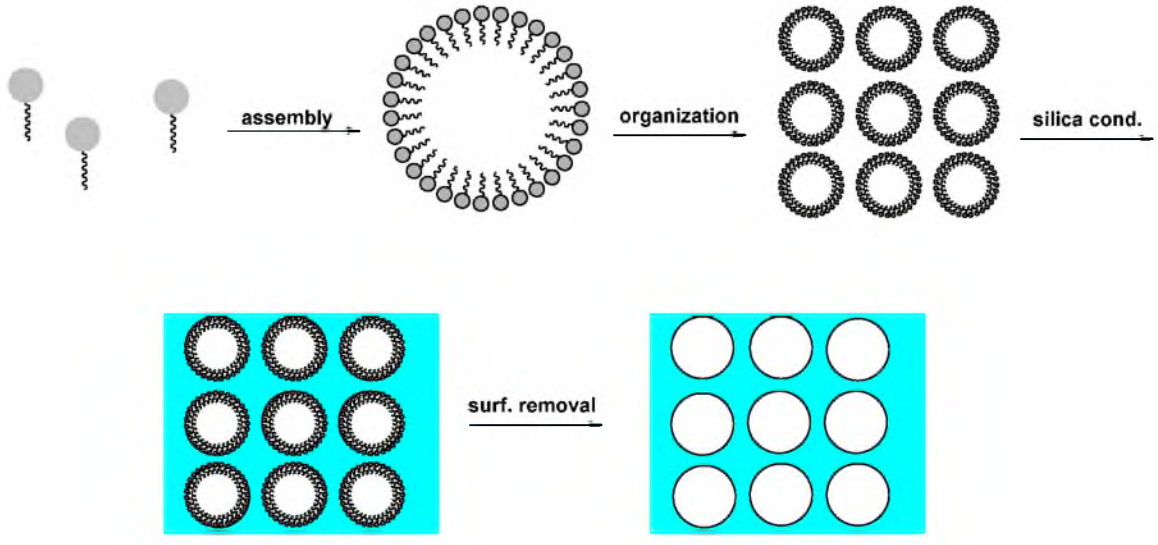

Scheme 1.6: Generation of mesoporous silica materials.

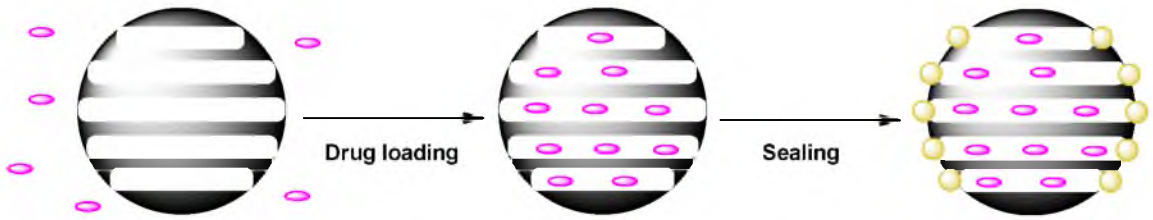

Scheme 1.7: Mesoporous particle loading.

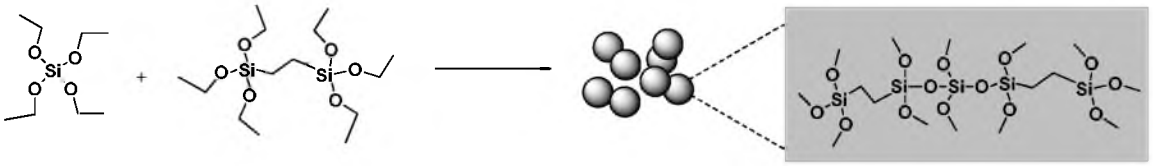

Scheme 1.8: Representation of co-condensation products.

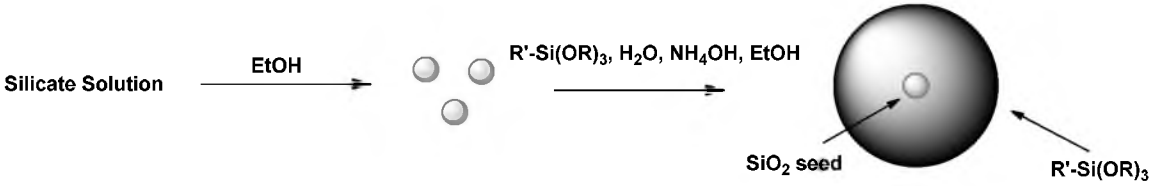

Scheme 1.9: Seeded ORMOSIL particle growth.

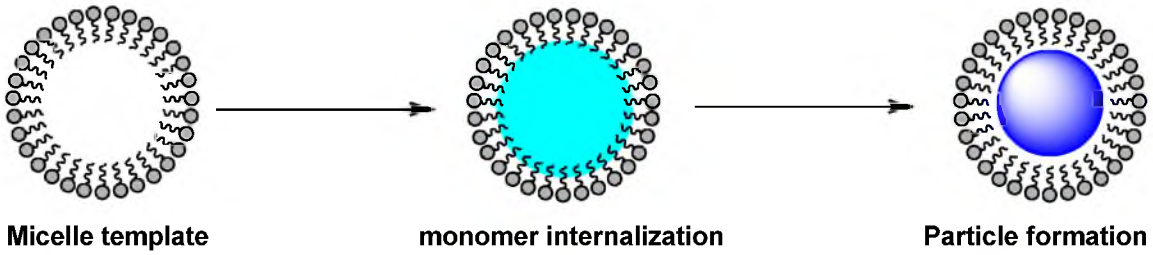

Scheme 1.10: Emulsion-mediated particle growth.

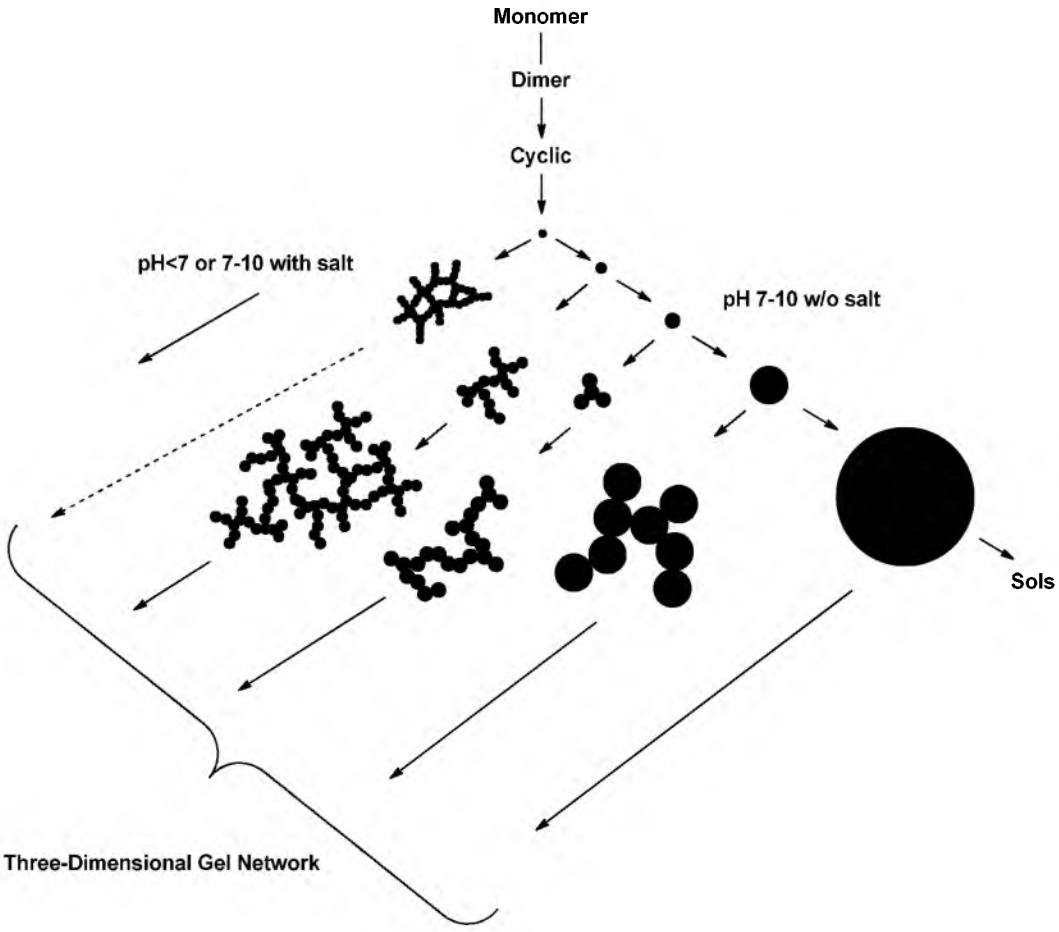

Figure 1.1: Sol-gel products resulting from different reaction conditions.[6]

1.11 References

[1] Berthod, A. *Journal of Chromatography,* **1991,** *549,* 1-28.

[2] Ambrogio, M.W.; Thomas, C.T.; Zhao, Y.-L.; Zink, J.; Stoddart, F. *Accounts of Chemical Research,* **2011,** *10,* 903-913.

[3] Hoffman, F.; Cornelius, M.; Morell, J.; Fröba, M. *Angew. Chem. Int. Ed.* **2006,** *45,* 3216-3251.

[4] Schmidt, H.; Wolter, H. *J. Non-Cryst. Solids* **1990,** *121,* 428-435.

[5] Brinker, C. J.; Scherer, G. W. *Sol-Gel Science.,* Academic Press, NY, (1990).

[6] Iler, R. K.; *The Chemistry of Silica,* John Wiley & Sons, NY (1979).

[7] Coenen, S.; De Kruif, C. J.; *Journal of Colloidal Interface Science,* **1988,** *124,* 104-110.

[8] P.C. Bird, U.S. Patent 2,244,325 (**1941**).

[9] Bechtold, M.F.; Snyder, O.E. U.S. Patent, 2,574,902 (**1951**)

[10] Alexander, G.B. U.S. Patent 2,750,345 (**1956**).

[11] Alexander, G.B.; McWhorter, J.R. U.S. Patent 2,833,724 (**1958**).

[12] Rule, J.M. U.S. Patent 2,577,484. (**1951**).

[13] Rule, J.M. U.S. Patent 3.012,972 (**1961**).

[14] Albrecht, W.L. U.S. Patent 3,440,174 (**1979**).

[15] Iler, R.K.; Wolter, F.J. U.S. Patent 2,631,134 (**1953**).

[16] Broge, E.C.; Iler, R.K. U.S. Patent 2,680,721 (**1954**).

[17] Stöber, W.; Fink, A.; Bahn, E. *J. of Colloid Interface Science,* **1968,** *26,* 62-69.

[18] Iler, R.K.; communication for Small Particles Technology

[19] Mattsson, and Otterstadt, J.-E. A., unpublished work, from Small Particles Technology

[20] Otterstedt, j.-E.; Brandreth, D.A. *Small Particle Technology*, Plenum Press, NY, (1998).

[21] Hiramatsu, H.; Osterloh, F. E. *Langmuir,* **2003,** *19,* 7003-7011.

[22] Kim, J.M.; Chang, S.M.; Kong, S.M.; Kim, -K.; Kim, I.-H.; Kim, K.-S.; Kim, W.S. *Mol. Cryst. Liq. Cryst.* **2008,** *492,* 245-256.

[23] Montalti, M.; Prodi, L.; Zaccheroni, N.; Battistini, G.; Marcuz, S.; Mancin, F.; Rampazzo, U.; Tonellato, U. *Langmuir,* **2006,** *22,* 5877-5881

[24] Rampazzo, E.; Bonacchi, S.; Montalti, M.; Prodi, L.; Zaccheroni, N. *J. Am. Chem. Soc.* **2007,** *129,* 14251-14256

[25] Bagwe, R.P.; Yang, C.; Hilliard, L.R.; Tan, W.; *Nano Lett.* **2004,** *20,* 8336-8342.

[26] Wang, L.; Yang, C.; Tan, W. ; *Nano Lett.* **2005,** *5,* 37-43.

[27] Zhao, X.; Bagwe, R.P.; Tan, W.; *Adv. Mater.* **2004,** *16,* 173-176.

[28] Bladeren, A.V.; Vrij, A. *Langmuir* **1992***, 8*, 2921-2931.

[29] Gao, D.; Wang, Z.; Liu, B.; Ni, L.; Wu, M.; Zhang, Z. *Anal. Chem.* **2008,** *80,* 8545-8553.

[30] Montalti, M.; Prodi, L.; Zaccheroni, N.; Falini, G.; *J. Am. Chem. Soc.* **2002,** *124,* 13540-13546.

[31] Bonacchi, S.; Rampazzo, E.; Montalti, M.; Prodi, L.; Zaccheroni, N.; Mancin, F.; Teolato, P. *Langmuir,* **2008,** *24,* 8387-8392.

[32] Smith, J.E.; Medley, C.D.; Tang, Z.; Shangguan, D.; Lofton, C.; Tan, W. *Anal. Chem.* **2007,** *79,* 3075-3082.

[33] Zhao, X.; Tapec-Dytioco, R.; Tan, W.; *J. Am. Chem. Soc.* **2003,** *125,* 11474-11475.

[34] Arduini, M.; Mancin, F.; Tecilla, P.; Tonellato, U. *Langmuir,* **2007,** *23,* 8632-8636.

[35] Zrazhevskiy, P.; Sena, M.; Gao, X. *Chem. Soc. Rev.* **2010,** *39,* 4326-4354.

[36] Bottrill, N.; Green, M. *Chem. Comm.***2011,** *47,* 7039-7050.

[37] Yi, D.K. ; Selvan, S.T.; Lee, S.S.; Papefthymiou, G.C.; Kundaliya, D.; Ying, J.Y. *J. Am. Chem. Soc.* **2005,** *127,* 4990-4991.

[38] Tan, T.T.; Selvan, S.T.; Zhao, L.; Gao, S.; Ying, J.Y. *Chem. Mater.* **2007,** *19,* 3112-3117.

[39] Darbandi, M.; Thomann, R.; Nann, T. *Chem. Mater.* **2005,** *17,* 5720-5725.

[40] Graf, C.; Dembski, S.; Hofmann, A.; Rhl, E. *Langmuir,* **2006,** *22,* 5604-5610.

[41] Gorelikov, I.; Matsuura, N. *Nano. Lett.* **2008,** *8,* 369-373.

[42] Bakalova, R.; Zhelev, Z.; Aoki, I.; Masamoto, K.; Mileva, M.; Obata, T.; Higuchi M.; Gadjeva, V.; Kanno, I. *Bioconjug. Chem.* **2008,** *19,* 1135-1142.

[43] Kirchner, C.; Liedl, T.; Kudera, S.; Pellegrino, T.; Munoz, J.A.; Gaub, H.E.; Stolzle, S.; Fertig, N.; Parak, W.J. *Nano. Lett.* **2005,** *5,* 331-338.

[44] Selvan, S.T.; Patra, P.K.; Ang, C.Y.; Ying, J.Y. *Angew. Chem. Int. Ed.* **2007,** *46,* 2448-2452.

[45] Li, Y.-F.; Chen, C. *Small* **2011,** *7,* 2965-2980.

[46] Na, H.B.; Song, I.C.; Hyeon, T. *Advanced Materials* **2009,** *21,* 2133-2148.

[47] Dreaden, E.C.; Mackey, M.A.; Huang, X.; Kang, B.; El-Sayed, M.A. *Chem. Soc. Rev.* **2001,** *40,* 3391-3404.

[48] Guerroro-Martinez, A.; Perez-Juste, J.;Liz-Marzan, L.M. *Advanced Materials* **2010,** *22,* 1182-1195.

[49] Wang, Y.; Angelatos, A.S.; Caruso, F. *Chem. Mater.* **2008,** *20,* 848-858.

[50] Such, G.K.; Tjipto, E.; Postma, A.; Johnston, A.P.R.; Caruso, F. *Nano Letters* **2007,** *7,* 1706-1710.

[51] Wang, Y.; Yan, Y.; Cui, J.; Hosta-Rigau, L.; Heath, J.K.; Nice, E.C.; Caruso, F. *Advanced Materials* **2010,** *22,* 4293-4297.

[52] Radhakrishnan, B.; Ranjan, R.; Brittain, W.J. *Soft Matter* **2006,** *2,* 386-396.

[53] Schepelina, O.; Poth, N.; Zharov, I. *Adv. Funct. Mater.* **2010,** *20,* 1962-1969.

[54] Abelow, A.E.; Zharov, I. *Soft Matter* **2008,** *5,* 457-462.

[55] Schepelina, O.; Zharov, I. *Langmuir,* **2008,** *24,* 14188-14194.

[56] Stamm, M.; *Polymer Surfaces and Interfaces* **2008,** 215-234**.**

[57] Beck, J.S.; Vartuli, J.C.; Roth, W.J.; Leonowicz, M.E.; Kresge, C.T.; Schmitt, K.D.; Chu, C.T.W.; Olson, D.H.; Sheppard, E.W.; Higgins, S.B.; Schlenkur, J.L.. *J. Am. Chem. Soc.,* **1992,** *114,* 10834-10843.

[58] Beck, J.S.; Chu, C.T.W.; Johnson, I.D.; Kresge, C.T.; Leonowicz, M.E.; Roth, R.J.; Vartuli, J.C. Mobile oil, *US Patent,* 5 108 725, **1992.**

[59] Kresge, C.T.; Leonowicz, M.E.; Roth, W.J.; Vartuli, J.C.; Beck, J.S. *Nature,* **1992,** *359,* 710-712.

[60] Monnier, A.; Schuth, F.; Huo, Q.; Kumar, D.; Margolese, D.; Maxwell, R.S.; Stucky, G.D.; Krishnamurty, M.; Petroff, P.; Firouzi. A.; Janicke, M.; Chmelka, B.F. *Science,* **1993,** *261,* 1299-1303.

[61] Alfredsson, V.; Anderson, M.W. *Chem. Mater.,* **1996,** *8,* 1141-1146.

[62] Ryoo, R.; Ko, C.H. *Chem. Commun.,* **1996,** 2467-2468.

[63] Bagshaw, S.A.; Prouzet, E.; Pinnavaia, T.J. *Science,* **1995,** *269,* 1242-1244.

[64] Prouzet, E.; Pinnavaia, T.J. *Angew. Chem. Int. Ed. Eng.,* **1997,** *36,* 516-518.

[65] Prouzet, E.; Cot, F.; Nabias, G.; Larbot, A.; Kooyman, P.; Pinnavaia, T.J. *Chem. Mater.,* **1999,** *11,* 1498-1503.

[66] Taney, P.T.; Pinnavaia, T.J. *Science, ,* **1995,** *267,* 865-867.

[67] Tanev, P.T.; Pinnavaia, T.J.; *Chem. Mater.,* **1996,** *8,* 2068-2079.

[68] Zhao, D.; Huo, Q.; Feng, J.; Chmelka, B.F.; Stucky, G.D. *Science,* **1998,** *279,* 548-552.

[69] Zhao, D.; Huo, Q.; Chmelka, B.F.; Stucky, G.D. *J. Am. Chem. Soc.,* **1998,** *120,* 6024-6036.

[70] Lai, C.-Y.; Trewyn, B.G.; Jeftinija, D,M.; Jeftinija, K.; Xu, S.; Jeftinija, S.; Lin, V.S.-Y. *J. Am. Chem. Soc.* **2003,** *125,* 4451-4459.

[71] Trewyn, B.G.; Slowing, I.I.; Giri, S.; Chen, H.-T.; Lin, V.S.-Y. *Acc. Chem Res.,* **2007,** *40,* 846-853.

[72] Lai, C.Y.; Trewyn, B.G.; Jeftinija, D.M.; Jeftinija, K.; Xu, S.; Jeftinija, S.; Lin, V.S. *J. Am Chem. Soc.* **2003,** *125,* 4451-4459.

[73] Giri, S.; Trewyn, B.G.; Stellmaker, M.O.; Lin, V.S.Y. *Angew. Chem. Int. Ed.* **2005,** *44,* 5038-5044.

[74] Pasqua, L.; Testa, F.; Aiello, R.; Cundari, S.; Nagy, B.J. *Macroporous Mesoporous Mater.* **2007,** *103,* 166-173.

[75] Wyndham, K.D.; O'Gara, J.E.; Walter, T.H,; Glose, K.H.; Lawrence, N.L.; Alden, B.A.; Izzo, G.S.; Hudalla, C.J.; Iraneta, P.C. *Anal. Chem.,* **2003,** *75,* 6781-6788.

[76] Blaaderen, A. V.; Vrij, A. *J. Colloid Interface Sci.* **1993**, *156*, 1–18.

[77] Burns, A.; Hooisweng, O.; Wiesner, U. *Chem. Soc. Re*V. **2006**, *35*, 1028–1042.

[78] Parida, S. K.; Dash, S.; Patel, S.; Mishra, B. K. *Ad*V. *Colloid Interface Sci.* **2006**, *121*, 77–110.

[79] Ohulchanskyy, T. Y.; Roy, I.; Goswami, L. N.; Chen, Y.; Bergey, E. J.; Pandey, R. K.; Oseroff, A. R.; Prasad, P. N. *Nano Lett.* **2007**, *7*, 2835–2842.

[80] Ottenbrite, R.M.; Wall, J.S.; Siddiqui, J.A. *J. Am. Ceram. Soc.* **2000,** *83,* 3214-3215

[81] Buining, P.A.; Liz-Marzan, L.M.; Philipse, A.P. *J. Colloid Interface Sci.* **1996,** *227,* 318-321.

[82] Arkhireeva, A.; Hay, J. N. *J. Mater. Chem.* **2003,** *13,* 3122-3127.

[83] Baumann, F.; Schmidt, M.; Deubzer, B.; Geck, M.; Dauth, J. *Macromolecules,* **1994,** *27,* 6102-6105.

[84] Arkireeva, A.; Hay, J.N.; Oware, W. *Journal of non-Crystalline Solids,* **2005,** *351,* 1688-1695.

[85] Kim, Y. B.; Kim, Y. A.; Yoon, K. *Macromol. Rapid Commun.* **2006**, *27*, 1247–1253.

[86] Ohulchanskyy, T.Y.; Roy, I.; Goswami, L.N.; Chen, Y.; Bergey, E.J.; Pandey, R.K.; Oseroff, A.R.; Prasad, P.M. *Nano Lett.* **2007,** *7,* 2835-2842.

[87] Jesson, , D.A.; Smith, P.A.; Hay, J.N.; Watts, J.F. *Journal of Mater. Sci.* **2007,** *42,* 3230-3237.

[88] Jesson, D.A.; Abel, M.-L.; Hay, J. N.; Smith, P. A.; Watts, J. F. *Langmuir* **2006**, *22,* 5144-5151.

CHAPTER 2

DESIGN AND SYNTHESIS OF BORON-CONTAINING SILICA NANOPARTICLES[i]

2.1 Introduction

Boron Neutron Capture Therapy (BNCT) is a form of cancer treatment that utilizes ^{10}B and a thermal neutron source. The two components of this binary system are innocuous in vivo until they are brought together and undergo fission. This fission reaction, more commonly known as a neutron capture event, occurs when a low-energy thermal neutron fuses with the nucleus of ^{10}B atom to form a transient unstable ^{11}B isotope. The ^{11}B isotope undergoes a fission reaction releasing a recoiling ^{7}Li ion and an alpha particle (Scheme 2.1). These fission products release a significant amount of energy capable of ionizing material within several micrometers of the reaction site.[1,2,3]

If this reaction can be confined near or inside a cancerous cell, cell death can occur from organelle damage, cell wall damage, or damage to the nucleus. The difficulty in this method lies with the incorporation of a sufficient amount of boron into a cancerous cell to ensure that a neutron capture event occurs.

---

[i] Parts of this chapter have been reprinted with permission from Brozek, E.; Zharov, I. Internal Functionalization and Surface Modification of Vinylsilsesquioxane Nanoparticles. *Chem. Mater.* **2009,** *21,* 1451-1456. Copyright 2013 American Chemical Society.

Approximately 10^9 boron atoms per cell are required to assure the capture efficiency of at least 85%. Additionally, the ratio of boron content in tumor to that in blood needs to be at least 3:1.[4,5] If the ratio is too low, there is a significant risk of damaging healthy tissue. This is especially important for brain cancer as brain damage can result from limited accumulation.

Two boron-containing moieties that have undergone clinical trials are mercaptoundecahydrododecaborate (BSH) and 4-dihydroxyboorylphenylalanine (BPA). BSH molecules contain a large number of boron (10 atoms),[6] which make them a good candidate for BNCT. BSH is uptaken by brain tumors, but the reason for the uptake remains unclear.[7] BPA was introduced based on the assumption that it would be uptaken in higher doses in cells that possess higher levels of melanin formation, as phenylalanine is the precursor for its synthesis.[7] BPA showed increased uptake in such cells, which made the drug more selective.[8,9]

Most of the boron-containing agents cannot deliver a sufficient number of boron atoms to cancer cells. In this respect, nanoparticles may provide a superior delivery modality due to the high boron content compared to other boron delivery agents.[10] So far, two methods have been reported for the preparation of boron-rich nanoparticles. One method involves ball milling of a boron powder by spinning the material in the presence of ball bearings. Boron nitride has been ball milled into a polydisperse powder of particles ranging from 40-500 nm in diameter, followed by surface functionalization.[11] The problem with the ball milling method is the general lack of control of size and shape of the resulting

particles. Additionally, the particles require surface stabilization to prevent aggregation, which limits useful surface modification. The second method involves the reduction of a tribromoboron salt by sodium naphthelinde in diglyme. This yields spherical elemental boron particles in the size range of 1-45 nm in diameter.[12] However, the particles formed through the reduction chemistry are highly sensitive to oxidation and require surface stabilization to prevent them from reacting with oxygen. Again, this limits the extent of useful surface functionalizations.

Boron-rich silica nanoparticles provide a promising alternative approach. If boron can be placed throughout a silica particle either via co-condensation, entrapment within the core, or bound to silica as an ORMOSIL, a large number of boron atoms could be delivered by a single particle. Additionally, the surface of the particle could be designed for the needs of the cancer therapy. The goal of this research project was to prepare new silica nanoparticles containing a large number of boron atoms.

In this chapter, the development of new boron-rich silica nanoparticles is described. Three approaches were examined in order to prepare the desired material. 1) Co-condensation of a silica precursor and activated boron source. 2) Generation of boron-containing trialkoxy-silica species and their hydrolysis and condensation to induce particle growth. 3) Synthesis of vinyl-containing silica particles and postmodification of the vinyl-handles throughout the particle body.

2.2 Experimental Section

2.2.1 General

All water-sensitive reactions were conducted under dry nitrogen atmosphere using dried glassware and anhydrous solvents. Hygroscopic liquids were transferred into reaction vessels by syringe through rubber septa. Where applicable, reactions were monitored by TLC using Merck silica gel 60F254 on aluminum plates and a potassium permanganate stain. Silicycle silica gel (Ultrapure, 230-400 mesh) was used for flash chromatography separations where applicable.

2.2.2 Reagents

All solvents were obtained from Mallinckrodt Baker or Fisher Scientific as reagent grade, except for hexanes and ethyl acetate that were of technical grade. THF was dried by distillation over sodium benzophenone ketyl under nitrogen; dichloromethane was dried by distillation over calcium hydride under nitrogen. Toluene was dried over 4 Å molecular sieves. All other solvents were used without further purification. The following reagents were all purchased and used without additional purification: glycerol (Mallinckrodt), boronic acid (99.9%, Mallinckrodt), NH_4OH (30%, Mallinckrodt), tetraethylorthosilicate (Alfa Aesar, +99.999), allylboronic acid pinacol ester (97%, Aldrich), vinyltriethoxysilane (97%, Aldrich), Grubb's 1st generation catalyst (Aldrich), 9-BBN (0.5 M in THF, Aldrich), acetlaldehyde (98.5%, Alfa Aesar), pinacol borane (97%, Aldrich), allyltriethoxysilane (Gelest), catecholborane (98%, Aldrich), Triethoxysilane

(Gelest), Karstedt's catalyst (Aldrich), BH_3.THF complex (1M stabilized, Acros organics), silicate solution (27% SiO_2, 10% NaOH, Aldrich), bromine (>99.5%, Mallinckrodt), 3-aminopropyltriethoxysilane (98%, Alrich), dansyl chloride (99%, Aldrich), 2,6-lutidine (99%, Aldrich).

2.2.3 Instrumentation

IR spectra were recorded in the range from 400 to 4000 cm^{-1} using a Bruker Tensor 37 IR Spectrophotometer as KBr pellets. Scanning electron microscopy (SEM) images were obtained using a Hitachi S3000N instrument at an accelerating voltage of 20 kV. Elemental analysis was conducted by Columbia Analytical Services using Inductively Coupled Plasma spectroscopy (ICP). Thermogravimetric Analysis (TGA) measurements were performed using a TA Instruments Q500 series TGA using a type P Platinel II thermocouple in an open platinum pan. The isotropic ^{11}B NMR data were collected using a 600 MHz Varian Infinity spectrometer using a 4.0 mm probe and a sample spinning speed of 10.0 kHz. Analysis was performed using a single pulse excitation at a frequency of 192.437 MHz and no decoupling. A total of 256 scans were acquired using a 2.0 μs 90 pulse and a 200 kHz spectral width with a 10 s delay between pulses. The spectrum was referenced to the ^{11}B resonance in sodium borate decahydrate at 2.1 ppm. A Branson 1510 sonicator was used for all sonications.

2.2.4 Synthesis

2.2.4.1 Attempted synthesis of borosilicate particles via activated boronic acid (Scheme 2.2).[13] Millipore water (21.9 mL) was placed into an Erlenmeyer flask (125 mL) and set to stir. Glycerol (9.22 mL, 128 mmol) was added to the flask, followed by boronic acid (2.35 g, 38 mmol). The solution was allowed to homogenize. Tetraethoxysilane (TEOS) (4.43 mL, 20 mmol) was dissolved in absolute EtOH (49.4 mL). The ethanoic TEOS solution was added to the boronic acid solution under continued stirring. Ammonium hydroxide (12.4 mL, 28%) was carefully added to the TEOS/boronic acid solution and the flask was sealed tightly with Parafilm. The final molar concentrations of the solution in absolute EtOH were as follows: 0.20 M TEOS, 0.96 M NH_4OH, 17.0 M H_2O, 0.38 M $B(OH)_3$. Shortly after the addition of NH_4OH, the solution became turbid and eventually white and opaque. The solution was stirred overnight at room temperature. The following day, a white precipitate was collected via centrifugation. The precipitate was washed seven times with water/ethanol mixtures containing increasing EtOH quantities (1:0, 3:1. 2:1, etc.). After the washing, a white solid was collected and dried under the nitrogen to yield a fine white powder. IR spectra were recorded for the powder in KBr pellets.

2.2.4.2 Olefin metathesis of vinyltriethoxysilane and allylboronic acid pinacol ester (Scheme 2.3):[14] Into a dry 3-necked round-bottom flask, dry methylene chloride (10 mL) was placed. Vinyltriethoxysilane (0.757 mL, 3.63 mmol) was added to the flask followed by allylboronic acid pinacol ester (0.140 mL, 0.73 mmol). Note: The silica:boron ratio needs to be kept at a minimum of

5:1 in order to prevent homometathesis of the boron source. A few milligrams of Grubb's 1st generation catalyst were added to the flask and the reaction mixture was set to reflux. The reaction progress was monitored via TLC. The product was collected by flash chromatography using silica as the stationary phase and 85:15 hexanes/ethylacetate eluent. Yields were typically between 50-60%.

2.2.4.3 Synthesis of functionally rich-trialkoxysilane particles via SiO_2 seeding method (Scheme 2.4).[15] A typical method for the synthesis of organically modified silica particles is as follows. Into a separate round-bottom flask, absolute ethanol (6.3 mL), ammonium hydroxide (8.4 mL, 30%), and vinyltriethoxysilane (0.84, 4 mmol) were all added and the contents set to stir. Into a separate vial, silicate solution (0.25 mL, 2.2%) was mixed with absolute ethanol (12.5 mL). The silicate solution was added to the previously prepared solution in a single addition. Within several hours of stirring, a white suspension was observed. The solution continued to stir overnight. The white precipitate was centrifuged down to yield a white solid. The solid was washed with mixtures of ethanol and water. After washing, the white precipitate was dried overnight over air to yield a fine white powder. IR, TGA, SEM, TEM, and elemental analysis data were collected.

2.2.4.4 Bromination of vinyl-containing ORMOSIL particles (Scheme 2.5). Dichloromethane (10 mL) was added to 0.25 g vinylsilisesquioxane nanoparticles (3.13 mmol based on monomer unit) and sonicated. To this solution, three equivalents of bromine (0.48 mL) were carefully added; the vial was then capped and sealed with Parafilm. The contents were briefly sonicated and stirred

overnight (~16 h.). The particles became much denser and precipitated out of solution more rapidly compared to nonbrominated particles while the color of the solution slightly lightened. The particles were collected by centrifugation and washed at least five times with dichloromethane to ensure all bromine was removed. Once washed, the particles were air dried and vacuum dried for at least 18 h. The particles were isolated as a fine white/off white powder. The powder was analyzed by IR spectroscopy, TGA, SEM, and elemental analysis (ICP). EA results: Si%: 13.05, C%: 9.125, H%: 1.315, Br%: 59.85.

2.2.4.5 Posthydroboration of vinyl-containing particles (Scheme 2.6). Vinylsilisesquioxane nanoparticles (0.25 g, 3.13 mmol based on monomer unit) were placed in a 25 mL round-bottom flask. To the vial, THF (3 mL) was added under nitrogen to disperse the particles. Three equivalents of 1.0 M BH_3·THF (9.5 mL) solution were then added. The contents were briefly sonicated to disperse the particles and vigorously stirred. At first, the particles dispersed evenly in the THF/BH_3 solution. After approximately 20 min., the particles began to precipitate out of the solution and appeared to cluster and could not be easily redispersed. The particles were sonicated again and stirred overnight. The solid was then collected via centrifugation at approximately 1800 rpm and washed several times with THF to remove excess BH_3. After the THF washings, the particles were washed with pure ethanol with a little water to remove any residual BH_3 while also converting the free borohydride groups to boric acids.[16,17] The particles were then rinsed several times with water to further remove any impurities and assure the conversion of the free hydrides. The boron-enriched

particles disperse evenly into pure water while the vinyl-particles are too hydrophobic to do so, offering an indication that a modification took place. The white solid was air dried and dried under vacuum for at least 18 h. The fine white powder was then analyzed by IR, TGA, SEM, ICP, and CP-MAS ^{10}B NMR. EA results: Si%: 23.45, C%: 16.44, H%: 3.785, B%: 3.585.

2.2.4.6 Amination of modified vinyl-containing particles (Scheme 2.7):[18] A general method was used for the amine functionalization of the surfaces of the particles and could be used for the vinyl, brominated, and boronated particles. An example of the procedure used is as follows: dry acetonitrile (6 mL) was added to vinyl-particles (26 mg) in a scintillation vial and sonicated to evenly disperse the particles. 3-Aminopropyltriethoxysilane (90 µL, 0.336 mmol) was added to the vial and the reaction mixture was stirred for approximately 20 hours. The particles were collected by centrifugation and washed several times with acetonitrile to remove any excess APTES. The white/off white solid was air dried then dried under vacuum overnight. The amine-modified particles were used without further characterization.

2.2.4.7 Dansylation of amine-modified ORMOSIL particles (Scheme 2.8):[19] A general method was used for the dansylation of the amine-functionalized particles and could be applied to the vinyl, bromine-, and boron-enriched aminated particles. An example of the procedure used is as follows: dry acetonitrile (10 mL) was added to amine-functionalized nanoparticles (13 mg) in a scintillation vial and sonicated to disperse the particles evenly. The vial was wrapped in aluminum foil and dansyl chloride (10 mg, 0.04 mmol) was added

followed by three drops of dry 2,6-lutidine. The vial was capped, wrapped in Parafilm, and the solution stirred for about 17 hours. The resulting particles were collected via centrifugation and washed five times with acetonitrile to remove any excess dansyl chloride. The particles were air dried then dried under vacuum overnight to yield a white/off white powder. The powder was irradiated with short-wave UV light and showed blue/green fluorescence. A control experiment was performed for nonaminated particles under the same conditions and they did not exhibit fluorescence.

2.3 Results and Discussion

2.3.1 Activated boronic acid

Our initial plan was to incorporate an activated boronic acid species into the matrix of a Stöber silica particle. There are several advantages to this design. First, the Stöber method has been exhaustively studied. Second, the Stöber method and its variations can yield particles over a wide size range, ranging from tens of nanometers to over a micron.[20,21,22] Third, the products derived from this synthesis would possess surfaces covered in silanols. This means the product could be easily surface-modified with targeting ligands, fluorescent tags, or any other functionality that could prove useful for in vitro or in vivo studies.[23-29] Fourth, silica and boronic acid have shown to have no toxicity in vivo.[30]

The aim was to introduce a boronic acid species that would participate in the hydrolysis/condensation process of the Stöber reaction (Scheme 2.9).

Glycerol was stirred with boronic acid in a water/ethanol solution in order to generate the reactive species. To the vessel, ethanol water, tetraethylorthosilicate, and ammonia hydroxide were added as is common in the Stöber method. It seemed reasonable to assume that activation of the boronic acid was the most important first step, especially considering how quickly silica particles can form in solution. Formation of the particles became apparent as the solution went from clear, to cloudy, to white and opaque. We used IR spectra in order to evaluate the product.

The IR spectrum provides several important observations (Figure 2.1). First, a very strong peak found at 1061 cm^{-1} represents a Si-O asymmetric vibration. This peak suggests the successful formation of a silica particle. A peak found at 952 cm^{-1} is typical of a Si-OH asymmetric vibration and suggests the preservation of the surface bound silanols. Additionally, a broad peak at 3435 cm^{-1} is representative of a –OH stretch, most likely due from H_2O or that from the silanols. A peak at 1631 cm^{-1} likely results from the scissoring vibration of H_2O, which is reasonable considering the conditions of the TEOS condensation.[31] This leaves the peak at 1401cm^{-1} to be assigned. At first, the presence of the peak at 1401 cm^{-1} appeared encouraging, as this range is typical of the B-O stretching vibration, and suggested some level of incorporation of boron into the silica particle. However, additional testing of our particles suggested otherwise. Specifically, the IR spectrum of the particles prepared by the Stöber method without the use of boronic acid was nearly identical. Thus, the peak likely represents another asymmetric Si-O-Si vibration and seems to

appear in other particles prepared by the Stöber method. Burning the particles was also attempted, as boron typically gives a green flame when burned. However, no green color was observed.

Reaction conditions were modified by increasing the amount of activated boronic acid in solution, changing the rate of addition of TEOS, changing the temperature, and/or changing the ammonia concentration. Unfortunately, none of these changes altered the final product. We explain this result by the structural differences between a xero-gel like product and a solid particle product. During an acid catalyzed sol-gel process, silica nuclei crosslink with each other, trapping reagents within the silica network. However, in a synthesis involving a base-catalyzed condensation, a nonporous structure is formed and no trapping occurs. Since the products formed during a base catalyzed method tend to be anionic in nature, there is a high degree of repulsion between the growing species. Thus, particle growth results from monomer addition to growing nuclei to yield a highly condensed network work as opposed to the porous network of an acid catalyzed gelation. Thus, it seems likely that only the pure silica particles are formed.[32]

2.3.2 Boron-containing trialkoxysilane

After the unsuccessful attempts to use a modified Stöber method to enrich a silica particle with boron, we decided to use a relatively knew and lesser-known method of synthesis. This method involves using an organically modified trialkoxysilane instead of TEOS as the sole silica source.[33,34] We were interested

in a trialkoxysilane precursor containing a boron moiety. If successful, every silica monomer throughout the particle would also contain a bound boron atom, thus impregnating the particle with a large amount of boron. However, there are also several drawbacks to this method. As previously stated, the trialkoxysilane particle formation methodology is relatively underdeveloped. As such, there was no clear indicator as to what precursor would be best to use. Additionally, it was unclear as to what effects using a trialkoxy-precursor might have on the surface chemistry of the resulting particles.

We decided to use the product of olefin metathesis of an allylboronic acid pinacol ester and a vinyl-triethoxysilane as it involved an already established synthesis. The synthesis of this compound was by no means facile, as it could take up to two days at reflux to form. However, the more significant problem, and one that would be seen throughout the studies in the generation of boron-containing trialkoxysilane precursors, was purification. Because the material has three alkoxy groups that are inherently reactive, purification could be problematic. First, they react with water leading to polymerization. Additionally, purification through standard chromatography techniques also proved difficult at times. Packed silica gel used in chromatography contains surface silanols. This means that it is possible for our material to covalently bind to these silanols and become trapped on the column.

Fortunately, we were able to prepare the desired precursor in quantities sufficient to attempt the preparation of the corresponding boron-containing silica nanoparticles. We used a seed growth method that utilized a silicate solution to

provide starting nuclei for silica nanoparticle growth. Conditions employed were similar to the Stöber method (use of NH_4OH as a catalyst in an ethanolic/aqueous solution) with some slight variations. Upon subjecting our new boron-containing precursor to this growth method, a white precipitate formed in solution. After washing and drying of the product as previously discussed, SEM images were recorded to examine the size and shape of the resulting particles.

The SEM images were encouraging (Figure 2.2). The particles were spherical, had relatively high monodispersities, and were below 200 nm in diameter. The IR spectrum was next recorded to check if a boron signal could be observed for the nanoparticles (Figure 2.3). Vinyl-containing particles were also synthesized to act as a reference for the boron-enriched particles. In the IR spectrum of vinyl-containing particles, there were several important features. First is the "silica" region from ~1000-1130 cm^{-1}, which represents the Si-O asymmetric stretches common in a silica particle. At 1411 cm^{-1}, one can see the peaks from the Si-C stretch, while at 1279 cm^{-1}, the Si-O asymmetric deformation can be observed. At 1604 cm^{-1}, the C=C peak can be clearly observed. Finally, one can see the C-H region between 2800-3100 cm^{-1}, and what seems to be a weak –OH stretch at 3436 cm^{-1}. Comparing this to the boron-containing sample, many similar features can be observed. For example, there is a significant "silica" region in the same area as in the vinyl-containing particles. Additionally, there are peaks in the C-H region ranging from 2800-3100 cm^{-1}, which is more complex compared to the vinyl-containing particles. However, there were also some significant changes found in the IR spectrum of boron-containing particles.

The new band found at 1635 cm^{-1} is similar to that of a C=C found in the starting material after metathesis of the allyl-boron and vinyl species. Particularly interesting were the bands at 1400 cm^{-1} and 787 cm^{-1}. As previously discussed, the peak at ~1400 cm^{-1} is common for a B-O stretching vibration while the band found at 787 cm^{-1} could be either a O-B-O stretch or B-C stretch. Overall, these data were very encouraging. We were able to reproducibly synthesize particles of uniform size and shape, with a distinct IR spectrum.

The final form of characterization was elemental analysis via Inductively Coupled Plasma Spectroscopy. Unfortunately, elemental analysis of the nanoparticles did not provide the expected calculated values and did not provide evidence of boron incorporation. In the expected structure, boron should have accounted for ~4.6% of the weight, and would have risen to ~8% if the carbon portion bound to the boron was cleaved. One could argue that silica content could be somewhat higher than expected due to using the silica seeds, but that does account for the observed small amounts of both carbon and boron. We speculate that the boron moiety decomposed under the Stöber conditions, which would explain the elemental analysis results. However, it is likely that some of the starting material participated in the condensation (estimated to account for 1/25 monomer units) which may explain the IR spectra observations.

To further compound the difficulties in generating a boron-containing silica particles, many issues in the preparation of boron-containing starting materials arose. We attempted to prepare a number of new precursors for particle synthesis (see Appendix). However, purification of these compounds was

difficult, often leading to low yields of impure products. Furthermore, when the new starting materials were isolated, they did not produce nanoparticles. Often, the only material recovered was from the silicate seed source, which was confirmed using IR spectroscopy. Thus, we concluded that the proposed boron-containing precursors were not compatible with the condensation conditions. Furthermore, boron-containing trialkoxysilane sources are difficult to synthesize and purify. Thus, we shifted our focus to the internal modification of pre-synthesized particles.

2.3.3 Internal functionalization of vinyl-containing particles

We decided to perform hydroboration inside vinyl-containing ORMOSIL nanoparticles. The benefit of this approach is that the particles are already formed with controlled sizes. However, this type of particle functionalization had never been reported. A vinyl-containing precursor was chosen as we were able to synthesize well-defined particles using this starting material. An SEM image of the vinyl-ORMOSIL particles is shown in Figure 2.4.

2.3.4 Bromination of vinyl ORMOSIL nanoparticles

The bromination of 237 ± 24 nm vinylsilsesquioxane nanoparticles has been performed using the conditions typical for double bond halogenations.[35] The SEM images of vinylsilsesquioxane and of the corresponding brominated nanoparticles are shown in Figure 2.4. There seems to be little difference between the two particle sizes, as the diameter of the brominated nanoparticles

was determined by SEM to be 232 ± 29 nm. There appears to be some agglomeration of the brominated particles, but this may be attributed to the sample preparation. Indeed, the unmodified particles were suspended in water, while the brominated particles were suspended in acetonitrile. The latter disperse very well in acetonitrile, thus leading to a high particle concentration in solution and a thick layer of the particles on the silicon wafer.

The IR spectra of the brominated particles (Figure 2.5) offered the initial insight into the chemical changes that took place inside the vinylsilisesquioxane particles. The stretch found at 960 cm^{-1} for the vinylsilsesquioxane particles[36] disappeared while the stretch at 1602 cm^{-1} was greatly reduced in intensity, suggesting that the double bonds have largely reacted. New bands at 874 and 650 cm^{-1} found for the brominated nanoparticles are within the range characteristic of the C-Br stretch. There is also a splitting of the 760 cm^{-1} band, which could result from an overlap with a C-Br stretch.

The TGA data gathered for the brominated vinylsilsesquioxane nanoparticles show a significant change compared to the unmodified vinylsilsesquioxane nanoparticles (Figure 2.6). The brominated particles show a very significant weight loss around 400 °C, which can be attributed to the presence of the heavy bromine atoms. Indeed, the monomer unit of the vinylsilsesquioxane particle is $SiO_{3/2}C_2H_3$ with molecular weight of 79.1 $g \cdot mol^{-1}$. Since each addition to the double bond introduces two bromine atoms at a molecular weight of 79.9 $g \cdot mol^{-1}$ each, the molecular weight of each monomer triples. This weight change is clearly observed in the TGA data when comparing

the vinylsilsesquioxane particles with weight loss of ~9% to the brominated particles with weight loss of ~60%. Assuming the additional weight loss of the brominated particles originates only from the bromine, the data suggest that nearly all of the vinyl groups in the particle have been reacted. This result is in good agreement with the elemental analysis which reveals that the particles contain 59.85..% bromine by weight. Compared to the maximum of 66 wt%, this suggests that ca. 90% of the double bonds have been brominated. Examining the bromine/carbon ratio leads to a similar conclusion. The maximum theoretical bromine-to-carbon weight ratio for the nanoparticles is 6.6, assuming that every vinyl group has been brominated. The average Br:C ratio obtained by the elemental analysis is 6.83, and is in good agreement with the theoretical calculation and TGA results. Silica and carbon contents are also within a few percent of the values calculated, assuming full incorporation of bromine.

2.3.4.1 Boron-containing ORMOSILs. The incorporation of boron into the nanoparticles has been performed using the standard hydroboration conditions.[35] The SEM images of the boronated particles (Figure 2.4) show little difference compared to the vinylsilsesquioxane particles (Figure 2.4), as the diameter of the former was determined by SEM to be 234 ± 23 nm. The inner pores of the boronated vinylsilsesquioxane nanoparticles were observed using TEM (Figure 2.7). The numerous small nanopores found within the unmodified particles became more difficult to observe after the boronation, suggesting that the pores are closing due to the functionalization.

The first compelling evidence that the hydroboration took place came from the changes in the IR spectrum of the boronated particles (Figure 2.8). The once very sharp and well-defined band found for the vinylsilisesquioxane particles at 1410 cm^{-1}, which is characteristic of the Si-C bonds, has been considerably broadened and became more intense, indicating the presence of the B-O vibration.[36] There is also a new band at 1712 cm^{-1} which is characteristic of the C-B-C stretch. The broad band centered around 3400 cm^{-1} suggests that the initially formed free hydrides of the borohydride have been converted to hydroxyl groups. There is also a considerable broadening around 770 cm^{-1}, which suggests the presence of O-B-O and/or B-C stretch.

The boronated nanoparticles also showed a significant change in TGA (Figure 2.9) compared to that of the vinylsilsesquioxane nanoparticles. However, it is important to note that the nature of the boron within the particles is somewhat ambiguous, which makes interpreting the TGA and elemental analysis data more complicated. It is unlikely that all of the boron atoms within the particles exist as a single boron atom covalently bound to a single carbon atom. It is more likely that some of the boron atoms form cross-linked divalent or trivalent species. Also, the borohydrides that are bound to less than three carbons are likely to be converted to boronic acid groups. This can add considerable weight to the particles, complicating the interpretation of both TGA data and elemental analysis. To establish the degree of hydroboration, the observed carbon and boron weight percent can be compared to that for $SiC_2H_6BO_{7/2}$, a monomer where every vinyl group has been hydroborated once. For this monomer unit, the

boron/carbon weight ratio is 0.45. The actual elemental analysis data give an average boron/carbon ratio of 0.22. Thus, comparing the experimental and theoretical data suggests that ca. one boron atom is attached per two vinyl groups. This method of estimating the boron content does not provide the exact chemical structure of the boronated species (singly boronated vs. cross-linked) but shows that there is a high degree of boronation of the nanoparticles.

For the TGA data (Figure 2.9), a weight loss averaging 21.3% for the boronated samples compared to ca. 9% weight loss for the unmodified vinylsilsesquioxane nanoparticles is observed, giving 12.3 wt% loss corresponding to the boron species. If each of the boron atoms in the nanoparticle was bound to a single vinyl group and carried two hydroxyl groups, each monomer unit would increase in weight from 79 to 122 $g \cdot mol^{-1}$. Using the estimated above boron-to-vinyl group ratio of 1:2, the average new monomer weight would be 100.5 $g \cdot mol^{-1}$ and the corresponding boron species content would be 21.4 wt%. The difference between the predicted and the observed weight percent for the boron species is likely due to some of the boron atoms being bound to more than one vinyl group, thus carrying fewer hydroxyl groups. The weight loss of the boronated particles is less dramatic and more gradual than that of the brominated particles. This may stem from a more gradual breakdown of the diverse species inside the boronated nanoparticles. For example, singly bound boron species may decompose at a different rate than a di- or trisubstituted boron species. Overall, these observations offer yet another

indication of how accessible the vinyl groups inside the nanoparticles are to functionalization.

We estimated the number of boron atoms in a single 237 nm organosilica nanoparticle using straightforward considerations. Assuming that the particle is comprised entirely of vinylsiloxane (which is a fair assumption given the molar ratio of the vinylsiloxane precursor to seed source of about 100:1), the volume of the sphere has been used to calculate the total number of vinyl groups available for the functionalization. Assuming that one half of the vinyl groups became boronated and estimating the density of the nanoparticle as 2 g/cm^3, this number of boron atoms per nanoparticle is ca. 5×10^7, which is within the range suitable for BNCT,[10] as discussed above.

Finally, we studied the boronated particles using CP-MAS ^{11}B NMR (Figure 2.10). There is no signal for boric acid (19.8 ppm) or borohydride (–1.1 ppm) in the spectrum, which confirms that all excess borohydride and the oxidized borohydride has been fully removed from the particles. The two peaks found for the boronated particles are both within the range of the R-B(OH)$_2$ and R-BH-R region. Unfortunately, a more precise peak assignment is not possible since boron can exist in several different forms inside the particles, as discussed above.

2.3.5 Surface modification of boron-containing nanoparticles

The ability to modify the surface of internally functionalized vinylsilsesquioxane nanoparticles is important for several reasons. Such

modifications would allow controlling the wettability of the particles, and would allow attaching a variety of moieties to the nanoparticle surface, ranging from fluorescent dyes to polymers to biological ligands.

A commonly used method for silica surface modification is amination.[23] We demonstrated the feasibility of the amination using a UV-active species. Dansyl chloride by itself does not fluoresce, but when coupled to an amine, will produce a sulfonamide moiety that fluoresces with a bright blue/green color. Thus, brominated and boronated nanoparticles were aminated using APTES. Both aminated and nonaminated nanoparticles were than treated with dansyl chloride. We found that only the amine-modified nanoparticles became fluorescent (Figure 2.11). This result indicates that the surface of the brominated and boronated vinylsilsesquioxane nanoparticles can indeed be aminated allowing further surface modifications, as discussed above.

2.4 Conclusions

In this study, we have successfully synthesized a boron-rich silica nanoparticle. Our initial efforts involved the synthesis using the Stöber method and an activated boronic acid species. However, co-condensation of TEOS and boronic acid species did not occur. We next attempted the condensation of trialkoxysilanes containing covalently bound boron moieties. However, they were difficult to synthesize and unstable, and did not provide the desired nanoparticles. Vinylsilsesquioxane nanoparticles, prepared using a modified Stöber method, have been successfully enriched with boron and bromine and

surface aminated following the enrichment. Our results demonstrate that the vinyl groups inside the nanoparticles are highly accessible for functionalization. The described internal functionalization method provides a new way for catalyst incorporation into silica nanoparticles, for their use as molecular sponges or in molecular recognition experiments, and for the preparation of nanoparticles that could exhibit unique internal and surface properties.

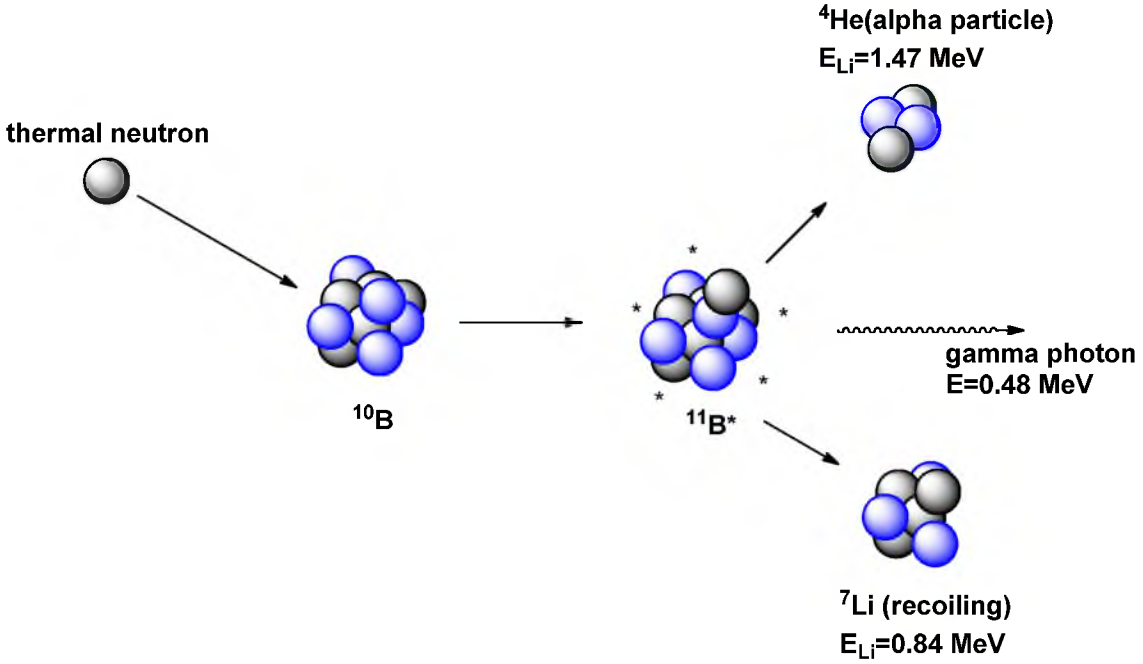

Scheme 2.1: Depiction of a ^{10}B nucleus neutron capture.

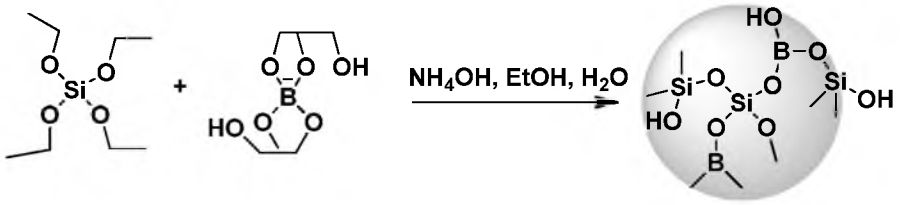

Scheme 2.2: Attempted synthesis of borosilicate particles via activated boronic acid

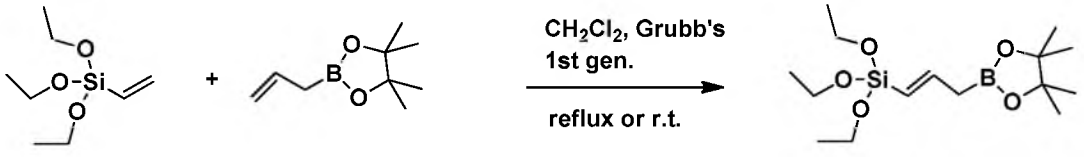

Scheme 2.3: Olefin metathesis of vinyltriethoxysilane and allylboronic acid pinacol ester

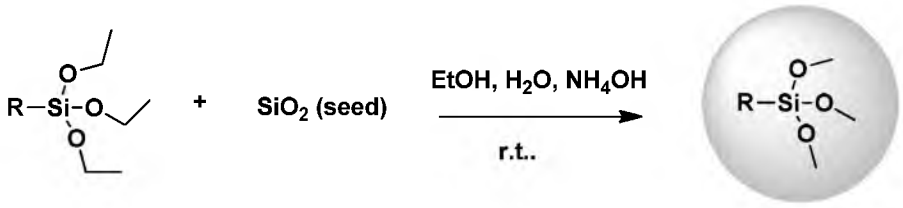

Scheme 2.4: Synthesis of functionally rich-trialkoxysilane particles via SiO_2 seeding method.

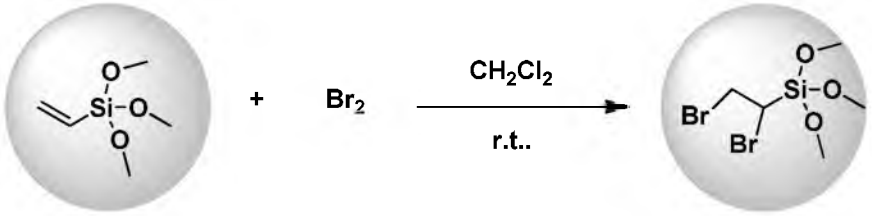

Scheme 2.5: Bromination of vinyl-containing ORMOSIL particles.

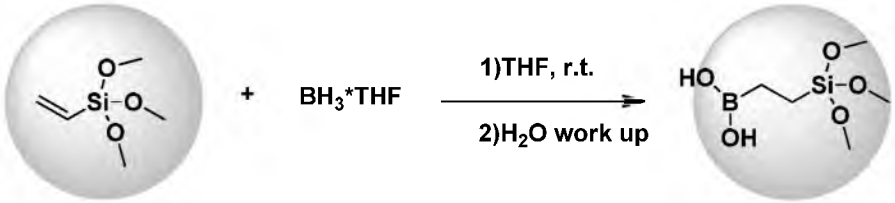

Scheme 2.6: Posthydroboration of vinyl-containing particles.

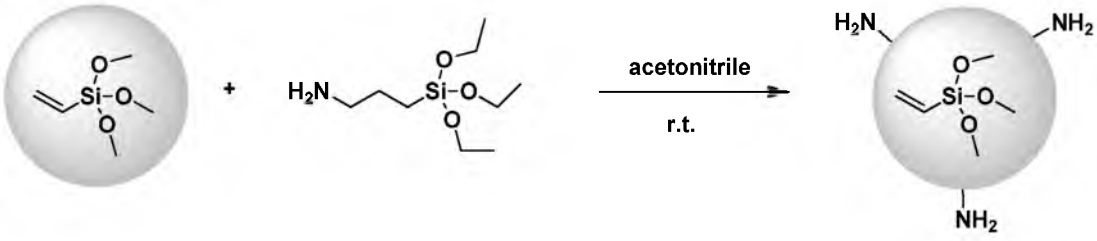

Scheme 2.7: Amination of modified vinyl-containing particles.

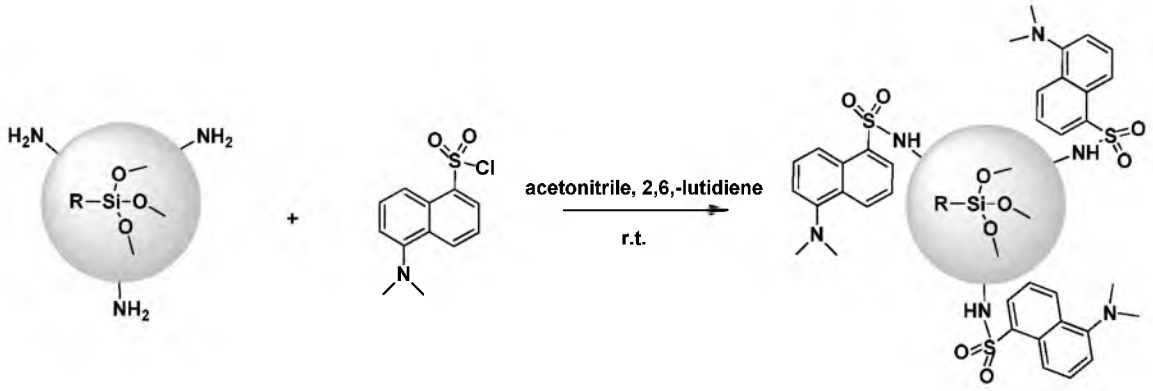

Scheme 2.8: Dansylation of amine-modified ORMOSIL particles

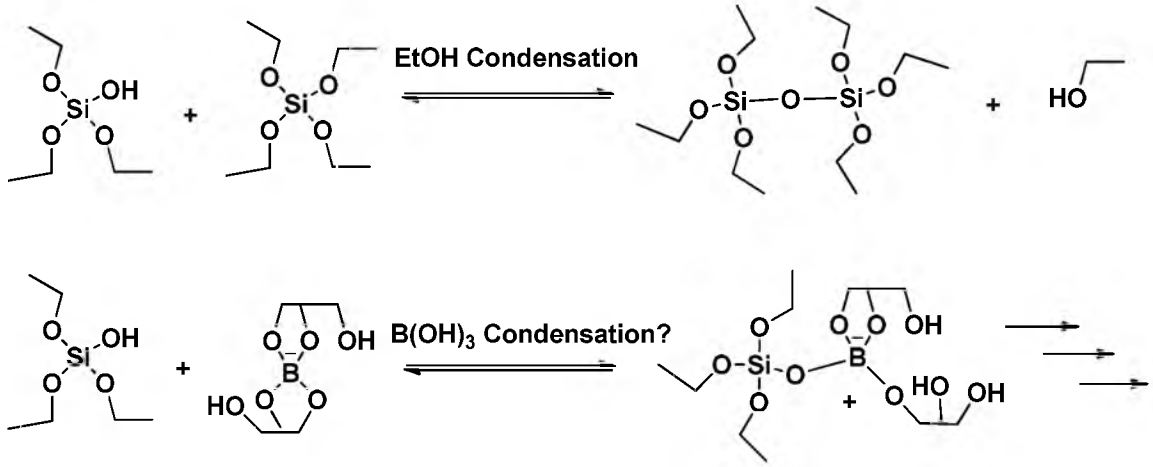

Scheme 2.9: Anticipated condensation reactions with TEOS.

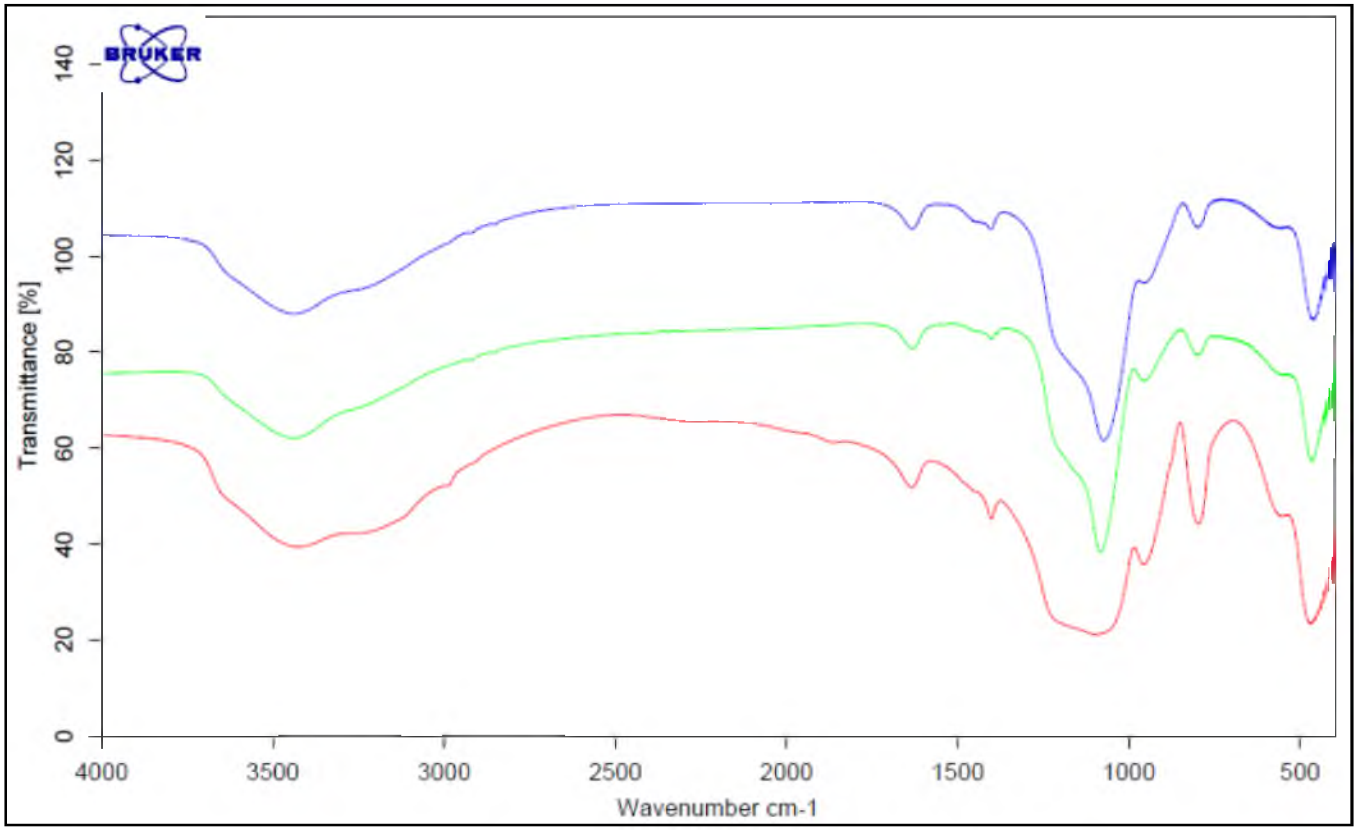

Figure 2.1: IR of proposed borosilicate particles.

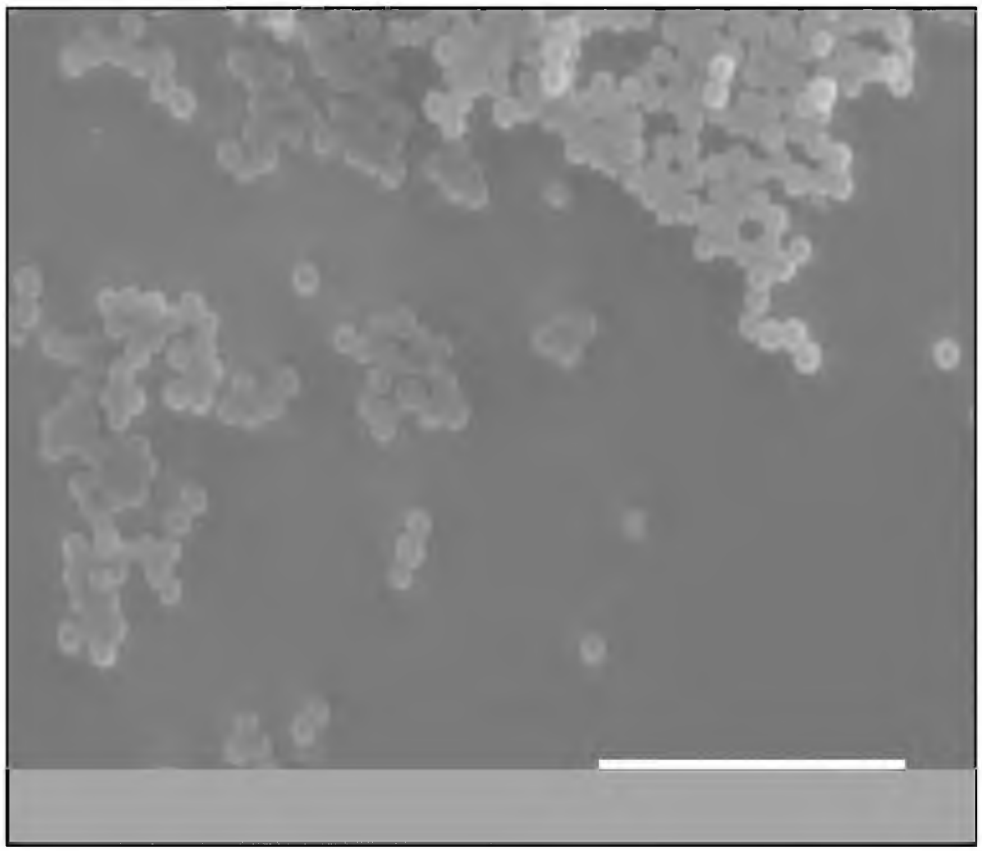

Figure 2.2: SEM image of particles formed with the pinacol borane vinyl silane metathesis. Scale bar is 2 µm.

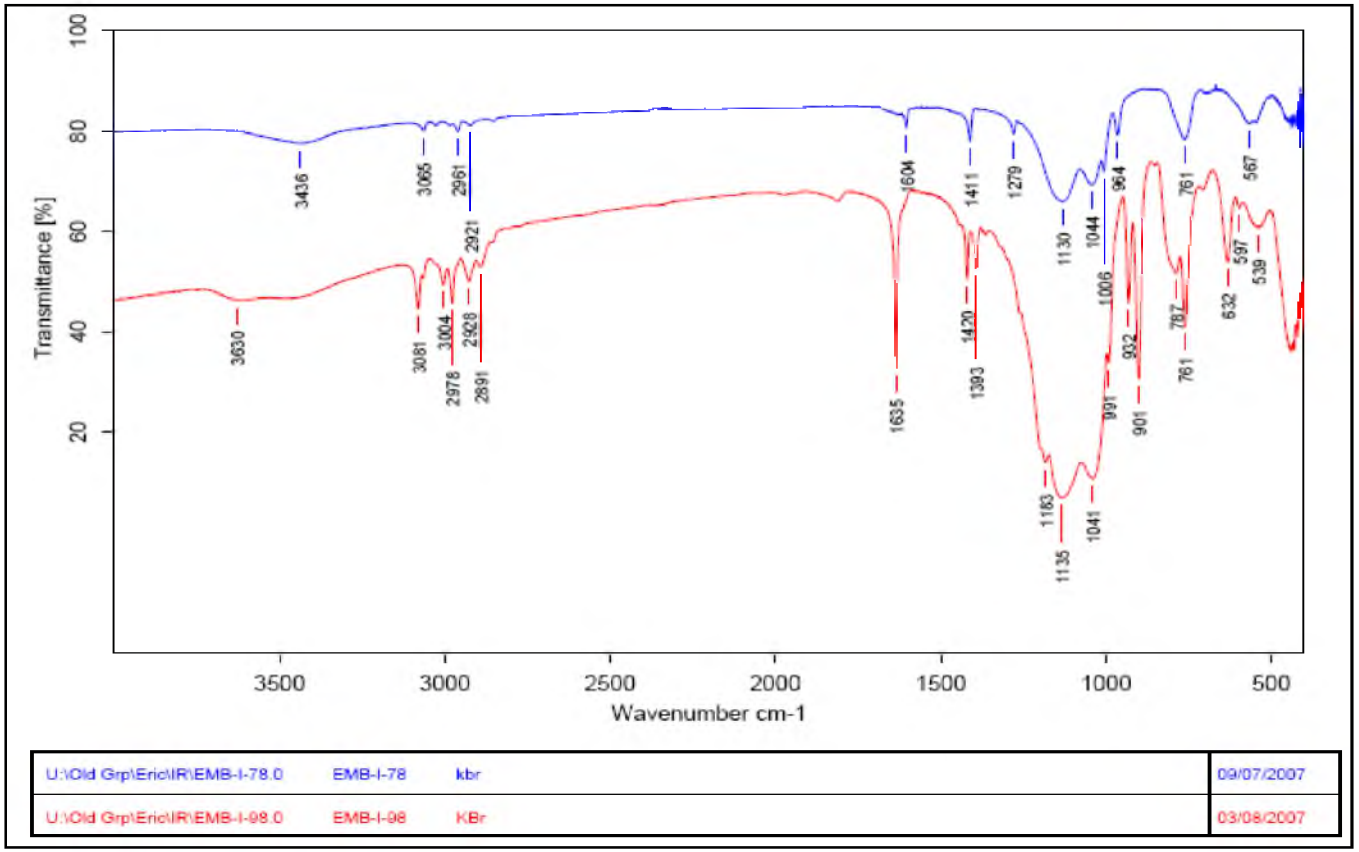

Figure 2.3: IR overlay of vinyl-containing particles and boron-rich particles.

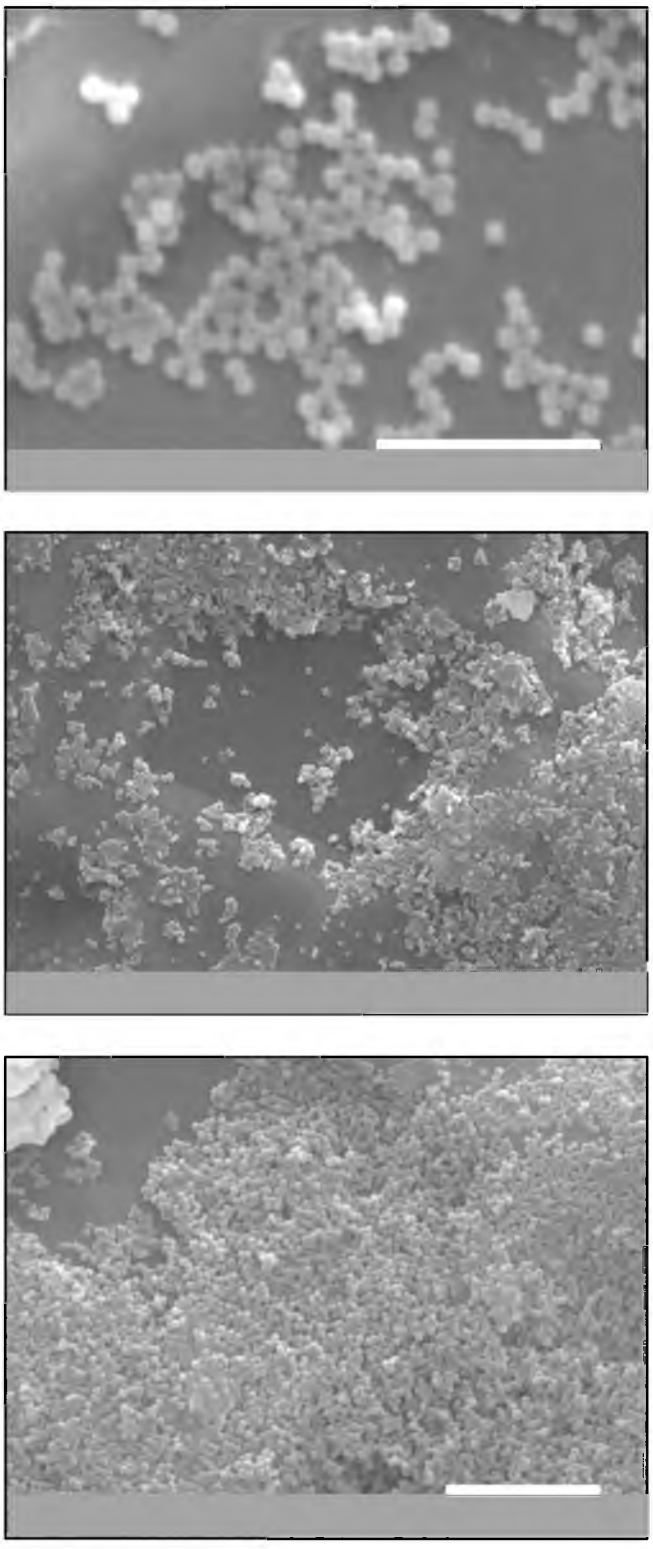

Figure 2.4: SEM images of vinyl (top), brominated (middle), and hydroborated (bottom) ORMOSIL products. Scale bars are 2.5 µm, 10 µm, and 5 µm.

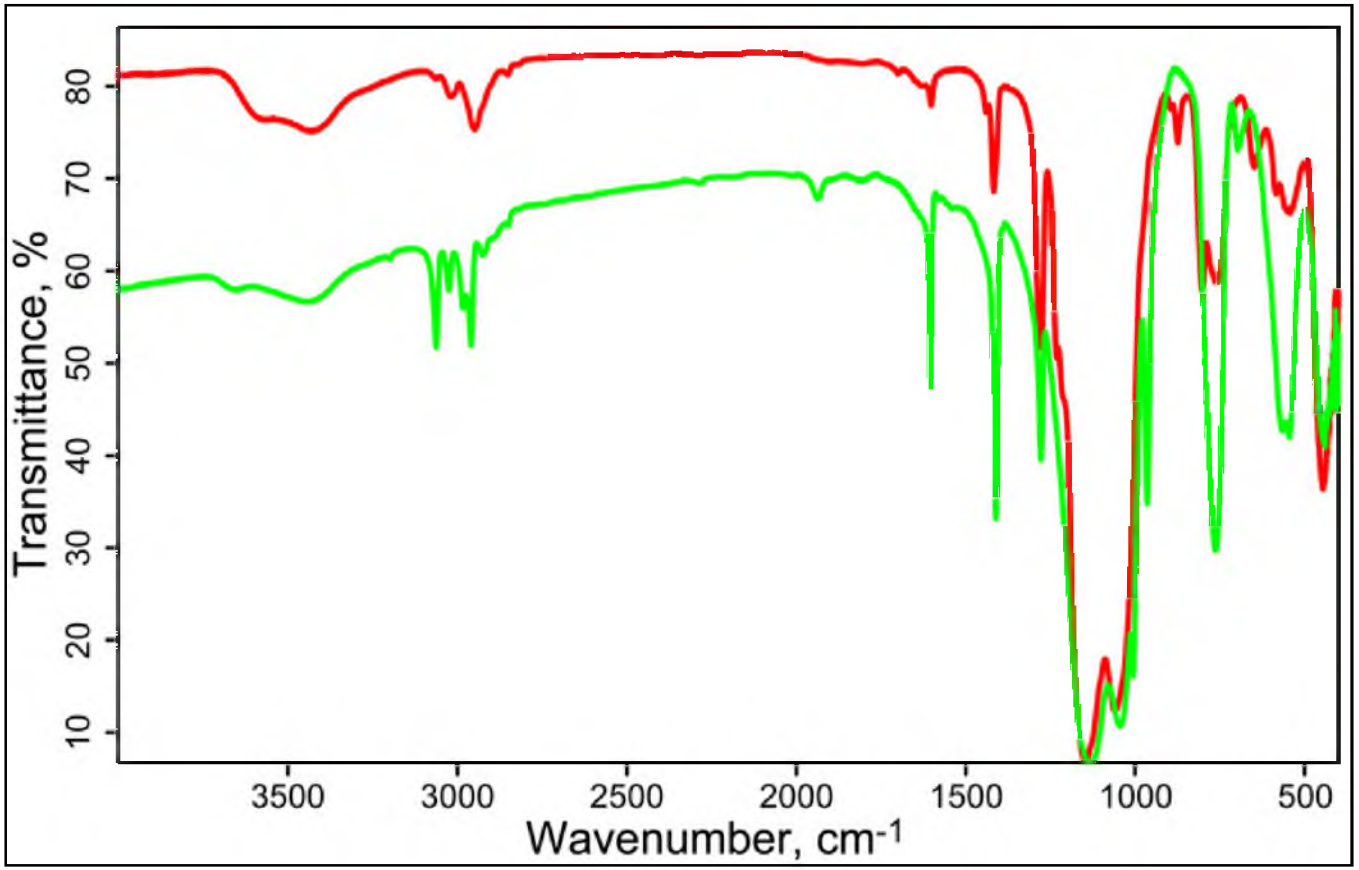

Figure 2.5: IR of vinyl and boronated particles. Vinyl (green), brominated (red).

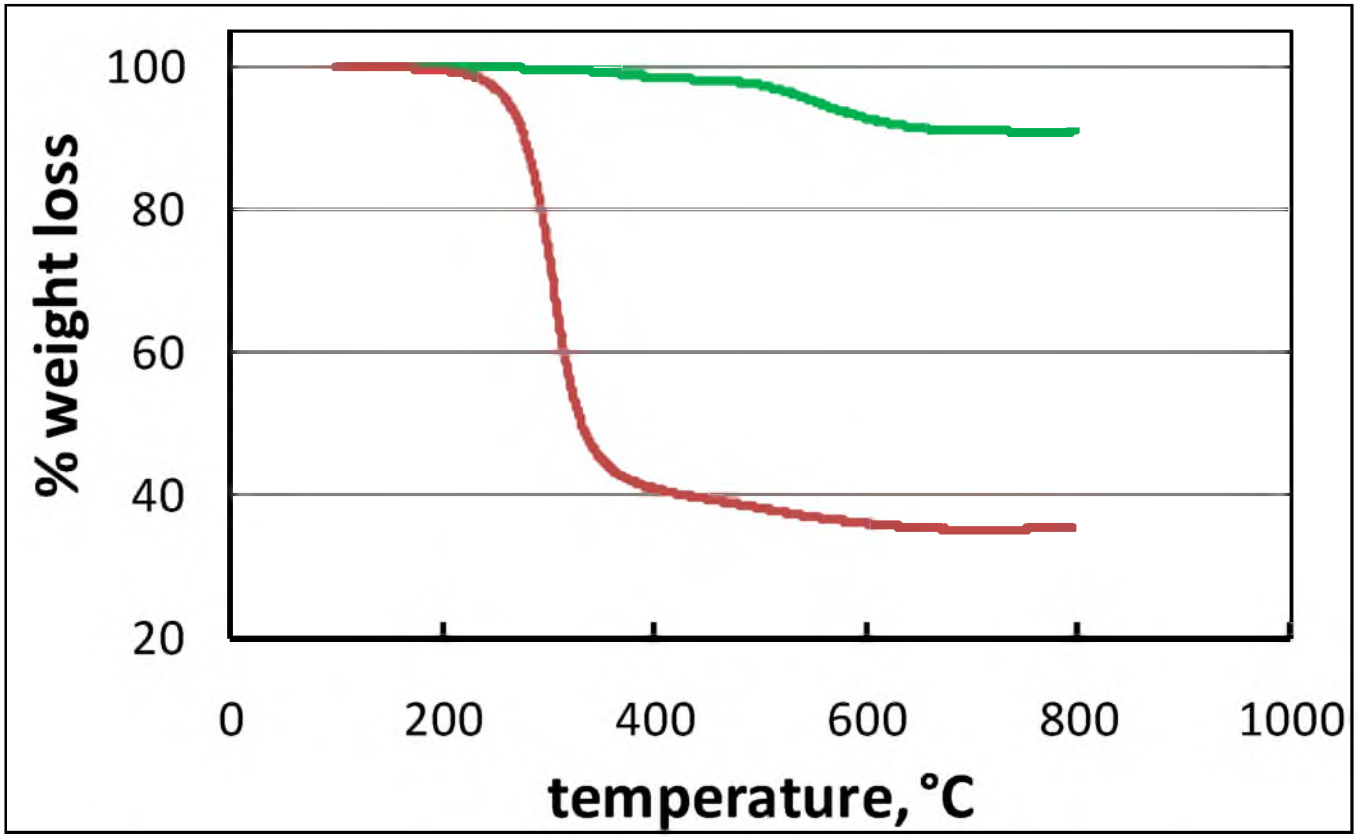

Figure 2.6: TGA data of vinyl ORMOSIL (green) and brominated ORMOSIL (red).

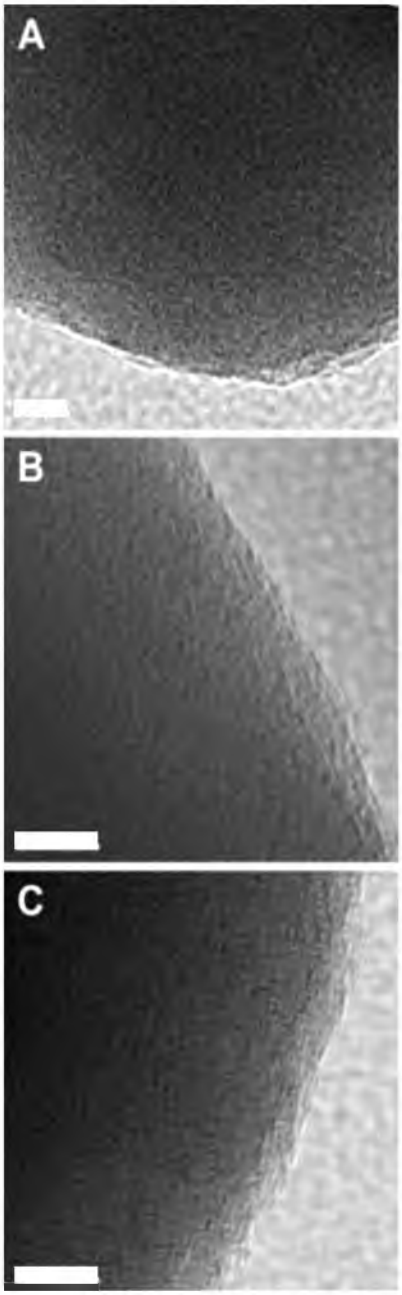

Figure 2.7: HR-TEM images of (A) unmodified, (B) brominated, and (C) boronated vinylsilsesquioxane nanoparticles. Scale bars are 10 nm.

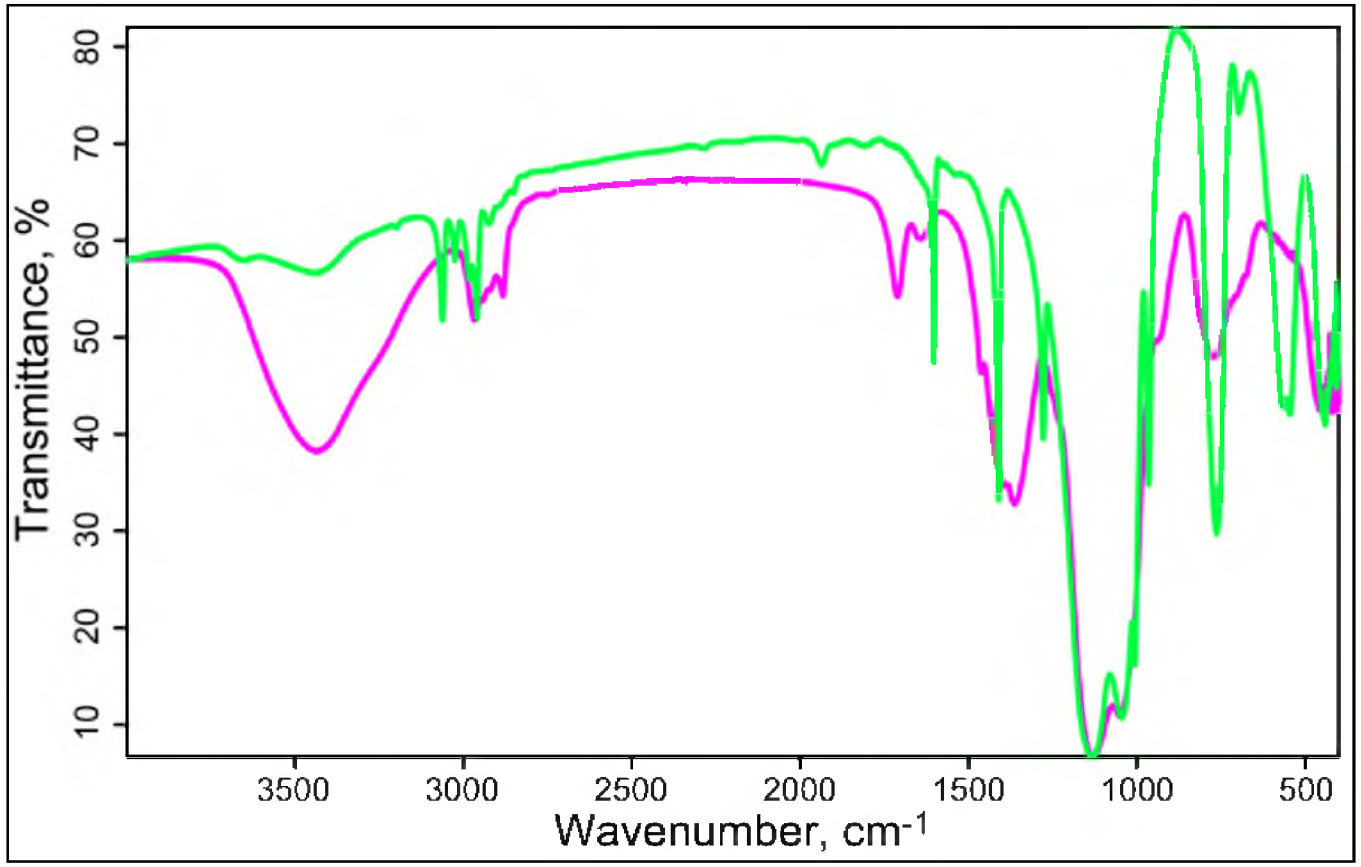

Figure 2.8: IR of hydroborated vinyl ORMOSIL. Green: vinyl, Purple: Hydroborated.

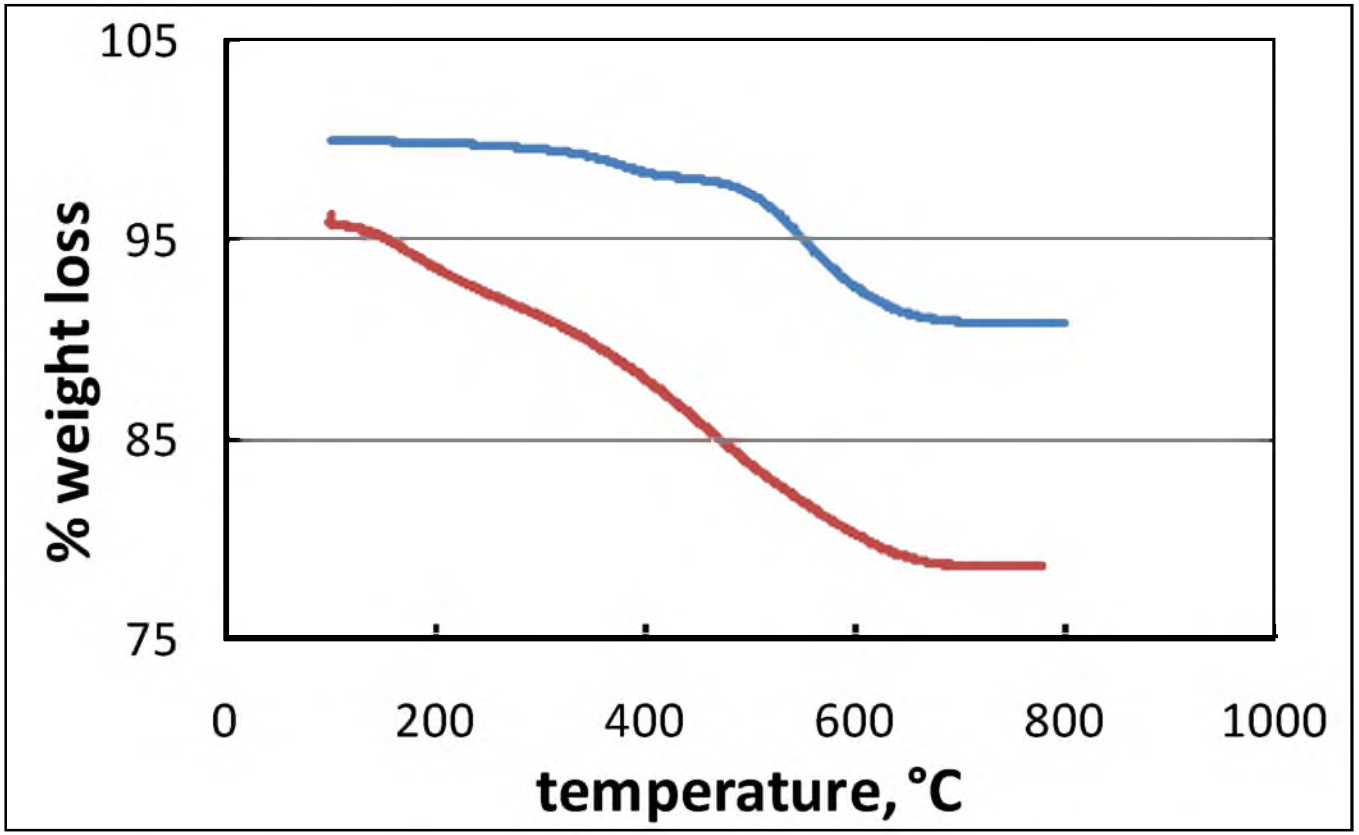

Figure 2.9: TGA of hydroborated ORMOSIL (red) and vinyl-ORMOSIL (blue).

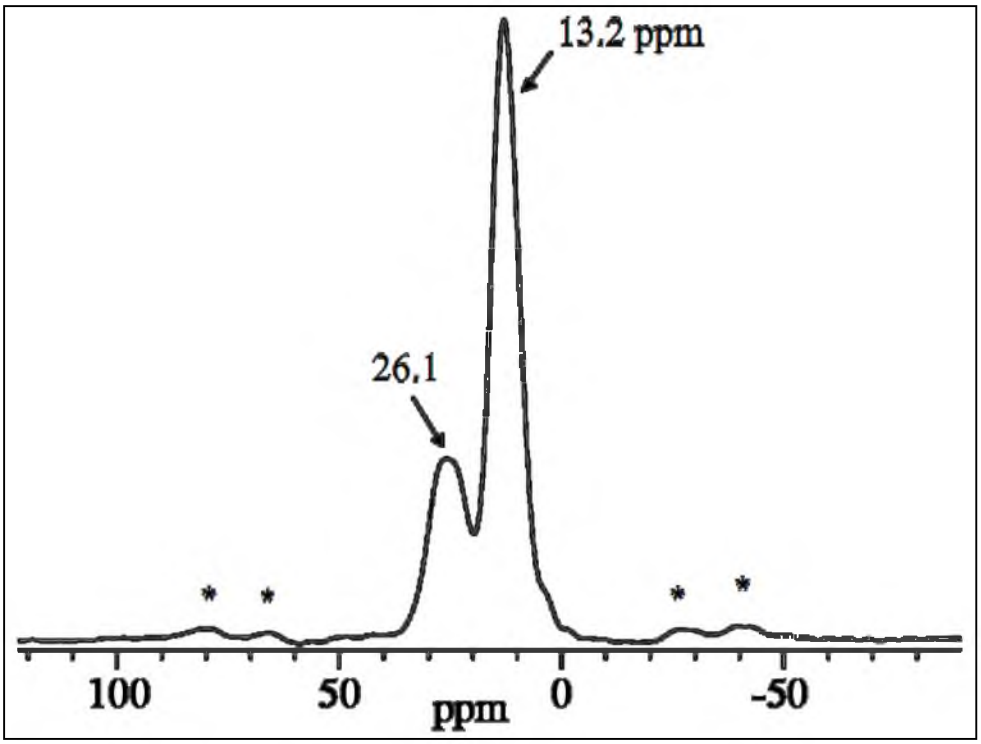

Figure 2.10: CP-MAS 10B NMR spectrum of the boronated vinyl-silane particles. *Spinning artifacts are marked with asterisks.

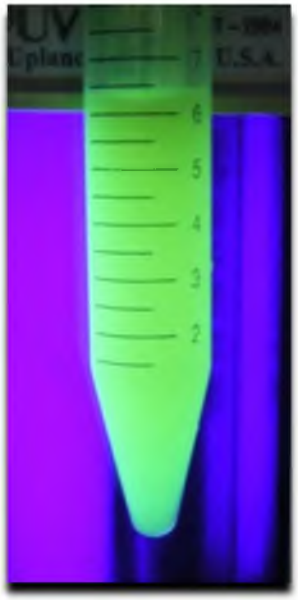

Figure 2.11: Picture of dansylated particles irradiated with long wave UV light.

2.5 References

[1] Krüger, P. G. *Proc. Natl. Acad. Sci. U.S.A.* **1940**, *26*, 181.

[2] Sweet, W. H.; Javid, M. *Trans. Am. Neurol. Assoc.* **1951**, *76*, 60-63.

[3] Conger, A. D.; Giles, N. H., Jr. *Genetics* **1950**, *35*, 397-419.

[4] Javid, M.; Brownell, G. L.; Sweet, W. H. *J. Clin. Invest.* **1952**, *31*, 604-610.

[5] Tolpin, E. I.; Wellum, G. R.; Dohan, F. C., Jr.; Kornblith, P. L.; Zamenhof, R. G. *Oncology* **1975**, *32*, 223-246.

[6] Soloway, A. H.; Hatanaka, H.; Davis, M. A. *J. Med. Chem.* **1967**, *10*, 714-717.

[7] Soloway, A. H.; Tjarks, W.; Barnum, B. A.; Rong, F.-G.; Barth, R. F.; Codogni, I. M.; Wilson, G. J.,*Chem. Rev.* **1998,** *98,* 1515-1562

[8] Belkhou, R.; Abbe´, J.-C.; Pham, P.; Jasner, N.; Sahel, J.; Dreyfus, H.; Moutaouakkil, M.; Massarelli, R. *Amino Acids* **1995**, *8*, 217-229.

[9] Coderre, J. A.; Glass, J. D.; Fairchild, R. G.; Roy, U.; Fand, I. *Cancer Res* **1987**, *47*, 6377-6383.

[10] A. H. Soloway, W. Tjarks, B. A. Barnum, F. G. Rong, R. F. Barth, I. M. Codogni and J. G. Wilson, *Chem. Rev.,* 1998, **98**, 1515.

[11] Mortensen, M. W.; Sørensen, P. G.; Björkdahl, O.; Jensen, M. R.; Gundersen, H. J. G.; Bjørnholm, T. *Applied Radiation and Isotopes,* **2005,** 315-324.

[12] Pickering, A. L.; Mitterbauer, C.; Browning, N. D.; Kaulzlarich, S. M.; Power, P. P. *Chem. Commun.* **2007,** 580-852.

[13] Tsvetkova, I. N.; Shilova, O. A.; Shilov, V. V.; Shaulov, A. Y.; Gomza, Y. P.; Khashkovskii, S. V. *Glass Physics and Chemistry,* **2006,** *32,* 218-227.

[14] Jankowska, M.; Pietraszuk, C.; Marciniec, B.; Zaidlewicz, M. *Synlett.* **2006,** *11,* 1695-1698.

[15] Arkhireeva, A.; Hay, J. N. *J. Mater. Chem.* **2003,** *13,* 3122-3127.

[16] Stockmayer, W. H.; Miller, R. R.; Zeto, R. J. *J. Phys. Chem.* **1961**, *65*, 1076-1077

[17] Pecsok, R. L. *J. Am. Chem. Soc.* **1953**, *75*, 2962-2964.

[18] Newton, M. R.; Bohaty, A. K.; Zhang, Y.; White, H. S.; Zharov, I. *Langmuir* **2006**, *22*, 4429-4432.

[19] White, H.; Murray, R.W. *Anal. Chem.* **1979**, *51*, 236-239.

[20] Hiramatsu, H.; Osterloh, F. E. *Langmuir,* **2003,** *19,* 7003-7011.

[21] Wang, W.; Gu, B.; Hamilton, W. *Journal of Physical Chemistry,* **2003,** *107,* 3400-3404.

[22] Kim, J. M.; Chang, S. M.; Kong, S. M.; Kim, J.; Kim, I.-H.; Kim, K.-S.; Kim, W.-S. *Molecular Crystals and Liquid Crystal,* **2008,** *492,* 245-256.

[23] Onclin, S.; Ravoo, B. J.; Reinhoudt, D. N. *Angew. Chemie Int. Ed.* **2005**, *44*, 6282-6304.

[24] Radhakrishnan, B.; Ranjan, R.; Brittain, W. J. *Soft Matter* **2006**, *2*, 386-396.

[25] Tsubokawa, N. *Polym. J.* **2007**, *39*, 983-1000.

[26] Buchmeiser, M. R. *Adv. Polym. Sci.* **2006**, *197*, 137-171

[27] Burns, A.; Hooisweng, O.; Wiesner, U. *Chem. Soc. Rev.* **2006**, *35*, 1028-1042.

[28] Pasqua, L.; Cundari, S.; Ceresa, C.l Cavaletti, G. *Current Medicinal Chemistry,* **2009,** *16,* 3054-3063.

[29] Knopp, D.; Tang, D.; Niessner, R. *Analytica Chimica, Acts,* **2009,** *647,* 14-30.

[30] Fadeel, B.; Garica-Bennett, A. E. *Advanced Drug Delivery Reviews,* **2010,** *62,* 362-374.

[31] Beganskienė, A.; Sirutkaitis, V.; Kurtinaitienė, M.; Juškėnas, R.; Kareiva, A. *Materials Science,* **2004,** *10(14),* 1392-1320.

[32] http://www.psrc.usm.edu/mauritz/solgel.html

[33] Arkhireeva, A.; Hay, J. N.; Oware, W. *Journal of Non-Crystaline Solids* **2005,** *315,* 1688-1695.

[34] Arkhireeva, A. Hay, J. N.; Lane, J. M.; Manzano, M.; Mater, H.; Oware, W.; Shaw, S. J. *Journal of Sol-Gel Science and Technology,* **2004,** *31,* 31-36.

[35] Smith MB, March J. March's Advanced Organic Chemistry: Reactions,

Mechanisms, and Structure. 5. Wiley-Interscience; 2007. p. 970.

[36] Villegas MA, Navarro JMF. J Mater Sci. 1988;23:2464–2478.

CHAPTER 3

SYNTHESIS AND INTERNAL FUNCTIONALIZATION OF NEW ORGANICALLY MODIFIED SILICA PARTICLE TYPES

3.1 Introduction

Our success in internal bromination and boronation of vinylsilisesquioxane nanoparticles led us to become interested in studying functional ORMOSIL nanoparticles and their internal modification. Organically modified silica (ORMOSIL) materials have been a growing field in materials chemistry since the discovery of the Stöber method[1] for the preparation of well-defined silica colloids. The Stöber silica particles are synthesized by the condensation of tetraorthosilicate (TEOS) in an aqueous/ethanolic media catalyzed by ammonium hydroxide. Under these conditions, TEOS hydrolyzes and cross-links to form spherical particles with sizes that can be easily tuned by altering the amount of ammonia.[1,2] These particles contain predominantly Si-O-Si bonds while their surfaces are covered with silanols (Si-OH) that can be further functionalized. Silica particles containing internal organic groups possess novel interesting properties,[3,4] and thus constitute an attractive synthetic target. One way to incorporate organic groups in silica nanoparticles, i.e., to prepare ORMOSIL

particles, is to use the co-condensation of TEOS and of a trialkoxyorganosilanes.[5] This method yields somewhat porous products incorporating organic functionalities, while maintaining control over the size and morphology of the final product. For example, particles with strong fluorescence have been synthesized by the co-condensation of a fluorescein-bound (3-aminopropyl)triethoxysilane and TEOS under Stöber-like conditions.[6,7] Silica particles can also be synthesized via co-condensation of TEOS and trialkoxyorganosilanes in the presence of a surfactant, providing varying degrees of porosity, and various shapes and morphologies depending on the nature of the surfactant and the organosilane.[8,9,10]

However, the above methods provide only a small degree of organic group incorporation. To solve this problem, ORMOSIL particles would have to be synthesized via condensation of an organosilane as a sole silica source. Arkhireeva and coworkers developed two methods that produced several hydrophobic ORMOSIL products (alkane, vinyl, phenyl). They were able to achieve this by using a micelle-mediated method or by seeding small SiO_2 nanoparticles to control the particle formation.[11,12] Other organic functional groups, such as thiol, phenyl-amine, and drug carry products, have also been incorporated, but require a variety of different conditions to produce.

In the previous chapter, we reported[13] internal bromination and boronation of vinyl-containing ORMOSIL particles[11] leading to materials with potential applications in boron neutron capture therapy. We demonstrated high degrees of internal modification and showed that these materials can be further surface-

modified. Given the promising behavior of these nanoparticles and their potential applications, we wished to examine other ORMOSIL particles containing internal reactive functional groups that could be modified, such as allyl, mercapto, cyano, and isocyanato groups. Our goal was to develop a general synthetic protocol that would easily yield functional ORMOSIL nanoparticles. Additionally, we wanted to examine the reactivity of the organic groups present throughout the particle body. If successful, we would expect two important outcomes: (1) the ability to produce various ORMOSIL particle types from a single particle source and (2) the ability to bind guest species inside the particles. Applications for such nanoparticles include drug delivery and imaging,[14] chemical clean-up,[15,16] and separations[17]. In this chapter, we describe the method we developed for the preparation of ORMOSIL particles and compare our method to other methods defined in the literature. We also describe our methods used to modify the organic functionalities of the new ORMOSIL particles.

3.2 Experimental Section

3.2.1 General

All water-sensitive reactions were conducted under a dry nitrogen atmosphere using oven-dried glassware and anhydrous solvents. Hydroscopic liquids were transferred into reaction vessels via syringe through a rubber septa.

3.2.2 Reagents

All solvents were obtained from Mallinckrodt Baker or Fisher Scientific as reagent grade, except for hexanes and ethyl acetate that were of technical grade. THF was dried by distillation over sodium benzophenone ketyl under nitrogen; dichloromethane was dried by distillation over calcium hydride under nitrogen. Toluene was dried over 4-Å molecular sieves. All other solvents were used without further purification. The following reagents were all used without further purification: tetraethylorthosilicate (+99.999, Alfa Aesar), butenyltriethoxysilane (Gelest), Vinyltrimethoxysilane (Gelest), allyltrimethoxysilane (Gelest), 2-cyanoethylltrimethoxysilane (Gelest), 3-cyanopropyltriethoxysilane (Gelest), 3-iso-cyanatopropyltrimethoxysilane (Gelest), 3-mercaptropropyltriethoxylsilane (Gelest) sodium hydroxide (Mallinchrodt), bromine(99.5%) (Mallinckrodt Chemicals) thionyl chloride(>99%, Aldrich) hydrogen peroxide(30%) (Aldrich), dansyl chloride (>99%, Fluka) and lithium aluminum hydride (97%, AlfaAesar), 2,6-lutidine (99%, Aldrich) silicate solution (27% SiO_2, ~14% NaOH, Aldrich).

3.2.3 Instrumentation

IR spectra were recorded from 400 to 4000 cm^{-1} using a Bruker Tensor 37 IR Spectrophotometer in KBr pellets. Scanning electron microscopy (SEM) images were obtained using a Hitachi S3000N instrument at an accelerating voltage between 20-25 kV. Thermogravimetric Analysis (TGA) measurements were performed using a TA Instruments TGA 2950 Thermogravimetric Analyzer in an open platinum pan. All drop-wise additions were made using a Razel

Syringe pump model A-99 with a 5mL syringe at an addition rate of about 3.8 mL/hr. A Branson 1510 sonicator was used for all sonications

3.2.4 Synthesis

3.2.4.1 Attempted synthesis of alkene-containing ORMOSIL particles via seeding method (Scheme 3.1).[11] An example procedure used to synthesize vinyl ORMOSILs is described. Allyl and butenyl precursors can be substituted for the vinyl precursor. Absolute ethanol (6.30 mL) and ammonium hydroxide (8.40 mL,) were placed into a round-bottom flask and vigorously stirred. To this solution, 0.84 mL (4 mmol) of triethoxyvinylsilane were carefully added in a single portion. In a scintillation vial, 0.25 mL of a 2.2% SiO_2 solution was added to absolute ethanol (12.50 mL). The vial was swirled and briefly sonicated to disperse the solution evenly. This seed solution was added in single portion shortly after the addition of the vinylsiloxane. The reaction flask was then sealed. The solution was stirred overnight, during which time a white precipitate formed. Following sonication, the precipitate was collected by centrifugation and washed several times with water and ethanol to remove ammonia and unreacted triethoxyvinylsilane. SEM images were obtained to determine particle size and shape.

3.2.4.2 Synthesis of alkene-containing ORMOSILs via an emulsion-mediated synthesis (Scheme 3.2).[10] A sample procedure used to synthesize vinyl ORMOSILs is described. Allyl and butenyl precursors can be substituted for the vinyl precursor. Sodium hydroxide (5 mL, 0.028 M) was added to a round-

bottom flask. Benzethonium chloride (0.031 g, 0.07 mmol) was added to the sodium hydroxide solution and stirred for 30 min. to equilibrate the emulsion. Vinyltrimethoxysilane (5.7 mL, 37 mmol) was added to the flask by syringe pump at a rate of 20 mL/hr for ~15 min. The solution was continuously stirred during the addition. The walls were scrapped with a spatula to keep the increasingly thick solution homogeneous. After 4 h. of stirring, the white suspension was dispersed in absolute ethanol and collected via centrifugation. The white precipitate was washed with 1:1 mixtures of ethanol and water and dried to yield a fine white powder. SEM images were obtained to determine particle size and shape if possible.

3.2.4.3 Attempted synthesis of alkene-containing ORMOSIL particles via Stöber-like conditions (Scheme 3.3).[1] A sample procedure used to synthesize vinyl ORMOSILs is described. Allyl and butenyl precursors can be substituted for the vinyl precursor. Vinyltriethoxysilane (0.7 mL, 3.31 mmol), Millipore water (3.07 mL, 0.17 mol), and absolute ethanol (7.8 mL) were added to a round-bottom flask. Ammonia hydroxide (30%, 1.87 mL) was next added to the flask and the contents were stirred. The calculated molarities of the reagents were as follows: Vinyltriethoxysilane 0.24 M, NH_4OH 1.03 M, H_2O 18.0 M. The solution became slightly opaque after 30 min. of stirring. The following day, the products were collected via centrifugation and washed several times with water and ethanol to remove ammonia hydroxide and unreacted vinyltriethoxysilane. SEM images were obtained to determine particle size and shape if possible.

3.2.4.4 General method for the synthesis of ORMOSIL particles (Scheme 3.4). A sample procedure used to synthesize vinyl containing ORMOSIL particles is described. More detailed information on synthesis of the other ORMOSIL particles using similar conditions can be found in Table 3.1. To a round-bottom flask, sodium hydroxide (1.6 mL, 1.1 M) was added. Absolute ethanol (20 mL) and Millipore water (20 mL) was added to the flask and the contents were stirred. Vinyltrimethoxysilane (1.0 mL, 6.5 mmol) was added via a syringe pump at a rate of 3.8mL/h. for ~15 min. Shortly after the addition of the vinyltrimethoxysilane precursor, the solution became turbid, eventually becoming an opaque white. The solution was stirred overnight and the white precipitate was collected the next day via centrifugation. The white product was washed several times with absolute ethanol and with a 1:1 mixture of ethanol:water. The product was dried overnight under a stream of air to yield a fine white powder. SEM images of the powder were obtained to determine particle size and shape. IR samples were prepared by crushing a small amount of the particles with KBr and pressing a tablet in a die set. TGA data were obtained for a neat sample of the dried particles.

3.2.4.5 Bromination of vinyl- and ally-containing ORMOSIL particles (Scheme 3.5). Alkene-containing nanoparticles (50 mg) prepared as described above were dispersed in 12 mL of chloroform in a round-bottom flask and briefly sonicated. Approximately four equivalents of Br_2 (~0.3 mL) were added directly to the particle suspension and the flask was sealed. The solution turned a dark red/orange color. The solution was occasionally shaken and sonicated to assure

homogeneity of the suspension. As alkene functionalities underwent functionalization, the particles began to settle out of solution rapidly, likely due to a dramatic increase in density. The solution was allowed to sit overnight. The following day, the product was collected by centrifugation and washed with $CHCl_3$ until a clear decantate was observed. The particles were than washed three more times to assure complete removal of elemental bromine. The white product was dried over air to yield a fine white powder. TGA, IR, and SEM were obtained as previously described.

3.2.4.6 Reduction of ethylcyano- and propylcyano-containing particles (Scheme 3.6). Cyano-containing nanoparticles (50 mg) prepared as described were dispersed in 15 mL of THF in a 20 mL scintillation vial with a stir bar. The particle solution was dispersed by stirring and sonication. A 10-equivalent excess of $LiAlH_4$ was carefully added to the particle slurry as a powder. The slurry turned grey from the $LiAlH_4$. The vial was briefly purged with nitrogen, capped, and sealed with Teflon tape. After stirring overnight, the smooth particle suspension was carefully quenched with 6 M HCl. Upon addition of the HCl, H_2 gas was rapidly generated. Additional HCl was added to bring the volume up to ~25 mL and allowed to stir overnight. Note: Stirring overnight was important as it fully dissolves the aluminum hydroxide residues. If this is not done, the gelatinous residues left behind from the quenching process are collected with the particles during centrifugation. We have not found a way to separate the particles from the gelatinous precipitate. However, the acid does not seem to degrade the particles in anyway. The particles were collected by centrifugation

and washed with copious amounts of water. A fine white powder is obtained. TGA, IR, and SEM were obtained as previously described.

3.2.4.7 Dansylation of the aminated ORMOSIL particles (Scheme 3.7).[18] The reduced cyno-containing ORMOSIL particles (25 mg) were dispersed in 10 mL acetonitrile in a vial and sonicated. The vial was wrapped in aluminum foil and 10 mg of dansyl chloride were added followed by a few drops of 2,6,-lutidene. The solution was stirred overnight. The resulting precipitate was collected by centrifugation and washed with water and ethanol. An identical reaction was performed for nonreduced cyano-containing particles as a standard. Under UV light, dansylated nanoparticles from the reduced cyano-containing nanoparticles fluoresced bright green/blue, while the dansylated nonreduced cyano-containing nanoparticles did not fluoresce.

3.2.4.8 Oxidative chlorination of thiol-containing particles (Scheme 3.8).[19] Dry acetonitrile (10 mL) was placed in a scintillation vial. H_2O_2 solution (0.24 mL) was added to acetonitrile, followed by a careful drop-wise addition of 0.056 mL of thionyl chloride. After the solution cooled down to room temperature, 50 mg of thiol-containing nanoparticles prepared as described above were added. The final molecular ratios of H_2O_2:$SOCl_2$:particles was 6:2:1. The suspension was briefly sonicated and stirred for 4 h. The particles where collected via centrifugation and washed with acetonitrile. An off-white powder was collected and dried. Some of the precipitate became glassy after drying, presumably due to partial gelling. TGA, IR, and SEM were obtained as described above.

3.3 Results and Discussion

3.3.1 Particle synthesis using methods found in the literature

Our attempts to synthesize new ORMOSIL particles with reactive organic functional groups using previously published methods[1,10,11] were unsuccessful. We first attempted to synthesize vinyl-containing OMROSILs using the seeded method we successfully used in previous experiments (see Chapter 1). However, the SEM images obtained from the vinyl-containing products showed that the particles aggregated and were no longer uniform in size and shape (Figures 3.1 and 3.2). Allyltrimethoxysilane and butenyltriethoxysilane were also used in an attempt to generate new alkene-rich ORMOSILs using the same seeded growth method. However, products were either sticky residues or rubbery films and showed no sign of individual particle growth. We hypothesize that the change in particle shape and morphology was due to the new silicate seed solution that was used to induce particle growth. The manufacturer of the silicate solution (Sigma-Aldrich) increased the concentration of sodium hydroxide used to stabilize the solution. The increased sodium hydroxide could alter the reaction rate of the condensation reaction and as a result change the particles' size and shape.

We next decided to use an emulsion-mediated method to synthesize our products (Scheme 3.2).[10] In an emulsion-mediated method, a surfactant is stirred in solution in order to generate micelles. When the silane precursor is mixed into the micellar solution, the silane enters the core of the micelle and will undergo condensation to form particles. The size of the particle is determined by

the size of the micelle. Smaller micelles yield smaller particles and larger micelles yield larger particles. In the literature, this method was used to successfully synthesize a variety of hydrophobic ORMOSIL particles, including vinyl, ethyl, and benzyl, while maintaining control of the diameters of product.[10] However, our attempts to synthesize alkene-containing ORMOSILs using the emulsion method were unsuccessful. The SEM images obtained for the vinyl-containing products revealed materials that were fully aggregated, partially aggregated, and nonaggregated particles within a single product (Figures 3.3 and 3.4).

Unfortunately, the nonaggregated products were observed in small quantities. Allyltrimethoxysilane and butenyltriethoxysilane were also used in the emulsion method. However, phase separation occurred between the aqueous solution and the silane precursor, suggesting the silane was poorly solvated. In the event a product was collected from allyl and butenyl solutions, the products were typically sticky and viscous. It was clear that the method was unfit for the synthesis of OMROSILs containing longer alkenes. However, it remains unclear why the emulsion method was unsuccessful for the vinyl precursor. It may have been due to the discrepancies between the published methods.[10,20]

Finally, the Stöber method was used to synthesize the vinyl-, allyl-, and butenyl-containing ORMOSILs by substitution of tetraethylorthosilicate with the alkene-containing starting materials (Scheme 3.3). However, the Stöber method did not generate a colloidal product. Sticky residues and rubbery materials much

like those seen in the previously discussed experiments were the only observable products. While this method formed pure silica nanoparticles if tetraethylorthosilicate was used, simple substitution of the silica precursor was inadequate to generate the desired ORMOSIL products.

After we were unsuccessful in generating new ORMOSIL products utilizing literary methods, we realized the literature was too specialized to generate our materials. It was at this point where we began developing our own unique method to generate the products previous methods failed to form.

3.3.2 Particle synthesis utilizing a new method

As we began to test different reaction conditions to generate ORMOSIL products using our own method, we observed early on that water and ethanol content and ratio play an important role in the outcome of the ORMOSIL particle products. We found three factors that require consideration when optimizing these reaction conditions: (i) the amount of ethanol necessary for the starting material dissolution in water; (ii) the amount of water necessary to achieve efficient starting material hydrolysis; (iii) the overall amount of the solvent necessary to avoid aggregation.

3.3.3 Effects of ethanol and water on particle formation

Ethanol plays an important role in helping to dissolve the silica precursors and thus facilitate the condensation process. If ethanol is not added, a phase separation of the starting material and water may result. Additionally, if the

ethanol content is too low, significant aggregation may be observed. The ethanol concentration was chosen such that homogeneous reaction mixtures were initially formed and nonaggregated suspensions persisted until the products were collected. For example, allyl- and vinyl-containing particles became largely aggregated in water. We hypothesized the particles were strongly hydrophobic and thus poorly solvated by water. Therefore, we increased the ethanol concentration incrementally and were able to obtain a homogeneous suspension in 1:1 mixture of ethanol/water (Table 3.1). Similarly, the mercaptopropyl-containing particles benefited from additional ethanol in terms of stability and homogeneity of the products. Both of the cyano-containing particles did not require a substantial addition of ethanol as the suspensions remained stable and agglomeration did not occur. Isocyanatopropyl-containing particles had to be prepared in pure ethanol because any addition of water beyond that present in NaOH led to gelation of the solution.

Water also plays an important role in the formation of these nanoparticles. If the water content is too low, hydrolysis is slow, and particle formation is either very slow or absent altogether. On the other hand, if water content is too high, the particles cannot be efficiently suspended in solution and significant aggregation may occur. For example, both of the cyano-containing particles formed in small quantities without the addition of water, but as the water concentration was incrementally increased, so did the amount of the particles that was collected. However, for particles that tend to aggregate in solution, high water concentrations were detrimental. Therefore, with particularly hydrophobic

particles, larger additions of ethanol were required to assure suspension of the product. The required water addition was tested by adding small aliquots of water to the reaction mixtures. When a homogeneous reaction mixture that rapidly became cloudy was obtained, the reaction conditions were considered acceptable.

The accepted ethanol and water amounts for the synthesis of each particle type are summarized in Table 3.1. It is possible that ethanol and water content and ratio could affect the size and shape of the final products as well, but in the present work, we decided to use our water:ethanol conditions and explore how the sodium hydroxide concentration affects the resulting materials. The relationship between the ethanol and water content and the particle size and shape will be studied at a later date.

3.3.4 Sodium hydroxide effect on particle sizes

In order to optimize the quantity of sodium hydroxide added, we started with the preparation of allyl-containing particles using low NaOH concentrations ranging from 0.03-0.1 M, as has been commonly used.[11] At these concentrations gel-like products were obtained. We hypothesized that at low NaOH concentrations, longer silica chains are formed due to few nuclei in solution, and thus gels are formed more readily. Conversely, if NaOH concentrations were too high (3-5 M), no particle formation was observed. We hypothesized that if the base concentration is too high, the silica precursor may rapidly ionize such that cross-linking would not occur due to electrostatic repulsion and lack of monomer

for nuclei growth. Additionally, we hypothesized that if the NaOH concentration is too high, etching and particle dissolution may occur. This led us to the more effective NaOH concentrations, 0.5-1.5 M, that were useful for all of the novel ORMOSIL particles reported herein.

In addition to controlling the formation of the nanoparticles, sodium hydroxide concentration affects the particle size within the 0.5-1.5 M range of concentration. The particle diameters as a function of NaOH concentration are given in Table 3.2. Increasing the concentration of NaOH typically yields particles that are smaller in diameter, and vice versa. This may be explained by assuming that at lower concentration of sodium hydroxide in solution, the particles grow larger as their surfaces carry a smaller negative charge, thus allowing them to ripen. It may also be due to the smaller number of activated nuclei formed in solution and generating fewer individual particles with larger diameters. Conversely, higher concentrations of NaOH in solution would generate a large population of growing nuclei and thus a large number of smaller particles. Additionally, partial etching of the products at higher concentrations of sodium hydroxide may also reduce the particle size.[21]

3.3.5 Nanoparticle size and morphology

As can be clearly seen in the SEM images (Figure 3.5), our conditions generate highly monodisperse, uniformly shaped, and spherical particles containing vinyl, allyl, thiol, cyanoethyl, and cyanopropyl functional groups. On the other hand, the thiol- and isocyanato-containing nanoparticles prepared at

lower NaOH concentration were highly polydisperse with a large population of both large and small particles. The size and polydispersity of thiol-containing particles decreased as the base concentration increased. The iscocyanato product was particularly polydisperse and formed nonspherical particles (Figure 3.5) at lower NaOH concentrations, and even under the best conditions, particle size and shape were not as consistent as the other products described above.

Particles did not show a change in size and shape after additional modification. This suggests the particles are porous enough for additional modification while still maintaining their initial structural integrity. However, the conditions we described were not subject to heat or other harsh conditions, which may alter the integrity of the products. Thiol-containing particles did seem to agglomerate to some extent after the modification, but shape and size remained the same. This may be due to either partial gelling after modification or partial loss in structural integrity after addition of thionyl chloride.

Interestingly, the 3-cyanopropyltriethoxysilane precursor formed very different structures when higher concentrations of sodium hydroxide were used with slightly lower water concentrations. The particles changed from spherical and submicron in diameter at 0.8-1.2 M concentration of NaOH to highly textured and large (>10 μm) particles at about 1.2 M concentration of NaOH (Figure 3.6). Presently, we are not certain why small changes in the amount of base in solution cause such a drastic change in shape. Indeed, to form silica structures with such an unusual shape typically requires a templating agent.[22] These products are currently undergoing further investigation.

3.3.6 Particle composition and reactivity: vinyl- and allyl-containing particles and products of their bromination

The products containing the vinyl and allyl functionalities throughout the particle bodies possessed many similarities. IR spectra on both of these products were collected and compared (Figures 3.7 and 3.8). The characteristic Si-O-Si absorptions at about 1130 cm^{-1} and 1030 cm^{-1} are typical of a silica-based particle and can be found in all of our product spectra. What we believe to be a series of C-H stretching vibrations can be found between 2800 cm^{-1} and 3000 cm^{-1}. Another characteristic peak can be found around 1250 cm^{-1}. This vibration is likely that of a Si-C stretch and is also common amongst the products. Most notable of the vinyl- and allyl-containing particles is the strong absorption found near 1600 cm^{-1}, representing the C=C stretching vibration and evidence of the preservation of the organic handle throughout our initial reaction conditions. Upon bromination, the IR spectrum of the products undergoes a considerable change. The strong absorbance found at 1600 cm^{-1} for both starting materials essentially disappears, suggesting loss of the double bond upon addition of the bromine. Additionally, there is a new peak found at ~850 cm^{-1}, which is in the range of a C-Br stretch.

TGA data (Figures 3.9 and 3.10) provided further insight into the degree of bromination of the C=C bond. Vinyl-containing particles showed ca. 8% weight loss. The allyl-containing particles showed a weight loss of 18 wt%. These values are smaller than expected (assuming complete combustion of the organic ligands and no additional reactivity in the TGA environment). Any lingering organic residues, ash, or incomplete combustion products will yield a lower

weight loss. However, these data are consistent with our previous results for vinyl-containing particles prepared in a different manner, whose composition was confirmed by elemental analysis.[16] Upon bromination, a significant weight loss is observed from both products. The brominated vinyl-containing particles lose 56% of their weight, while the brominated allyl-containing particles lose 66% of their weight. If we assume the weight loss comes from only the bromine addition, we calculate a near quantitative conversion of the alkene functionality to the brominated product. Again, this is consistent with our previous work. These data clearly demonstrate the accessibility of the double bond found within the particle bodies, and that they are prone to additional modification.

3.3.7 Particle composition and reactivity: Cyano-containing nanoparticles and products of their reduction

Like the previously described alkene-containing products, the cyano-containing products shared many of the same characteristics. For example, the IR spectra collected had several distinct characteristics (Figures 3.11 and 3.12). The most important IR peak observed is the band found at ~2250 cm^{-1}. This band represents the -C≡N stretch, and confirms the preservation of the cyano-organic functionalities during initial particle synthesis. Reduction of the cyano groups results in expected changes in the IR spectrum. The two most notable changes include the reduced intensity of the -C≡N stretch found at 2250 cm^{-1}, suggesting that cyanos groups have been reduced to amine groups. Additionally, several new peaks are observed around ~1600-1700 cm^{-1}. This is likely representative of the N-H bend and a partial reduction of the -C≡N to

-C=N-H. Additionally, there is increased signal intensity found in the 3400 cm^{-1} region, which offers further evidence of the reduction chemistry.

TGA data were also collected on the cyno-containing particles and their reduced products. The cyanoethyl-containing particles lost ~30% of their weight while particles containing the slightly longer cyanopropyl functionality lost ~40% of their weight (Appendix A). The reduced nanoparticles showed little or no additional weight loss. Reduction chemistry adds very little molecular weight to the product, and as a result, TGA data were not useful in further characterizing these particles. However, we conducted a simple test that demonstrates the formation of amine groups upon reduction of cyano-containing nanoparticles. Dansyl chloride fluoresces brightly upon covalent attachment to an amine. As described above, the reduced cyano-containing particles and the unmodified cyano-containing particles were both exposed to dansylation conditions. Only the reduced product fluoresced (Figure 3.13). No signs of chemical leeching were observed. The nonreduced starting material showed no fluorescence. No significant change in IR or TGA was observed after the dansylation, even under conditions with higher concentrations of dansyl chloride. The dansyl chloride that covalently attached to the particle surface may have clogged the pores of the particle and thus prevented further functionalization. Thus, the absolute extent of reduction for cyano-containing nanoparticles is presently not determined. It appears that the 3-cyanopropyl particles undergo a higher degree of modification based on the IR spectra, where the cyano peak is more diminished and the amine peaks are amplified. These particles could be of considerable importance

given the versatile reactivity of the amine groups and difficulty in preparing amine-containing silica nanoparticles using other techniques.

3.3.8 Particle composition and reactivity: Thiol-containing particles and products of their oxidative chlorination

The IR spectra for the thiol-containing particles possess many of the same characteristics discussed above (Figure 3.14). The important peaks found for these particles include a stretching vibration of S-H at ~2552 cm^{-1}. Additionally, a peak found at 694 cm^{-1} is likely due to the C-S stretching vibration. Upon oxidative chlorination of the thiol-containing particles with thionyl chloride, the peak at 2552 cm^{-1} disappears, and a new peak is found at 1374 cm^{-1}. The new peak can be attributed to S=O asymmetric stretch, commonly found in sulfonyl chlorides or sulfates. The disappearance of the S-H suggests conversion to the sulfonyl chloride.

TGA was also useful in analyzing these nanoparticles as oxidative chlorination adds a substantial amount of weight to the starting material (Figure 3.5). Thiol-containing particles showed weight loss of ~44 wt%. The particles that underwent oxidative chlorination showed weight loss of about ~55 wt%. Assuming that all of the additional weight loss resulted from the modification of the thiol groups in the starting particles, we calculate the ca. 77% conversion of these groups into sulfonyl chloride groups. If higher concentrations of the thionyl chloride and hydrogen peroxide are used to convert the thiol functionality, larger weight losses are observed by TGA. This would suggest an increased conversion of the thiol. However, recovery of the product decreases. This may

be due to the thionyl chloride reacting with the crosslinked silica network and causing the particle to dissolve.

It is important to note that silanols on the surface of silica particles have been reacted with thionyl chloride for Si-Cl bonds.[23] However, it is unlikely that the weight loss observed from the TGA data is from this surface modification. In our experience, surface functionalizations rarely show significant weight loss unless the modification is a polymer.

3.3.9 Particle composition and reactivity: Isocyanate-containing particles

The IR spectrum of the particles prepared using the isocyanate-containing precursor was less conclusive (Figure 3.16). The asymmetric stretch typically found at ~2250 cm^{-1} for the N=C=O group which was observed for the starting material is absent for these particles, which clearly indicates that isocyanate groups undergo a transformation. One possibility is the decarbonylation through hydroxide addition to yield CO_2 and a terminal amine. However, a carbonyl-like vibration is present at 1689 cm^{-1}. It may correspond to such groups as secondary amide, urea, or carbamic acid. While we are unable to ascertain the exact structure of these groups, it is most likely a carbamic acid anion or a urethane-like structure, considering the alkali preparation conditions in the presence of both ethanol and water. The very strong peak at 1469 cm^{-1} may represent an amide-like structure of a urea.

TGA data of the isocyanate-containing particles yielded some very interesting results. The material showed the weight loss of ~50 wt% (Appendix

A). If the isocyanate group did convert to an amine under our conditions, the molecular weight of the silica/organic monomer would decrease from 136 to 110 Da, much closer to that of the ethylcyano group, and one would expect a similar weight loss for these two particle types. Instead, we observed a significantly higher weight loss for isocyanate-containing materials, suggesting at least a partial preservation of the isocyanate moiety, or that of a urea-like or a carbamic-like functionality, as discussed above.

3.4 Conclusions

In this chapter, we described a simple set of conditions to prepare ORMOSIL particles with a variety of internal organic functional groups. We described general considerations for ORMOSIL particle formation, based on the chemical nature of the starting organotrialkoxysilane (hydrophobicity, hydrophilicity, etc.) We also demonstrated that similar precursors provide common chemical trends. For example, both the allyl- and vinyl-containing trialkoxysilane precursors require larger amounts of ethanol to prevent agglomeration and to yield well-defined particles, while the cyano-containing precursors yield particles without the need for a large amount of ethanol. Through our study, were able to make three consistent observations: (i) a higher base concentration results in larger populations of particles that are smaller in size; (ii) a lower base concentration or higher water concentration can improve yields; (iii) the formation of a smooth and nonaggregated suspension often results in spherical and submicron particles.

We also demonstrated that organic functional groups present throughout the particle body are accessible and reactive. Also, one functional particle type may be used as a precursor for multiple nanoparticles via the internal functional group transformations. This suggests that ORMOSIL nanoparticles could be of considerable use in a variety of fields.

Future work includes the continuing effort to develop new functional ORMOSIL particle types. We are also testing these new materials as a stationary phase in solid phase extractions. Finally, we are developing methods that will yield particles with multiple functionalities by co-condensation of different organically modified trialkoxysilanes.

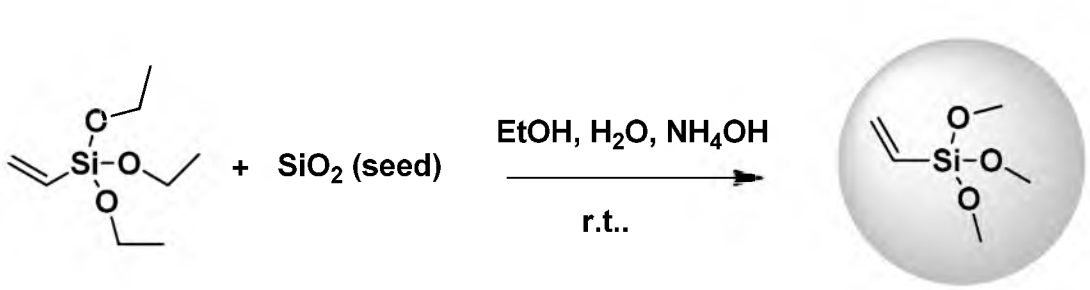

Scheme 3.1: Attempted synthesis of alkene-containing ORMOSIL particles via seeding method

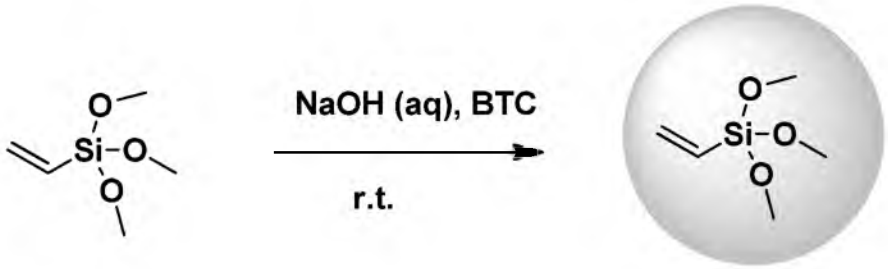

Scheme 3.2: Synthesis of alkene-containing ORMOSILs via an emulsion-mediated synthesis

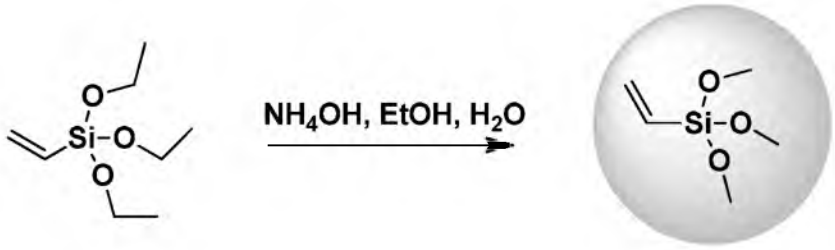

Scheme 3.3: Attempted synthesis of alkene-containing ORMOSIL particles via Stöber like conditions

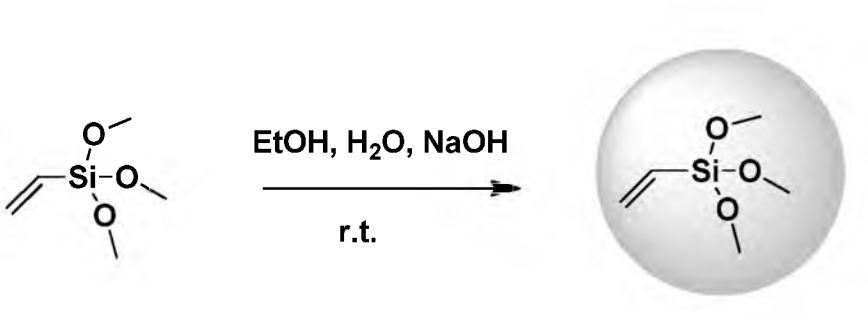

Scheme 3.4: General method for the synthesis of ORMOSIL particles

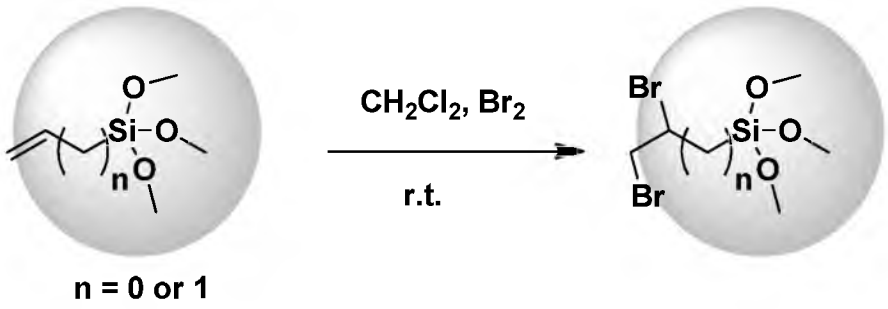

Scheme 3.5: Bromination of vinyl- and ally-containing ORMOSIL particles

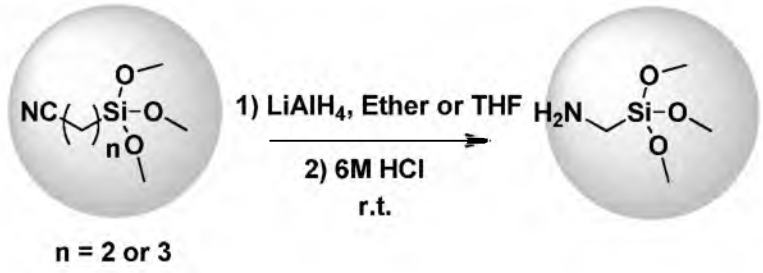

Scheme 3.6: Reduction of ethylcyano- and propylcyano-containing particles.

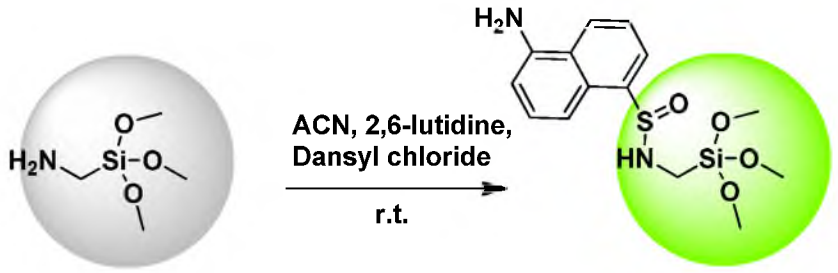

Scheme 3.7: Dansylation of the aminated ORMOSIL particles

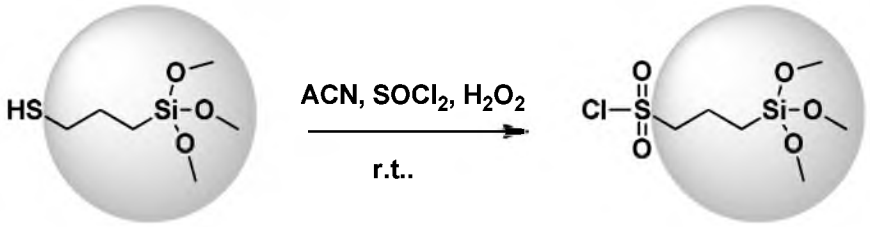

Scheme 3.8: Oxidative chlorination of thiol-containing particles

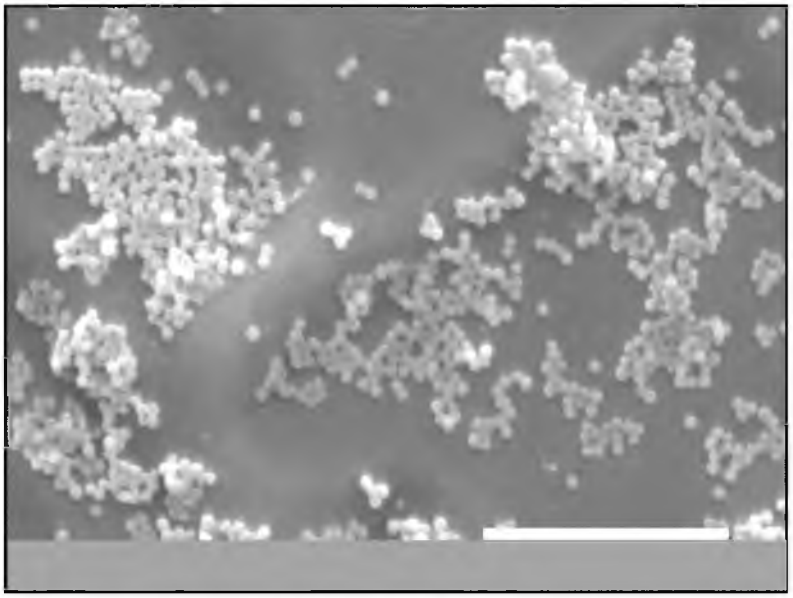

Figure 3.1: Previously prepared vinyl ORMOSIL products. Scale bar is 5 µm.

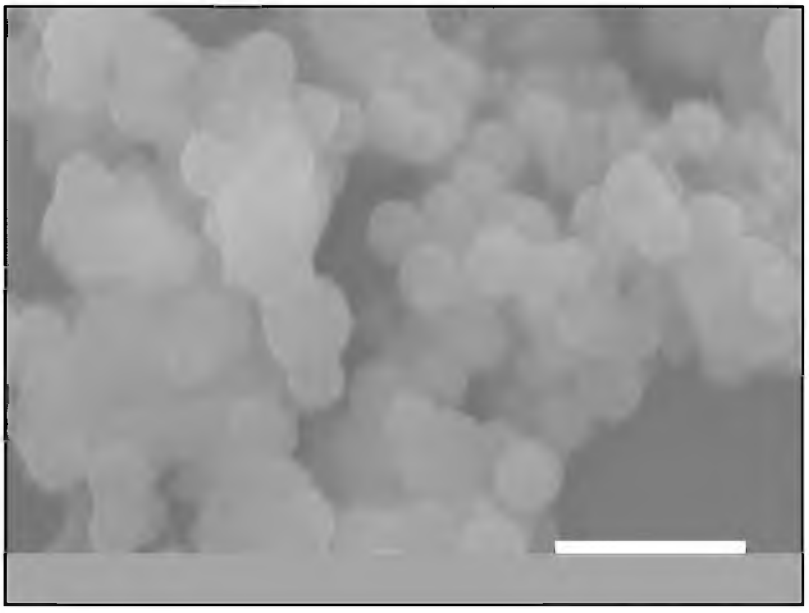

Figure 3.2: Vinyl ORMOSIL products formed with the new silicate seed source. Scale bar is 2 µm.

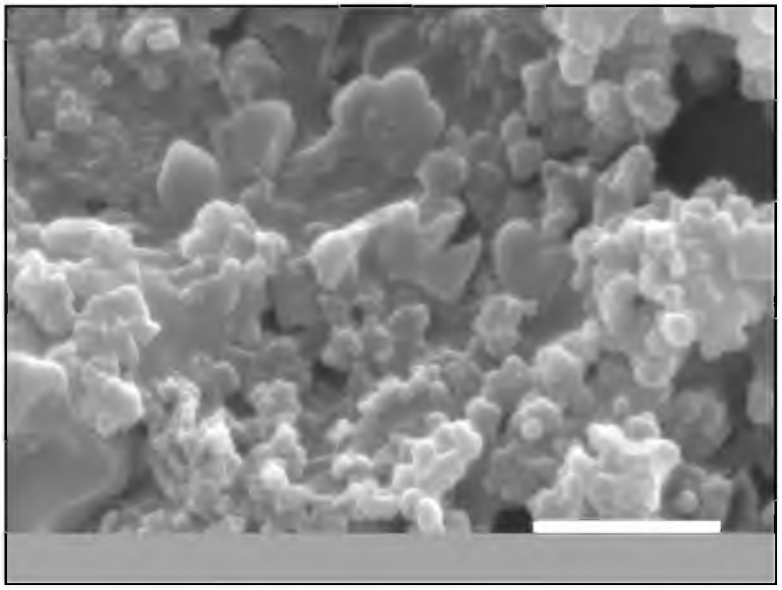

Figure 3.3: Aggregated vinyl products from the emulsion method. Scale bar is 2.5 µm.

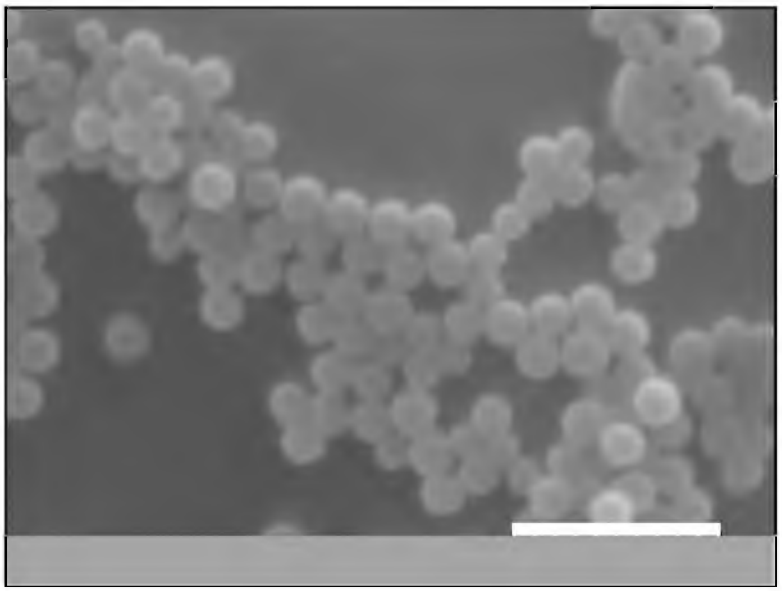

Figure 3.4: Nonaggregated vinyl products from the emulsion method. Scale bar is 1 µm.

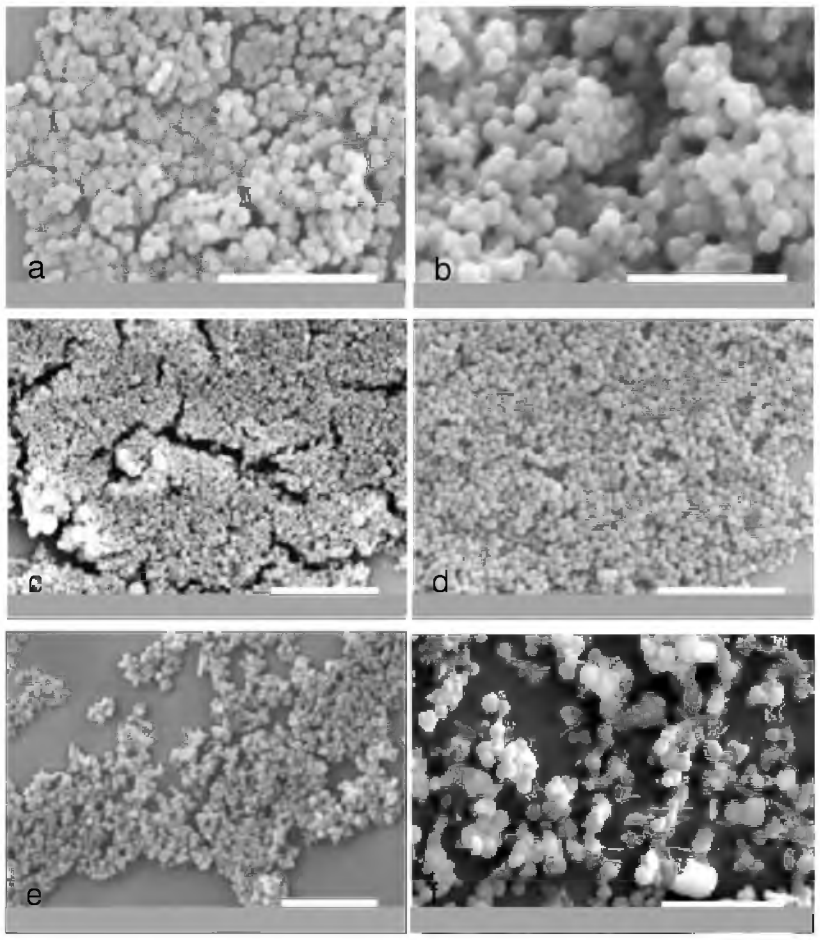

Figure 3.5: SEM images of (a) vinylsilane particles, (b) allylsilane particles, (c) mercaptosilane particles, (d) ethylcyano particles, (e) propylcyano particles, (f) isocyanato particles. Scale bars are 5 µm, 5 µm, 10 µm, 10 µm, 5 µm, and 10 µm.

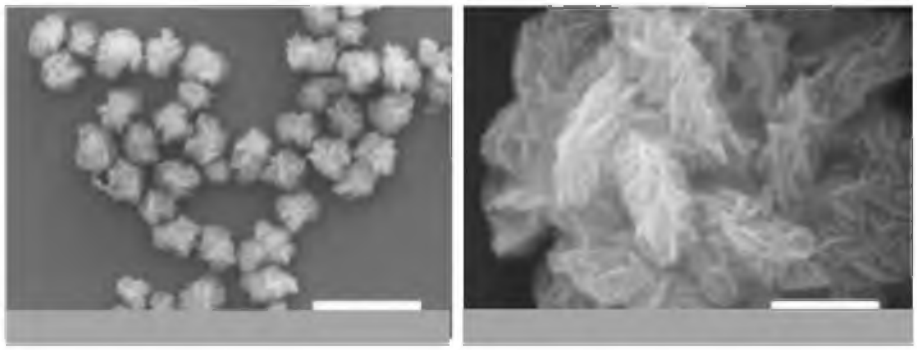

Figure 3.6: SEM of propylcyano particles prepared with higher concentration of sodium hydroxide. Scale bars are 25 µm and 2.5 µm.

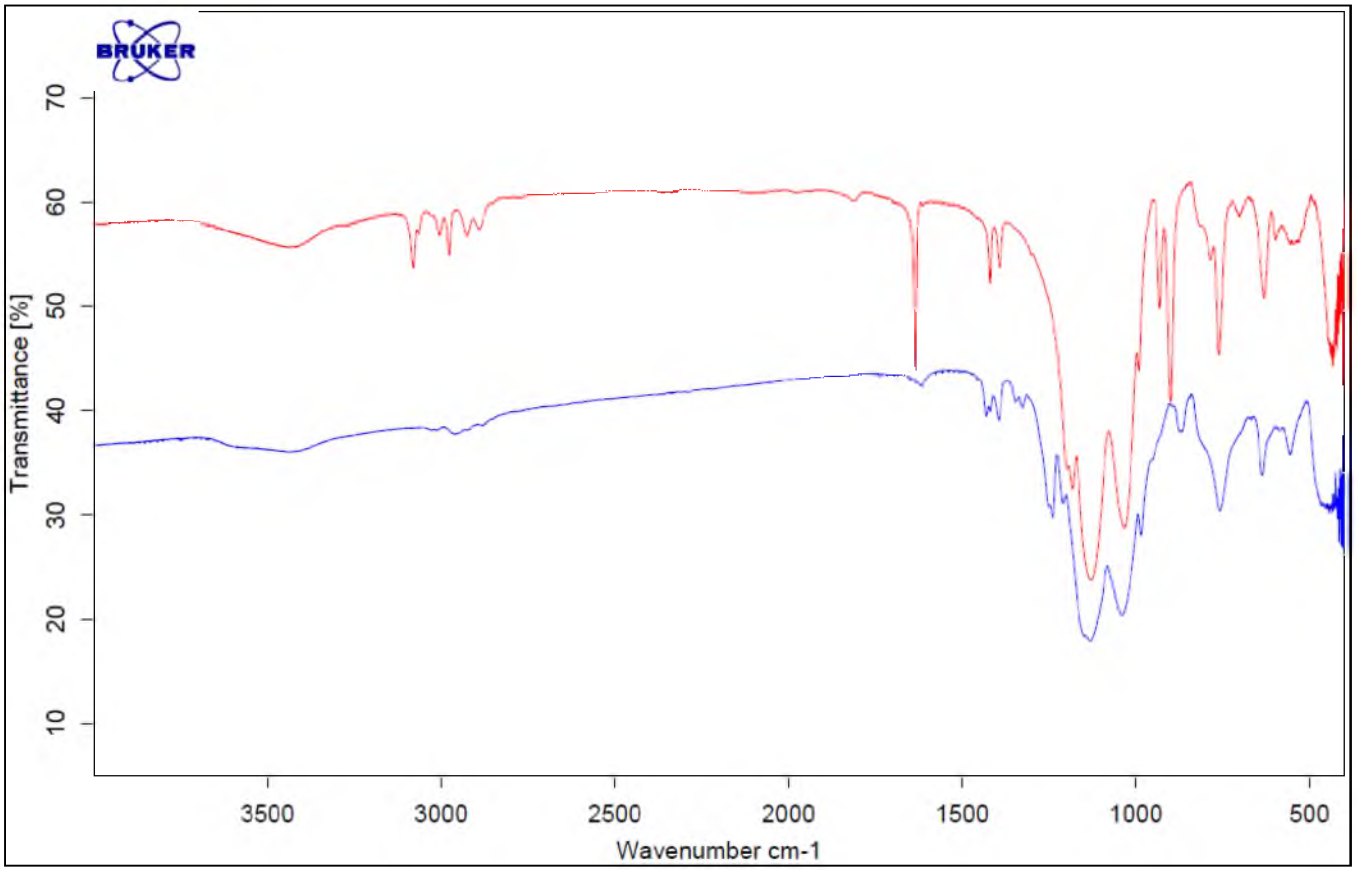

Figure 3.7: IR spectra of vinyl (red), brominated vinyl (blue) ORMOSILs. Offset for clarity.

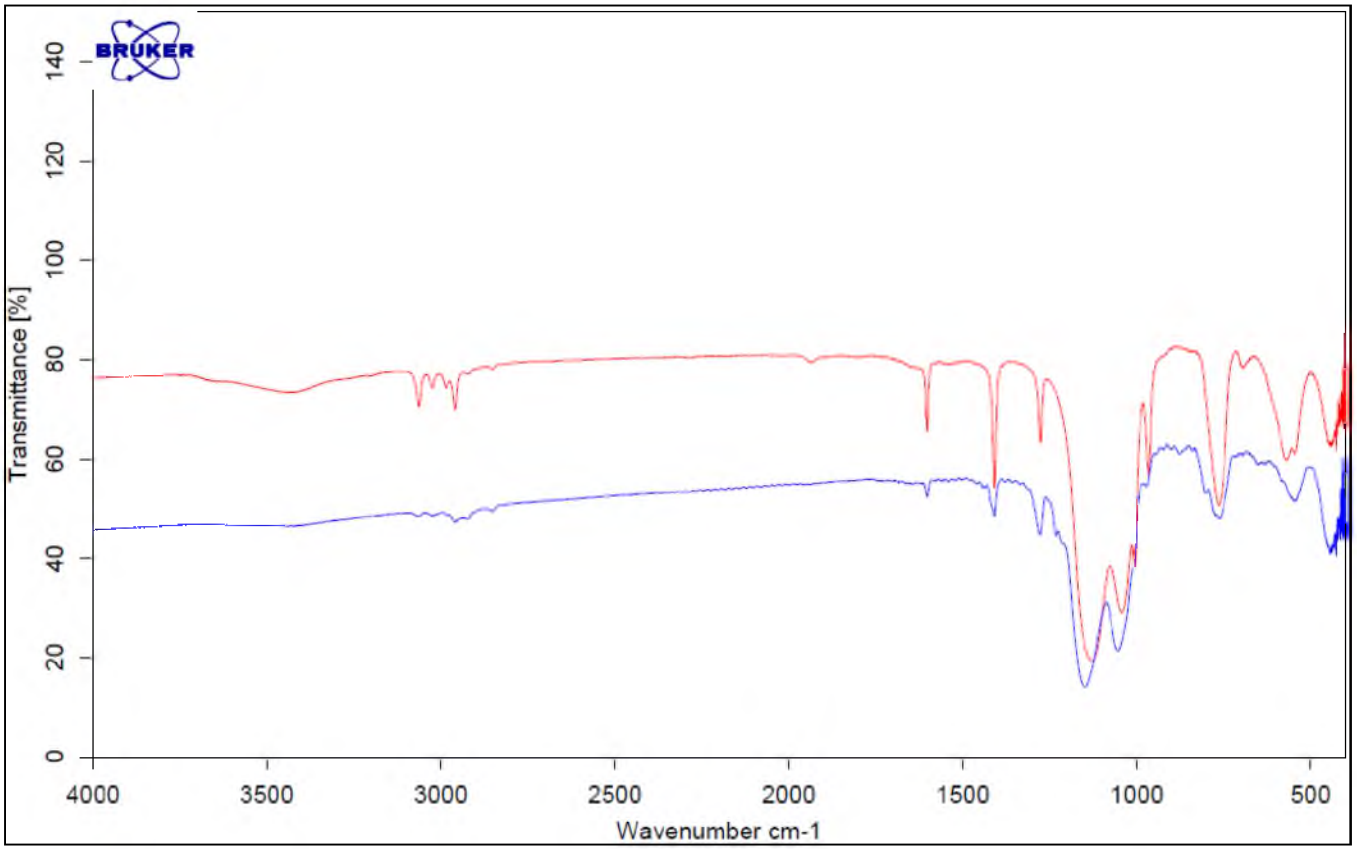

Figure 3.8: IR spectra of allyl (red), and brominated allyl (blue) ORMOSILs. Offset for clarity.

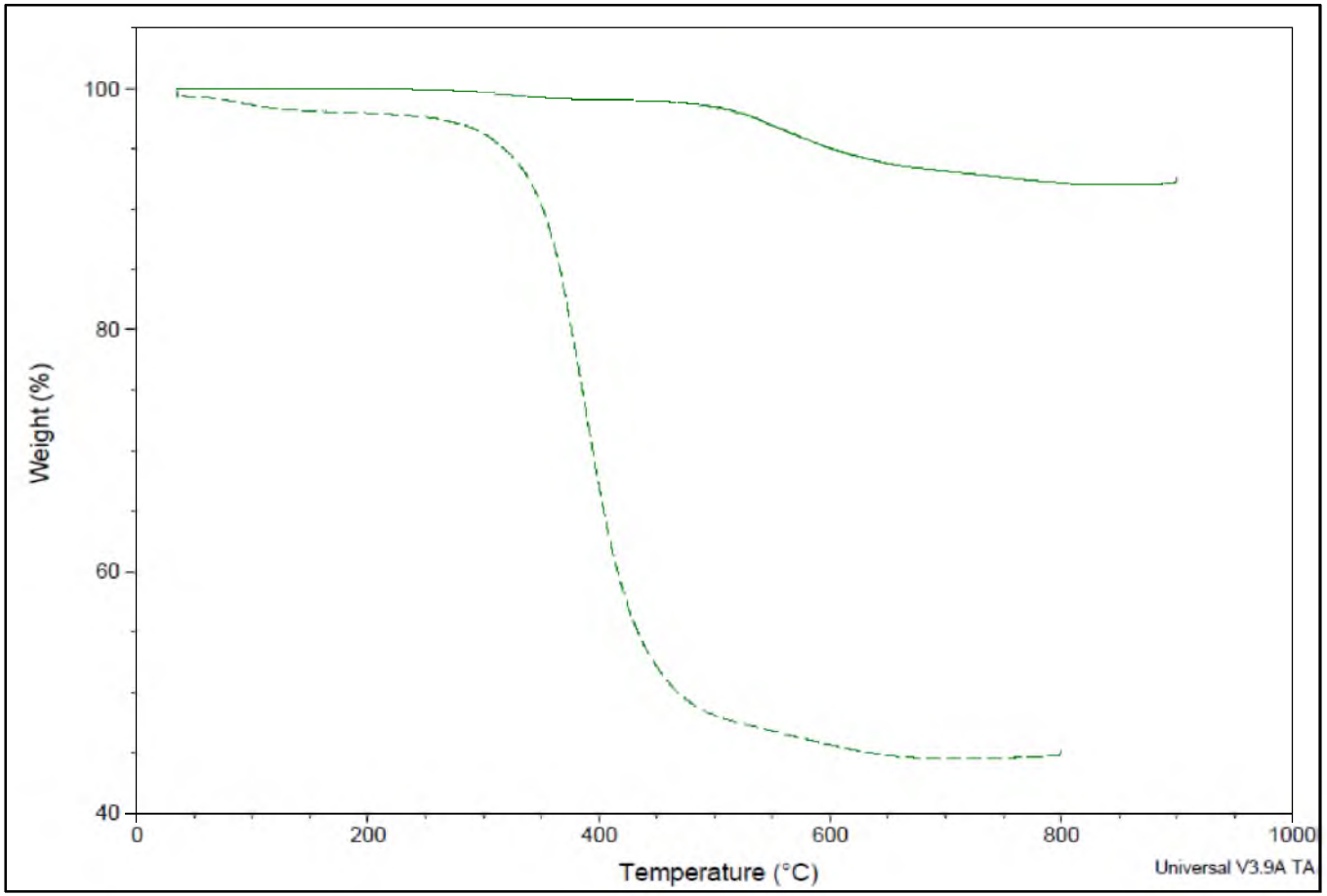

Figure 3.9: TGA data of vinyl (solid), brominated vinyl (dashed) ORMOSILs.

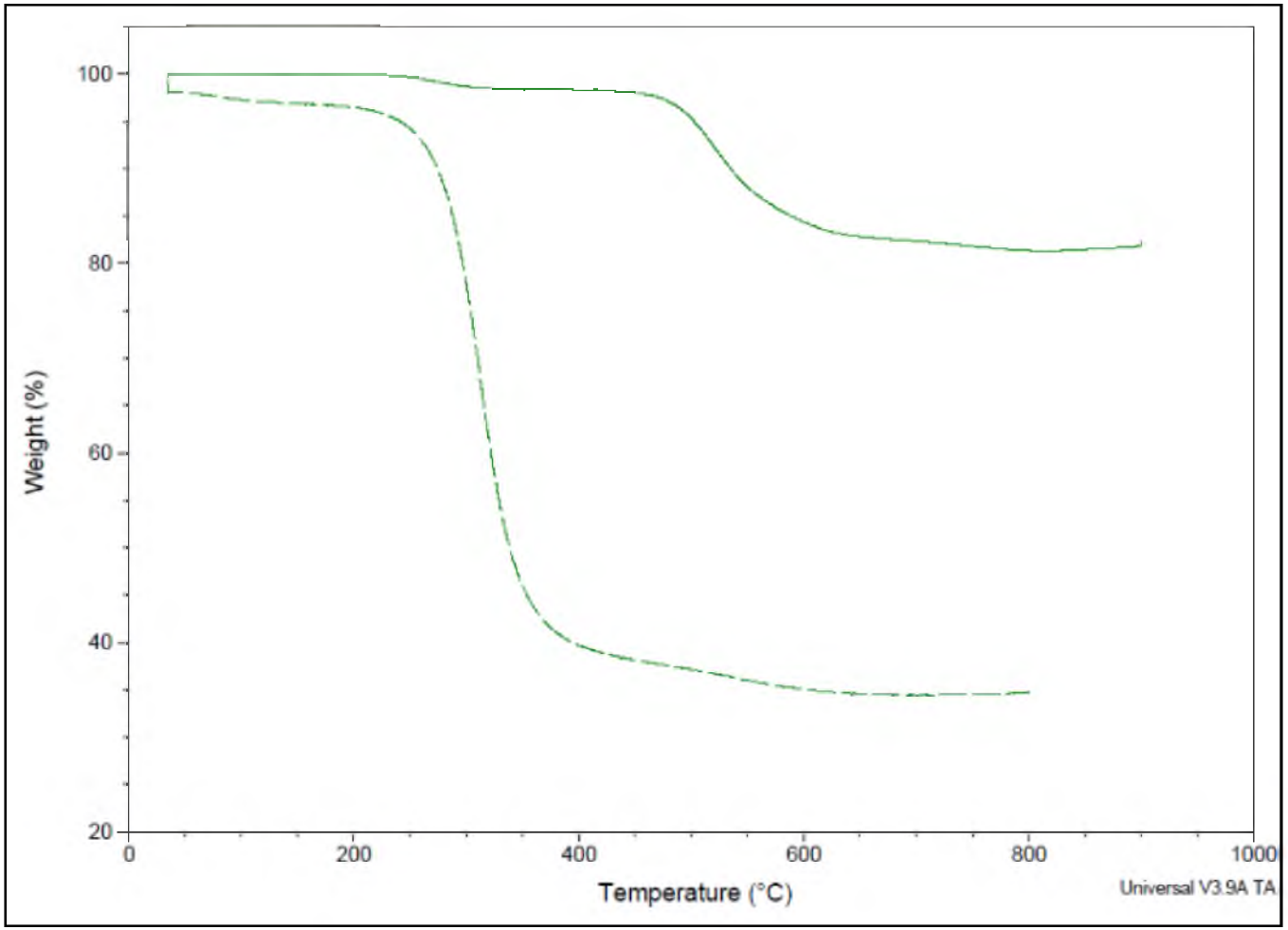

Figure 3.10: TGA data of allyl (solid), and brominated allyl (dashed) ORMOSILs.

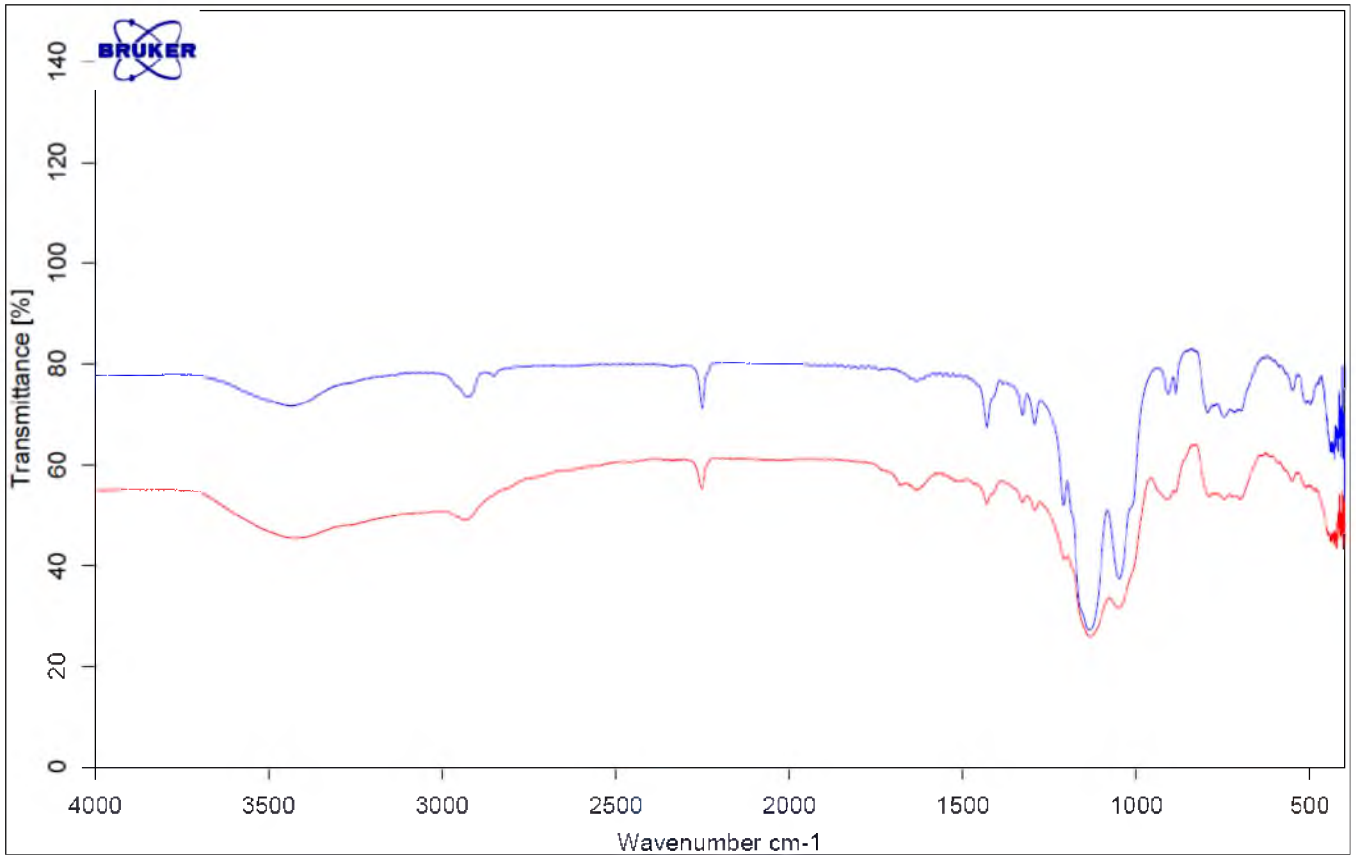

Figure 3.11: IR spectra of cyanoethyl (blue), reduced cyanoethyl (red) ORMOSILs. Offset for clarity.

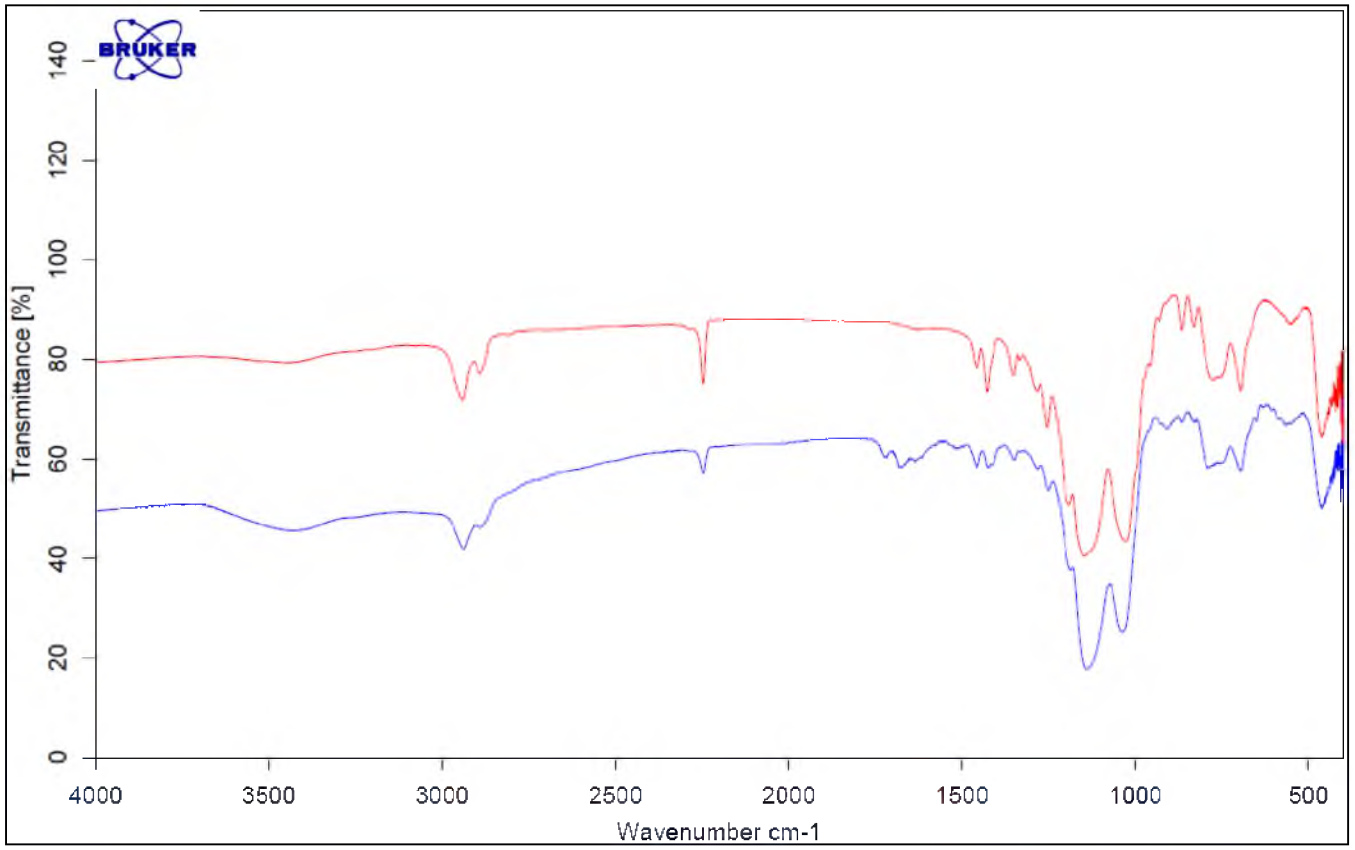

Figure 3.12: IR spectra of cyanopropyl (red), and reduced cyanopropyl (blue) ORMOSILs. Offset for clarity.

Figure 3.13: Digital picture of dansylated cyanopropyl (left), and dansylated reduced cyanopropyl (right) ORMOSILs.

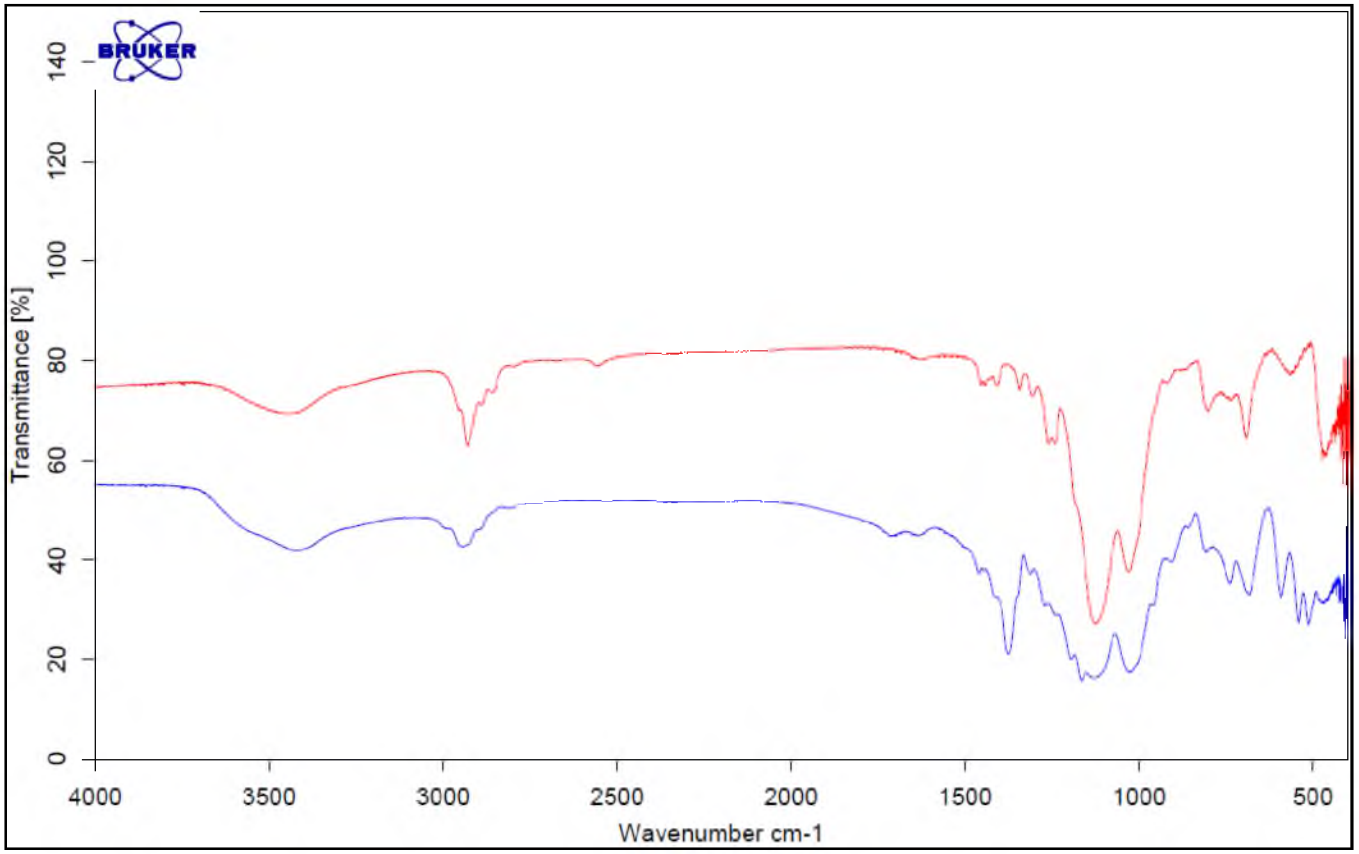

Figure 3.14: IR spectra of thiol (red), and oxidatively chlorinated thiol (blue) ORMOSILs. Offset for clarity.

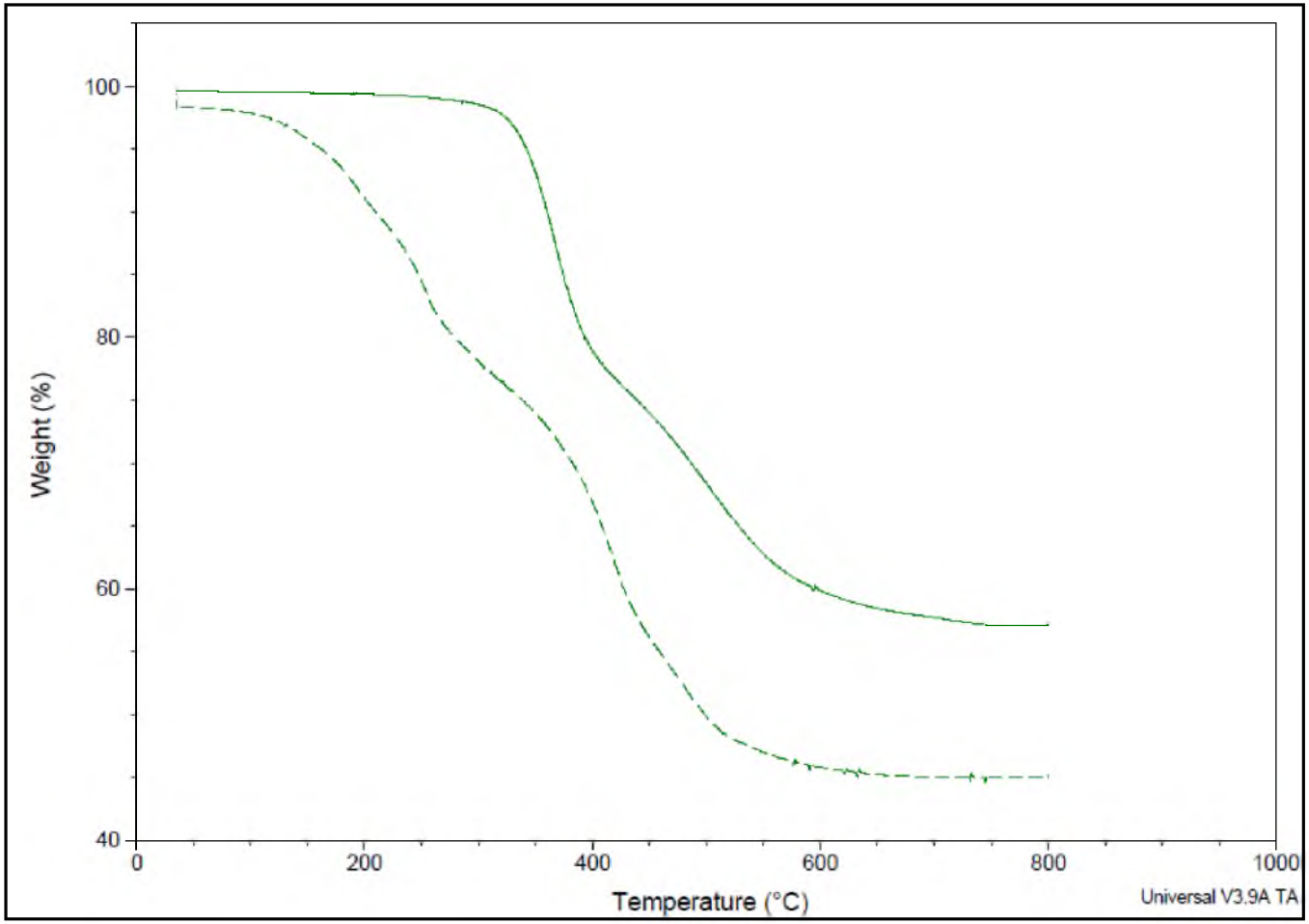

Figure 3.15: TGA data of thiol (solid), and oxidatively chlorinated thiol (dashed) ORMOSILs.

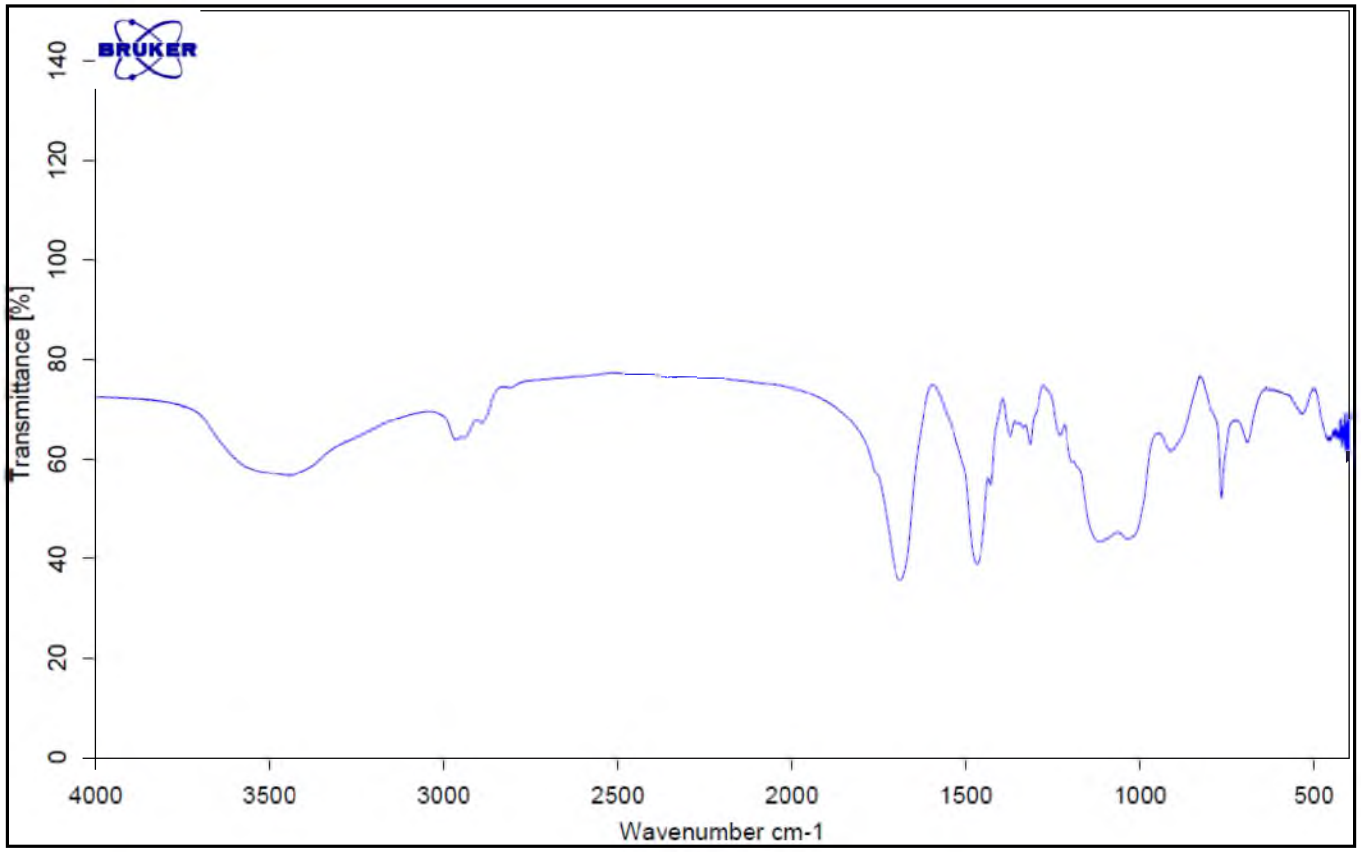

Figure 3.16: IR spectrum of 'isocyanato' ORMOSIL.

Table 3.1. Solvent amount per 1 mL of the silane precursor for the formation of the ORMOSIL nanoparticles.

siloxane organic group	solvent volume, mL H_2O	EtOH
isocyanatopropyl	0	11
cyanoethyl	15	2.25
cyanopropyl	15	2.25
vinyl	20	20
allyl	20	20
mercaptopropyl	20	20

Table 3.2: Nanoparticle diameter (nm) as a function of NaOH concentration during the formation of the ORMOSIL nanoparticles.

	sodium hydroxide concentration, M							
siloxane organic group	0.6	0.9	1.0	1.1	1.2	1.3	1.4	1.5
vinyl	-	200-500	-	300-400	-	500-600	-	-
allyl		700-1000		500-600		500-700		
cyanoethyl	-	-	700-900	-	500-600	-	x	-
cyanopropyl	2000	1000	-	-	600-700	-	-	-
mercaptopropyl	-	1000-2000	-	600-2000	-	300-1000	-	300-400
isocyanatopropyl	-	-	600-2000	800-1200	-	700-2500	-	>1500

3.5 References

[1] Stöber, W.; Fink, A.; Bohn, E. *Colloidal Interface Sci.* **1968**, *26*, 62.

[2] Wang, W.; Gu, B.; Hamilton, W. *J. Phys. Chem. B* **2003,** *107,* 3400-3404.

[3] Dash, S.; Mishra, S.; Patel, S.; Mishra, B.K. *Advances in Colloid and Interface Science* ***2008,*** *140, 77-94.*

[4] Yoshitake, H. *Journal of Materials Chemisty* **2010,** *20,* 4537-4550.

[5] Wan, Y.; Zhang, D.; Hao, N.; Zhao, D. *Int. J. Nanotechnology,* **2007,** *4,* 66-99.

[6] Blaaderen, A.; Vrij, A. *Langmuir,* **1992,** *8,* 2921-2931

[7] Burns, A.; Hooisweng, O.; Wiesner, U. *Chem. Soc. Rev.* **2006**, *35*, 1028-1042.

[8] Trewyn, B.G.; Giri, S.; Slowing, I. I.; Lin, V. S. *Chem. Comm.;* **2007,** 3236-3245.

[9] Radu, D.R.; Lai, C.-Y.; Huang, J.; Shu, X.; Lin, V. S.-Y, *Chem. Comm.* **2005,** 1264-1266.

[10] Trewyn, B.G.; Slowing, I. I.; Giri, S.; Chen, H.-T.; Lin, V. S.-Y. *Acc. Chem. Res.* **2007,** *40,* 846-853.

[11] Arkhireeva, A.; Hay, J. N.; Oware, W. *J. Non-Crystalline Solids,* **2005,** *351,* 1688-1695

[12] Arkhireeva, A.; Hay, J. N. *J. Mater. Chem.* **2003***, 13,* 3122-3127.

[13] Brozek, E.; Zharov, I. *Chem. Mater.* **2009,** *21,* 1451-1456.

[14] Kumar, R.; Roy, I.; Ohulchanskky T. Y.; Vathy, L. A.; Bergey, E. J.; Sajjad, M.; Prasad, P. N. *ACSNano,* **2010,** *4(2),* 699-708.

[15] Li, H.; Gui, X.; Zhang, L.; Wang, S.; Ji, C.; Wei, J.; Wang, K.; Zhu, H.; Wu, D.; Cao, A. *Chem. Commun.* **2010,** *46,* 7966-7968.

[16] Frenkel-Mullerad, H.; Avnir, D. *Chem. Mater.* **2000,** *12,* 3754-3759.

[17] Berthod, A. *J. Chrom.* **1991,** *549,* 1-28.

[18] White, H. S.; Murray, R. W. *Anal. Chem.* **1979,** *51,* 536-239.

[19] Bahrami, K.; Khodaei, M. M., Soheilizad, M. *J. Org. Chem.* **2009,** *74,* 9287-9291.

[20] Arkhireeva, A.; Hay, J.N.; Lane, J.M.; Manzano, M.; Masters, H.; Oware, W.; Shaw, S.J. *Journal of Sol-Gel Science and Technology* **2004,** *31,* 31-36.

[21] Zukoski, C. F.; Look, J.-L.; Bogush, G. H. *Adv. In Chemistry Series,* **1994,** *234,* 451-465.

[22] Jin, R.-H.; Yuan, J.-J. *Macromol. Chem. Phys.,* **2005,** *206,* 2160-2170.

[23] Kasseh, A.; Ait-Kadi, A.; Riedl, B.; Pierson, J.F. *Polymer* **2003,** *44,* 1367-1375.

CHAPTER 4

SYNTHESIS OF TRI-FUNCTIONAL ORMOSIL PARTICLES: PROOF OF PRINCIPLE FOR ORMOSILS WITH DRUG DELIVERY APPLICATIONS

4.1 Introduction

Nanoparticle-based drug delivery agents are materials that take advantage of the unique physical properties of nanosized architectures to deliver a therapeutic agent. They span a variety of materials, such as inorganic nanoparticles, micellar capsules, or dendritic polymers.[8] Their small size, large surface areas, porosity, and targeting ability give them advantages over traditional delivery methods. A targeting ligand may be covalently bound to the nanoparticle surface to increase specificity toward a desired site (i.e., a receptor for endocytosis).[9-12] A controlled response may release a drug over time or under specific conditions, which limits exposure of healthy tissue to the drug.[9-12] Additionally, covalent attachment of a drug to a nanoscale scaffold or internalization into the nanoparticle body may reduce toxicity by limiting the kinds of cells/tissue the drug would come in contact with.[9-12]

In the previous chapters, we described new methods to synthesize a variety of ORMOSIL particles. We also demonstrated that organic functionalities

of the ORMOSIL particles can undergo further chemical modification. In this chapter, we discuss our efforts to design a particle that contains three components for imaging, targeted delivery, and therapy. These more complex particles are designed to demonstrate potential applications of ORMOSIL products in the field of drug delivery. The therapeutic component is boron atoms, reactive nuclei suitable for neutron capture therapy.[13] The imaging component is fluorescein isothiocyanate. The fluorescent dye would allow the particles to be tracked easily during in vitro studies.[14] The targeting component is folic acid that is covalently attached to the particle surface. Folic acid can bind to the folate receptors that are common to many cancer cell lines.[15] If the folic acid that is covalently attached to the particle surface comes into contact with the folate receptor of the cell, then it is likely to be internalized by the cell through endocytosis.[16] We first attempted to synthesize a particle with these three components by using a series of internal chemical modifications and surface functionalizations using the methods described in the previous chapters. When these attempts to generate the particle proved ineffective, we developed a method that utilized a tri-condensation reaction to bring all of the components together in a single step. The organic functionalities of the tri-condensed species were then modified to yield the final product comprised of the therapeutic agent, a targeting ligand, and a fluorescent label.

4.2 Experimental Section

4.2.1 General

All water-sensitive reactions were conducted under a dry nitrogen atmosphere using oven-dried glassware and anhydrous solvents. Hygroscopic liquids were transferred into reaction vessels via syringe through rubber septa.

4.2.2 Reagents

All solvents were obtained from Mallinckrodt Baker or Fisher Scientific at reagent grade, except for hexanes and ethyl acetate that were of technical grade. THF was dried over sodium benzophenone ketyl under nitrogen; dichloromethane was dried over calcium hydride under nitrogen. Toluene was dried over 4-Å molecular sieves. All other solvents were used without further purification. The following reagents were used without further purification: NH_4OH (30%, Mallinckrodt), vinyltriethoxysilane (Gelest), allyltrimethoxysilane (Gelest), BH_3•THF complex (1 M stabilized, Aldrich), fluorescein isothiocyanate (Aldrich), rhodamine B isothiocyanate (Aldrich), 3-aminopropyltriethosilane (98%, Aldrich), 3-aminopropyltrimethoxysilane (Fluka), tetraethylorthosilicate (+99.999%, Alfa Aesar), dansyl chloride (99%, Aldrich), folic acid (98%, Aldrich), 1-ethyl-3-(3-dimethylaminopropyl) carbodiimide) (Fluka), RPMI-1640 medium (ATCC).

4.2.3 Instrumentation

IR spectra were recorded in KBr pellets in 400 to 4000 cm^{-1} range using a Bruker Tensor 37 IR Spectrophotometer. Scanning electron microscopy (SEM) images were obtained using a Hitachi S3000N instrument at an accelerating voltage between 20-25 kV. Thermogravimetric Analysis (TGA) measurements were performed using a TA Instruments TGA 2950 Thermogravimetric Analyzer in an open platinum pan. All drop-wise additions were made using a Razel Syringe pump model A-99 with a 5 mL syringe at an addition rate of about 3.8 mL/hr. A Branson 1510 sonicator was used for all sonications.

4.2.4 Synthesis

4.2.4.1 Covalent attachment of fluorescein isothiocyanate to 3-aminopropytriethoxysilane (Scheme 4.1).[17] Absolute ethanol (9.3 mL) was placed in a scintillation vial. In the dark, fluorescein isothiocyanate (5.3 mg, 0.014 mmol) was added to the vial. Finally, 3-aminipropyltriethoxysilane (0.73 mL, 3.12 mmol) was added to the solution. The scintillation vial was capped, wrapped in aluminum foil, and stirred overnight. The solution was stored in the refrigerator for later use.

4.2.4.2 Covalent attachment of folic acid to 3-aminopropyltriethoxysilane (Scheme 4.2).[18] Dimethylsulfoxide (10 mL) was placed in a round-bottom flask. 1-Ethyl-3-(3-dimethylamino-propyl)carbodiimide (150 mg, 1 mmol) and folic acid (66 mg, 0.15 mmol) were next added to the flask. The solution was stirred until the solution became homogenous (for at least 30 min.). 3-

aminopropyltriethoxysilane (40 µL, 0.17 mmol) was added in a single portion to the solution and the contents of the flask were stirred overnight. The vessel was sealed and stored in a refrigerator for later use.

4.2.4.3 Hydroboration of alkene-rich ORMOSILs (Scheme 4.3). Hydroboration conditions are described in Chapter 2, Scheme 2.8. Identical conditions and work-up were utilized for all hydroboration reactions conducted to an alkene-containing ORMOSIL.

4.2.4..4 General method for surface functionalization of ORMOSIL particles (Scheme 4.4). An example of the surface functionalization with folic acid-modified silanes is described. ORMOSIL particles (25 mg) were dispersed in 15 mL of dimethylsulfoxide in a round-bottom flask and set to stir. The previously prepared folic acid solution (5 mL) was added in a single portion followed by 34 µL of ammonium hydroxide. The solution was stirred overnight and an orange precipitate was collected by centrifugation. The particles were washed four times with dimethylsulfoxide and 1:1 mixture of ethanol and water.

4.2.4.5 Silica shell growth on the surface of ORMOSIL particles (Scheme 4.5). A general method to grow layers of silica on the surface of OMROSIL particles is described. It was used for all particle types. ORMOSIL particles (50 mg) were placed in a round-bottom flask. A Stöber stock solution (6 mL) was added to the particles and briefly sonicated to homogenize the solution. The solution was stirred for ~20 min. Tetraethylorthosilicate (50 µL) was added in a single portion and the solution was stirred overnight. The precipitate was

collected by centrifugation and washed with 1:1 mixture of ethanol and water. The products were dried and SEM images were obtained.

4.2.4.6 Tri-condensation of trialkoxysilanes with -amine, alkene, and FITC functional groups (Scheme 4.6). Water (40 mL) and ethanol (40 mL) were placed in a round-bottom flask and magnetically stirred. Sodium hydroxide (1.3 M, 3.23 mL) was added to the flask and stirred for 10 min. The flask was wrapped in aluminum foil to keep out light. Allyltrimethoxysilane (2.0 mL) was added to the vessel by syringe pump at a rate of 3.8 mL/h. As the allyltrimethoxysilane was being added from the syringe pump, 4 mL of the previously prepared FITC solution (Scheme 4.1) was added all at once. After half of the allyltrimethoxysilane addition was complete, another 4 mL of the FITC solution were added all at once. After addition of the allyltrimethoxysilane was complete, 2 mL of the FITC solution were added to the flask. The solution became turbid after several hours of stirring. The flask was sealed and continued to stir overnight. The precipitate was collected by centrifugation and washed several times with 1:1 water and ethanol until the decantate was colorless. The solution was then washed three more times. A yellow precipitate was collected and dried to yield a fine yellow powder. SEM, TGA, IR and Elemental Analysis were obtained for the powder.

4.2.4.7 Attachment of folic acid to the surface of tri-functionalized particles (Scheme 4.7). 1-Ethyl-3-(3-dimethylaminopropyl)carbodiimide (150 mg, 0.96 mmol) and folic acid (70 mg, 0.16 mmol) were placed into a round-bottom flask containing 10 mL dimethylsulfoxide The solution was stirred for about 30 min., or

until a uniform transparent yellow solution was observed. The previously prepared tri-functional OMROSIL particles (100 mg) were suspended in DMSO (5 mL) and briefly sonicated. The particle suspension was added to the folic acid solution, flask wrapped in aluminum foil, and solution stirred for 72 h. The resulting suspension changed from yellow to dark orange. The folic acid-modified particles were collected by centrifugation and washed with DMSO and 1:1 ethanol and water mixtures. The particles were rinsed with small amounts of dilute HCl to liberate any noncovalently bound folic acid.[19] The particles collected were yellow/orange, presumably due to the surface-bound folic acid. The persistence of fluorescence was confirmed via UV light. The products were analyzed by IR, SEM, TGA, and Elemental Analysis.

4.3 Results and Discussion

4.3.1 Early synthetic strategies

We first approached the synthesis of a three-component particle by conducting a series of surface modifications for the previously synthesized boron-containing ORMOSIL nanoparticles, prepared as discussed in Chapter 1. When we functionalized the particle surface with the fluorescein dye, the particles changed color from white to light yellow. If the particles were exposed to 365 nm UV light, the particles fluoresced bright green. The folic acid module was next covalently attached to the particle surface using a similar surface modification method. Unfortunately, this method involving multiple surface modifications did not yield stable products. Within several days of functionalizing a particle surface

with fluorescein, the fluorescence color changed from green to blue and eventually disappeared. We concluded that fluorescein that was covalently attached to the surface was quenching from exposure to air, light, and/or water.[20] Modifying the particle surface with the folic acid also proved problematic. There was no qualitative or quantitative indicator to suggest that folic acid had covalently attached to the surface. The particles did not undergo any significant change in color, nor was there any significant change in the IR spectrum or TGA of the product. We modified the method by attempting to grow a thin layer of silica on the ORMOSIL particle surface. We rationalized that if the dye could be protected with a layer of silica, then fluorescence would be preserved and a new layer of silanols could be modified with folic acid.[21]

We first attempted to grow a thin silica shell on the surface of vinyl-containing ORMOSILs. SEM images were obtained for these new particles and revealed that our method was unsuccessful. SEM images of the "silica-coated vinyl-containing nanoparticles" did not appear as if a layer of silica had grown on the surface (Figure 4.1). A large population of very small particles was also observed, which suggests that the tetraethylorthosilicate was forming individual silica particles rather than growing on the vinyl-containing nanoparticle surface. In addition, fluorescent vinyl-containing nanoparticles were still quenching within days after being subjected to silica shell growth conditions, suggesting the dye was not protected. SEM images of the "silica-coated boron-containing nanoparticles" showed that some of the particles grew in size while others did not (Figure 4.2). The particles that underwent growth were much larger in diameter

and their surfaces were no longer homogeneous like the surface of the starting materials. Unfortunately, the boron-containing particles that had been functionalized with a dye were still quenching. It seemed reasonable to conclude that the silica surface growth was not successful on the majority of the particles or that the silica shell was not protecting the dye.

4.3.2 The tri-condensation method

Next, we decided to employ a different synthetic method, a co-condensation, which had been particularly useful in the past for those studying silica.[22,23] Co-condensation is simultaneous hydrolysis and condensation of at least two silane precursors (often, tetraethylorthosilicate and an organically modified silane) to generate a hybrid structure.[24,25] The resulting products possess a significantly higher concentration of the organic groups throughout the particle body compared to traditional surface modification/grafting. We hypothesized that if the three components could be co-condensed together, then the dye would be protected and the surface modification would easily follow. However, there is no example in the literature describing a co-condensation of two or more organosilanes.

We attempted to synthesize our three-component material (Scheme 4.6) by adapting our methods described in Chapter 3 for the allyl-containing nanoparticles. The allylsilane had to be used in the highest concentration to ensure maximum boron loading. The concentration of fluorescein was chosen to resemble a method[17] used to generate dye-doped silica particles.

4.3.2.1 Qualitative observations of tri-condensation products. The particles collected from the tri-condensation reaction were yellow (Figure 4.3) and hydrophobic. We believe that the hydrophobicity of the product was due to the large number of alkene groups introduced by the allyl-silane precursor. SEM showed spherical particles 300-500 nm in diameter (Figure 4.4). It is unclear if particles in this size range would be useful for in vivo work; however, they can be useful for in vitro studies and are more easily characterized (SEM, TEM, etc.) and thus perfectly suited as a model. The particles fluoresced bright green upon exposure to 365 nm UV light (Figure 4.5).

The alkene functionalities of the nanoparticles were hydroborated, as previously described.[26] After the hydroboration, the particles became hydrophilic and dispersed easily in water, which is consistent with our previous results. Although the particles changed color from yellow to white (Figure 4.3), they fluoresced a bright green color (Figure 4.4). This suggested that at least some of the fluorescein-trialkoxysilane was internalized within the particle body and was not affected by the hydroboration. This would indicate that the dye was now properly protected for the first time. Indeed, the fluorescence lifetime of the particles could be measured in months instead of days.

Covalent attachment of the folic acid to the particle surface was achieved through the formation of a new amide bond between the carboxcylic acid of the folic acid and the primary amines on the particle surface. We believe the amide bond was formed on the carboxcylic acid found at the gamma position of the folic acid, as has been shown in the literature.[27] The benefit of utilizing the coupling to

the aminated surface instead of the surface modification with organosilane has to do with the retention in particle size of the starting material. Surface modifications with silanes can increase the diameter of a silica particle if the alkoxysilanes form multiple layers on the surface. This was observed in some of our earlier experiments that exposed particles to a series of surface modifications with alkoxysilanes.[28] By coupling folic acid to the amines that are already on the particle surface, the increase in particle diameter is negligible.

After the surface modification, the color of the particles changed from white to yellow/orange (Figure 4.3). This color change was consistent with those in other reports describing modification of silica with folic acid.[19] The particles were washed with a 1.0 M hydrocholoric acid solution to remove any non-covalently bound folic acid from the particle surface. The color persisted even after multiple acid washes. Furthermore, we performed a control experiment where boron-containing nanoparticles that did not possess any amine functionalities were surface-modified with folic acid using the same conditions. These nanoparticles did not undergo color change even after a prolonged exposure to the folic acid solution.

After the particles were washed and dried, a sample of the particles were resuspended in ethanol and irradiated with 365 nm UV light. The particles fluoresced a green/blue color (Figure 4.5). The slight color change may be a result of the new environment of the dye (boron, folic acid, etc.).[29] Furthermore, the fluorescence of the products persisted for months instead of days, showing that the dye was protected.

4.3.2.2 IR and TGA data for tri-functional particles. The IR data that were obtained for the tri-functional nanoparticles and their functionalized products displayed many characteristics consistent with our previously synthesized ORMOSIL particles (Figure 4.6). The tri-functional particles displayed the typical Si-O-Si vibrations observed at ~1010 cm^{-1} (bending) and ~1110 cm^{-1} (stretching). Symmetric deformations of the Si-C bond were observed at ~1410 cm^{-1} and 1430 cm^{-1}. The C=C stretching vibration is clearly observed near 1600 cm^{-1}. A series of C-H stretching vibrations can be found between 2800 cm^{-1} and 3200 cm^{-1}. A weaker O-H stretching vibration can be seen at 3400 cm^{-1}, which is likely due to surface silanols. Many of the absorptions characteristic of fluorescein or amines are not readily observed in the IR spectrum of the tri-functional particles. It is likely that fluorescein is in such a small concentration that it cannot be detected. The absorptions observed for the amines may be overlapping in other peaks of the spectrum or may be also present in a relatively low concentration.

The IR spectrum of the hydroborated tri-functional particles showed many characteristics similar to our previously described hydroborated products. The C=C stretching vibration found at 1600 cm^{-1} essentially disappears. Two new broad absorptions are observed near 1400 cm^{-1}, which is characteristic of the B-O vibration, and 700 cm^{-1}, which is characteristic of either a C-B or O-B-O stretch. Additionally, the O-H stretch observed at 3400 cm^{-1} increased in intensity, most likely due to the oxidation of the free borohydrides to hydroxyl groups. The spectrum offers strong evidence of the conversion of the alkene to

boronic acid moieties. For reasons previously discussed (see Chapter 2), the exact chemical structure of the boron species remains unclear.

Finally, the IR spectrum of the folic acid-modified particles was nearly identical to the hydroborated product. The only clear difference was near 1700 cm^{-1}, where a weak absorption could be representative of either a carboxylic acid or imine functionality. In our experience, surface modification products are difficult to characterize with IR spectroscopy due to the low ratio of the surface groups relative to the bulk particle. However, the small change that was observed for the folic acid-modified product may be a qualitative indicator that folic acid was successfully covalently bound to the particle surface.

The TGA data collected for the three particles showed increasing weight loss with each functionalization (Figure 4.7). The tri-functional particles showed the weight loss of 19.3%. These data are consistent with TGA data we have collected for similar ORMOSIL particles. After the hydroboration of the alkenes of the starting material, TGA displayed a more significant weight loss of 30.8%. This value is comparable to our results for the hydroboration of a vinyl-containing nanoparticles. After the folic acid functionalization, the nanoparticles displayed a weight loss of 33.3%. This small increase in weight loss is somewhat surprising considering the substantial molecular weight of folic acid (441.4 g/mol). Thus, we conclude that most of the folic acid was bound to the surface of the particles rather than inside the particles.

4.4 Conclusions

We successfully synthesized ORMOSIL particles containing three functionalities: boronic acid, fluorescein, and folic acid. We were able to achieve this by developing a method to co-condense three different organosilane precursors to yield tri-functional particles. They were then functionalized to yield a product containing a therapeutic agent, a fluorescent label, and a targeting ligand. Our study demonstrated that increasingly complex ORMOSIL particles can be synthesized in a simple and straightforward manner and that the organic functionalities found throughout the particle bodies can be selectively functionalized. In vitro and in vivo studies need to be conducted for the particles to determine if they are viable for drug delivery.

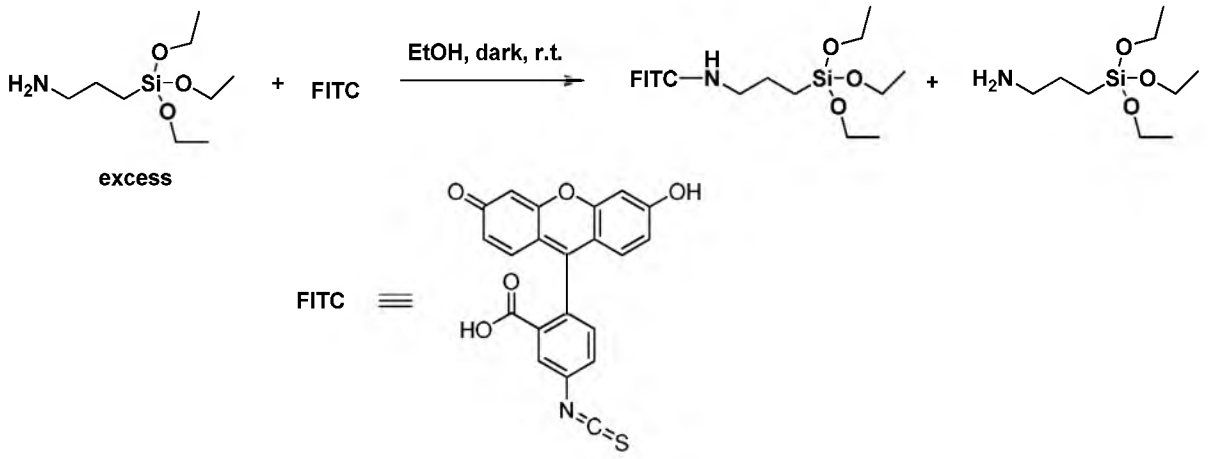

Scheme 4.1: Covalent attachment of fluorescein isothiocyanate to 3-aminopropytriethoxysilane

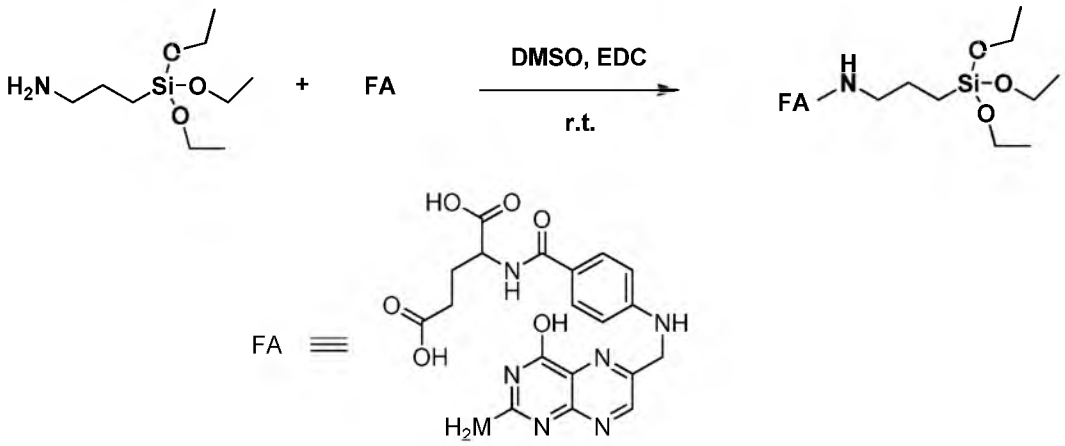

Scheme 4.2: Covalent attachment of folic acid to 3-aminopropyltriethoxysilane

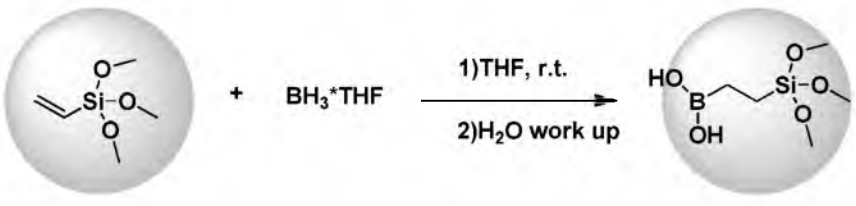

Scheme 4.3: Hydroboration of alkene-rich ORMOSILs.

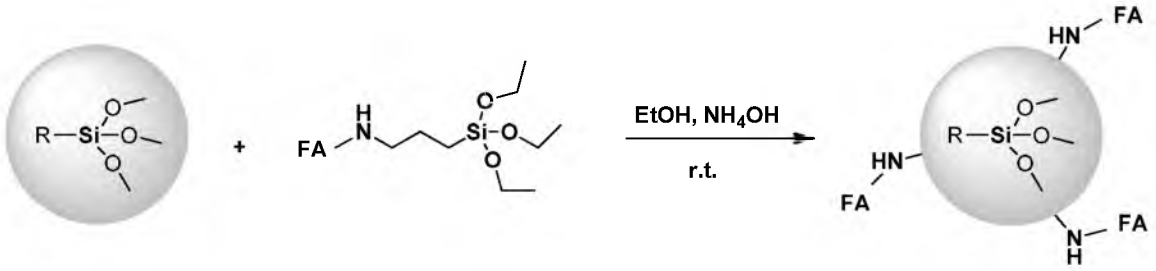

Scheme 4.4: General method for surface functionalization of ORMOSIL particles

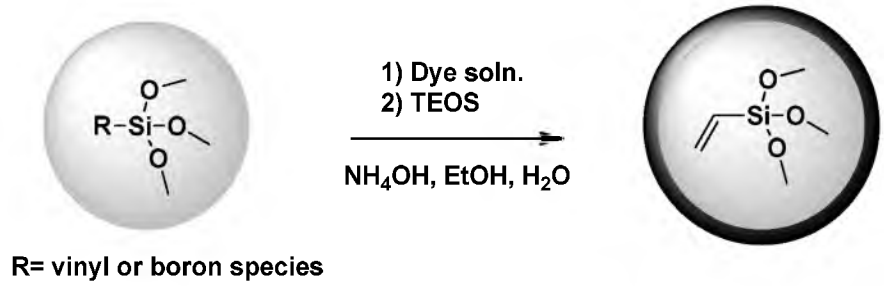

Scheme 4.5: Silica shell growth on the surface of ORMOSIL particles.

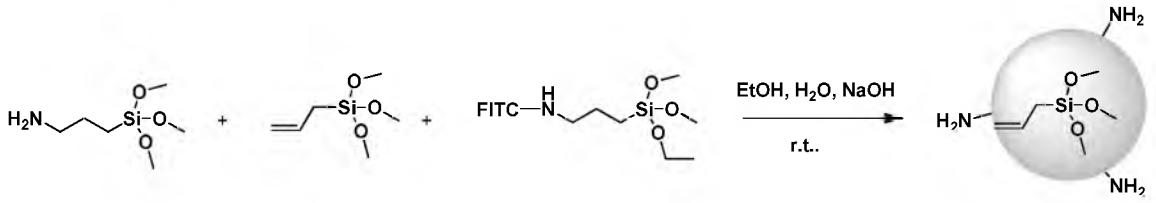

Scheme 4.6: Tri-condensation of trialkoxysilanes with -amine, alkene, and FITC functional groups

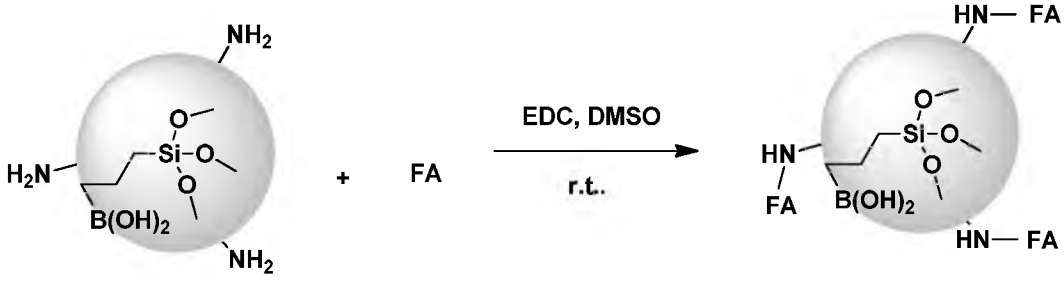

Scheme 4.7: Attachment of folic acid to the surface of tri-functionalized particles

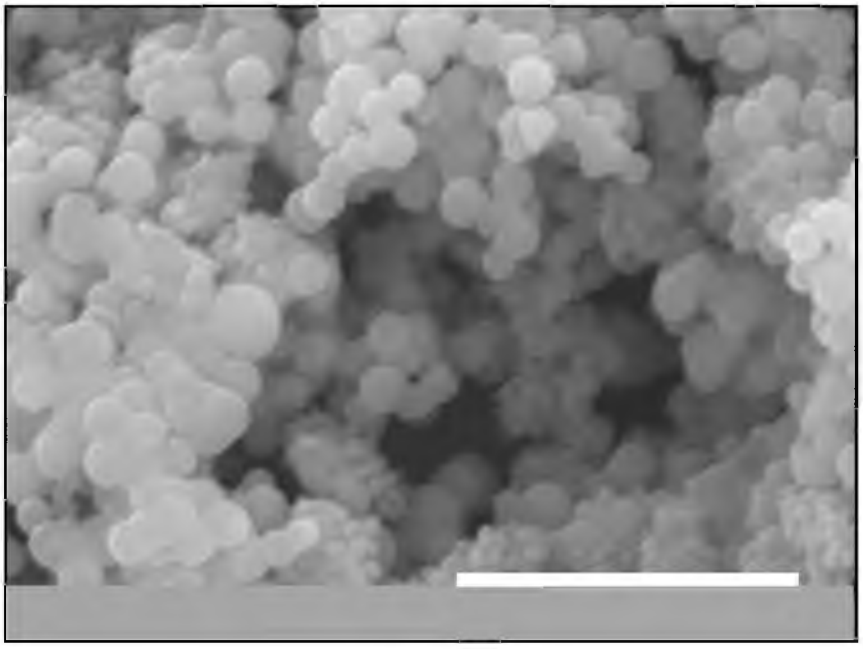

Figure 4.1: SEM image of vinyl-ORMOSILs after silica shell growth. Scale bar is 5 µm.

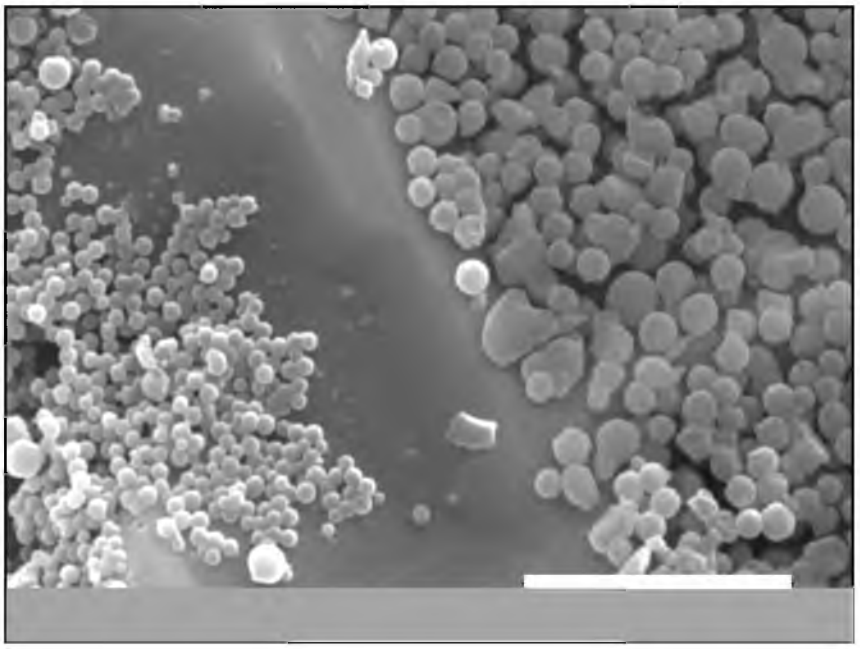

Figure 4.2: SEM image of boron rich OMOSILS after silica shell growth. Scale bar is 5 µm.

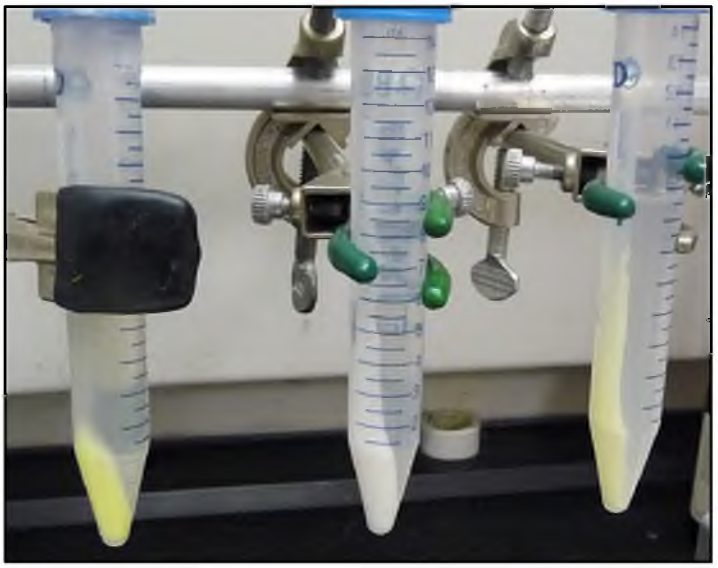

Figure 4.3: Photograph of products of the tri-condensation reaction (left), hydroborated tri-condensation product, (middle) and the folic acid functionalized hydroborated product (right).

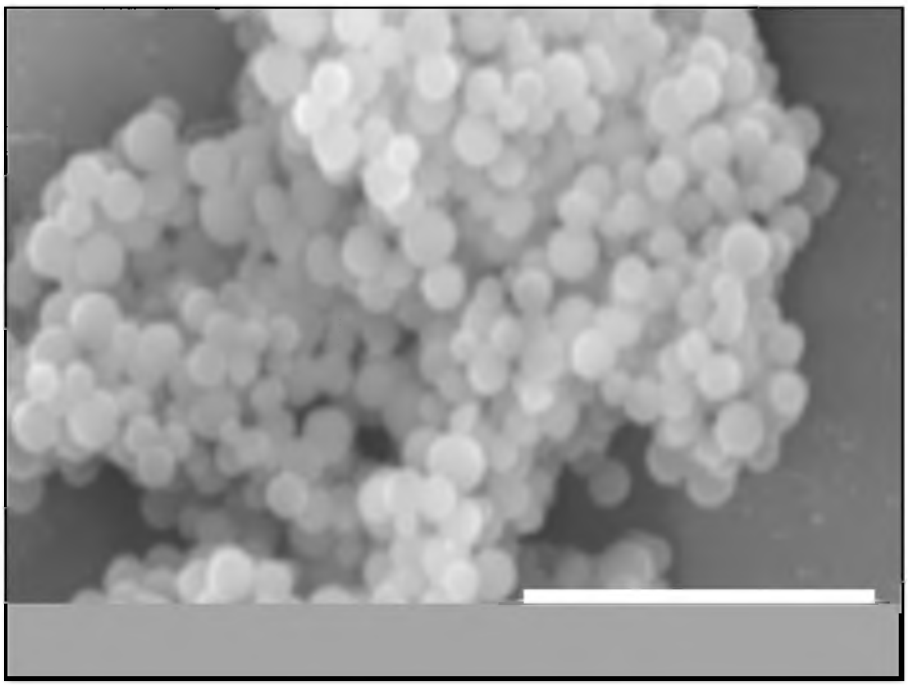

Figure 4.4: SEM image of tri-functional ORMOSIL particles. Scale bar is 5 µm.

Figure 4.5: Photograph of nanoparticles exposed to 365 nm UV light: tri-condensation reaction (left), hydroborated tri-condensation product (middle), and folic acid functionalized hydroborated product (right).

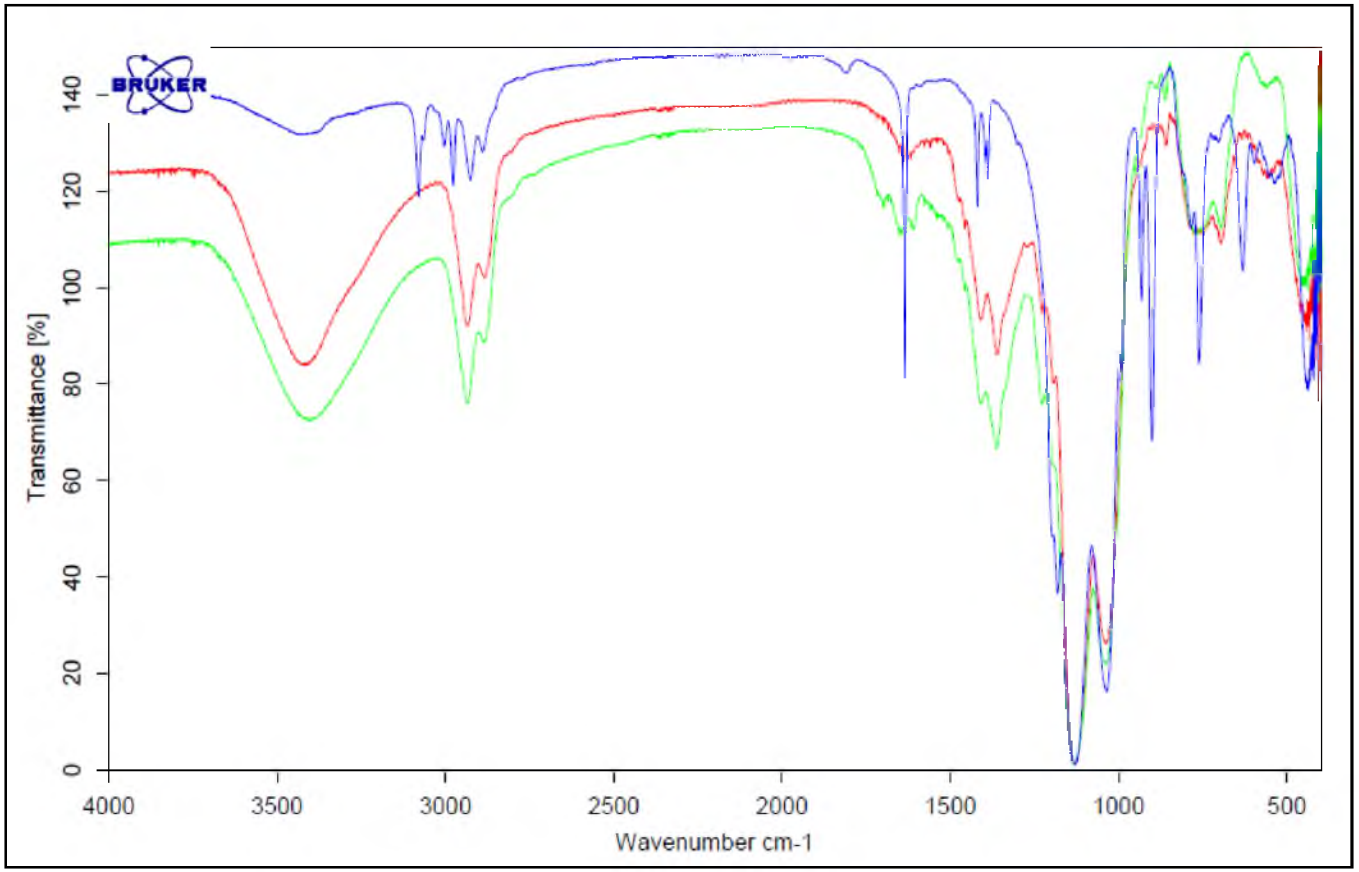

Figure 4.6: IR spectra of tri-functional starting material (top, blue), hydroborated product (red, middle), and folic acid modified hydroborated product (bottom, green). Offset for clarity.

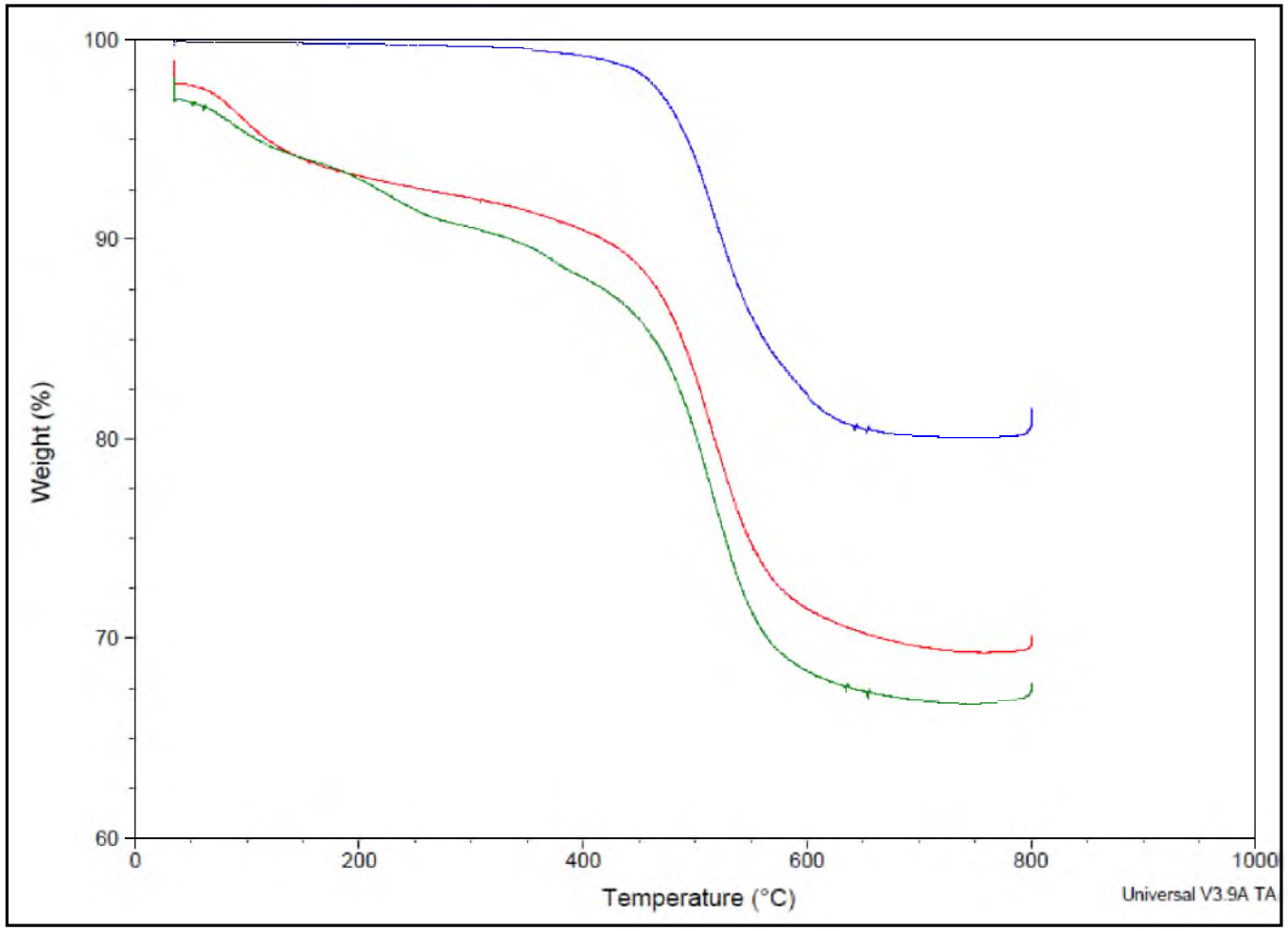

Figure 4.7: TGA data of tri-functional starting material (top, blue), hydroborated product (red, middle), and folic acid modified hydroborated product (bottom, green).

4.5 References

[1] Khalil, N.M.; Mainardes, R.M. *Curr. Drug Delivery* **2009,** *6,* 261-273.

[2] Tyrrell, Z.L.; Shen, Y.; Radosz, M. *Progress in Polymer Science* **2010,** *35,* 1128-1143.

[3] Gao, W.; Chan, J.M.; Farokhzad, O.C. *Molecular Pharmaceutics* **2010,** *7*(6), 1913-1920.

[4] Kabanov, A., Batrakova, E.V.; Melik-Nubarov, N.S.; Fedoseev, N.A.; Dorodnich, T.Y.; Alakhov, V.Y.; Chekhonin, V.P.; Nazarova, I.R.; Kabanov, V.A.. *Journal of Controlled Release* **1992,** *22,* 141-157.

[5] Bae, Y.; Jang, W.-D.; Nishiyama, N.; Fukushima, S.; Kataoka, K. *Mol. BioSyst.* **2005,** *1,* 242-250.

[6] Hawker, C.J.; Fréchet, *J. Am. Chem. Soc.* **1990,** *112,* 7638-7647.

[7] J.F.G.A. Jansen, de Brabander van den Berg, E.M.M.; Meijer, E.W. *Sci.* **1994,** *266,* 1226-1229.

[8] De Groot, F.M.H.; Albrecht, G.; Kockkoek, R.; Beusker, P.H.; Scheeren, H.W. *Angew. Chem. Int. Ed.* **2003,** *42,* 4490-4494.

[9] van Dongen, S.F.N.; Hoog, H.-P.M.; Peters, R.J.R.W.; Nallani, M; Nolte, R.J.M.; van Hest, J.C.M. *Chem. Rev.***2009,** *109,* 6212-6274.

[10] Farokhzad, O.C.; Langer, R. *ACS Nano* **2009,** *3,* 16-20.

[11] Bharali, D.J.; Mousa, S.A. *Pharmacology & Therapeutics* **2010,** *128,* 324-335.

[12] Petros, R.A.; DeSimone, J.M. *Nature Rev.* 2010, ***9,*** **615-627.**

[13] Soloway, A.H.; Tjarks, W.; Barnum, B.A.; Rong, F.-G.; Barth, R.F.; Codogni, I.M.; Wilson, J.G. *Chem. Rev.* **1998,** *98,* 1515-1562.

[14] Duan, Y.; Liu, M.; Sun, W.; Wang, M.; Liu, S.; Li, Q.X. *Mini-Rev. in Org. Chem.* **2009,** *6,* 35-43.

[15] Low, P.S.; Kularatne, S.A. *Current Opinion in Chemical Biology* **2009,** *13,* 256-262.

[16] Plow, P.S. *Current Opinion in Chemical Biology* **2009,** *13,* 256-262.

[17] Blaaderen, A.; Vrij, A. *Langmuir,* **1992,** *8,* 2921-2931

[18] Slowing, I.; Trewyn, B.G.; Lin, V.S.-Y. *F. Am. Chem. Soc.* **2006,** *128,* 14792-14793.

[19] Pasqua, L; Tet, F;Aiel R.; Cunari, S;Nagy, J.N *Microrous Mesoporous Materials* **2007,** *103,* 166-173

[20] Johnson, I.; Spence, M.T.Z. *Molecular Probes Handbook: A Guide to Fluorescent Probes and Labeling Technologies 11th Edition* **2010**.

[21] Burns, A.; Ow, H.; Wiesner, U. *Chem. Soc. Rev.* **2006,** *35,* 1028-1042.

[22] Dash, S.; Mishara, S.; Patel, S.; Mishra, B.K. *Advances in Colloid and Interface Science* **2008,** *140,* 77-94.

[23] Yoshitake, H. *journal of Materials Chemistry* **2010,** *20,* 4537-4550.

[24] Wyndham, K.D.; O'Gara, J.E.; Walter, T.H,; Glose, K.H.; Lawrence, N.L.; Alden, B.A.; Izzo, G.S.; Hudalla, C.J.; Iraneta, P.C. *Anal. Chem.,* **2003,** *75,* 6781-6788.

[25] Ohulchanskyy, T. Y.; Roy, I.; Goswami, L. N.; Chen, Y.; Bergey, E. J.; Pandey, R. K.; Oseroff, A. R.; Prasad, P. N. *Nano Lett.* **2007**, *7*, 2835–2842.

[26] Brozek, E.; Zharov, I. *Chemistry of Materials* **2009,** *21,* 1451-1456.

[27] Wang, S.; Lee, R.J.; Mathias, C.J.; Green, M.A.; Low, P.S. *Bioconjugate Chemistry* **1996,** *7,* 56-62.

[28] Brozek, E.; Zharov, I. *unpublished results.*

[29] Olympus America. Microscopy Resource Center: Solvent Effects on Fluorescence Emission. http://www.olympusmicro.com/primer/java/jablonski/solventeffects/index.html

CHAPTER 5

CONCLUSIONS AND FUTURE WORK

This thesis described new methods to synthesize and modify Organically Modified Silica particles. This was accomplished by first studying the post-modification of vinyl functionalities of vinyl ORMOSIL particles. This was the first time an ORMOSIL particle was shown to be functionalized throughout the entire particle body. New types of ORMOSIL particles were next synthesized in an effort to better understand how new ORMOSILs can be formed and how well they undergo additional modification As a result, new families of ORMOSIL particles were synthesized by a new and easy-to-use method. The particles were also able to undergo further postmodification. Finally, a new hybrid particle was synthesized in order to demonstrate proof of principle of how these new ORMOSIL particles could find use in drug delivery. A tri-condensation reaction was used to synthesize particles with three distinct organic functionalities. The organic functionalities were postmodified in such a way to yield a product with a fluorescent label, a targeting ligand, and a drug. Early in vitro studies have begun on the particle to test for toxicity and the ability for the particle to target folic acid receptors.

Additional research within the ORMOSIL field is currently underway that has used many of the lessons learned through this study as a template. For example, highly porous vinyl ORMOSIL particles are being developed using a micellar solution as template. These highly porous particles may have a range of applications as an antifogging agent, in chemical separations, or in drug delivery. A new hybrid ORMOSIL particle is also being synthesized that is degradable under near biological conditions. If these particles are able to fully dissolve and break down in biological conditions, they will likely become a new prime candidate for silica-based drug delivery applications. Solid Phase Extraction cartridges are also being developed using ORMOSIL particles as the stationary phase. Extraction of an analyte from a biological matrix is an expensive and time-consuming process in any analytical laboratory. Solid Phase Extraction cartridges can help efficiently and easily purify a sample in preparation for analysis. This can also act as a vaulting point for using ORMOSIL particles for other forms of chromatography such as high-pressure liquid chromatography. The ability to form a variety of particle types with different diameters and different organic functionalities that can be further modified make ORMOSIL particles versatile and potentially useful candidates for a variety of applications.

APPENDIX

ADDITIONAL SYNTHETIC CONDITIONS AND DATA FOR SELECT PRODUCTS

A.1 Attempted synthesis of borosilicate particles via seeding method (Scheme A.1).[1] The same procedure was used as described in 2.2.4.1, but TEOS was added using an addition funnel in order to slowly grow the size of the silica nanoparticles. IR spectra were recorded in KBr pellets. *Note:* The above two reaction conditions were also altered in attempts to optimize the conditions. The changes included: ratio of $B(OH)_3$:TEOS, rate of addition of TEOS, NH_4OH concentration, and temperature.

A.2 Preparation of α-pinene borohydride (Scheme A.2).[2] Dry THF (15 mL) was placed into a 3-neck round-bottom flask. Pinene (8.5 mL, 55 mmol) was next added to the flask. Finally, 10 M borane methylsulfide complex (2.5 mL) was carefully added to the flask with stirring. The rate of addition was controlled to prevent overheating. After the addition was complete, a clear solution was observed. Stirring was stopped and the product was allowed to slowly re-crystallize overnight. The next day, the solution with crystals was put into an ice bath to maximize yield. The liquid phase of the solution was removed with a

syringe and the crystals were washed several times with dry THF. After washing, the crystals were stored in freshly dried THF in the freezer until needed. No further characterization was conducted do to high reactivity.

A.3 Hydroboration of vinyltriethoxysilane with α-pinene borohydride (Scheme A.3). Into an ice bath-cooled 3-neck round-bottom flask, dry THF (15 mL) was added. α-Pinene borohydride (1.1 g, 4 mmol) was added as a suspension to the flask. Finally, vinyltriethoxysilane (0.55 mL, 2.6 mmol) was added to the flask dropwise. The contents of the flask were continually stirred at 0° C and allowed to warm to room temperature after the addition was complete. TLC was used to monitor the reaction progress. Due to difficulties in purification, the product obtained was used as is.

A.4 Oxidation of 2-(dipineneboro)ethyltriethoxysilane with acetaldehyde (Scheme A.4). The previously prepared solution was cooled in an ice bath. Acetaldehyde (0.9 mL, 16 mmol) was added in a single portion to the solution. The solution was stirred overnight. The solvent was removed and the contents were used as is, without further purification.

A.5 Catalytic hydroboration of allyltriethoxysilane with pinacolborane (Scheme A.5).[3] Dry dichloromethane (15 mL) was added to a 3-neck round-bottom flask. Allyltriethoxysilane (0.2 mL, 0.89 mmol) was added to the flask. Pinacolborane (0.26 mL, 1.8 mmol) was next added to the flask. Finally, about 2 mol% Wilkinson's catalyst was added to the flask and the solution was stirred for 48 h. Disappearance of the starting material was confirmed by TLC, and the product was isolated by flash chromatography using a 9:1 hexane:ethyl acetate

mixture. Product yields were between 15-50%. The collected product was used as obtained.

A.6 Catalytic hydroboration of allyltriethoxysilane with catecholborane (Scheme A.6).[4] Conditions identical to those described above were used replacing pinacolborane with catecholborane. Typical yields were between 40-50%.

A.7 Catalytic hydrosilation of allylboronic acid pinacol ester (Scheme A.7).[5] Dry tetrahydrofuran (10 mL) was added to a round-bottom flask. To the flask, triethoxysilane (0.77 mL, 4 mmol) was added. Allylboronic acid pinacol ester (0.5 mL, 2.7 mmol) was next added to the flask followed by ~2-3 mol% Karstedt's catalyst. The solution was stirred overnight. 2mol% of the Karstedt's catalyst and 1.5 eqs. of triethoxysilane was added after TLC showed incomplete reaction of the allylboronic acid pinalcol ester. The product was isolated via flash chromatography with an 85:15 hexane:ethylacetate elutant. Typically, yields were <40%.

A.8 Attempted hydroboration of vinyltriethoxysilane (Scheme A.8). Dry tetrahydrofuran (30 mL) was added to a round-bottom flask at 0° C. Vinyltriethoxysilane (3 mL, 14.4 mmol) was added into the cold THF solution and set to stir. 1M BH_3.THF (4.8 mL, 4.8 mmol) was carefully added to the solution. The solution was stirred for 3 h. at 0° C, then warmed to room temperature and stirred for another hour at room temperature. The product could not be isolated.

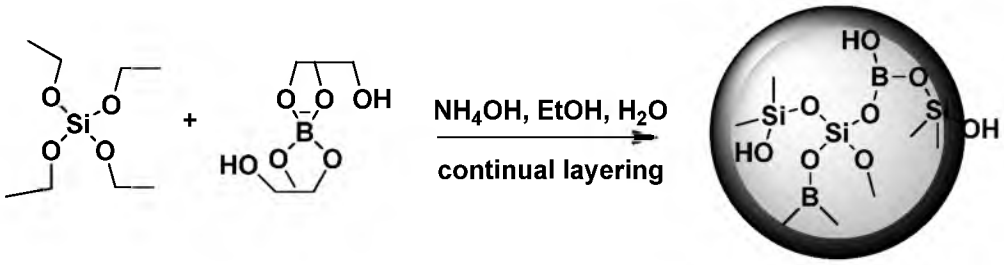

Scheme A.1: Attempted synthesis of borosilicate particles via seeding method

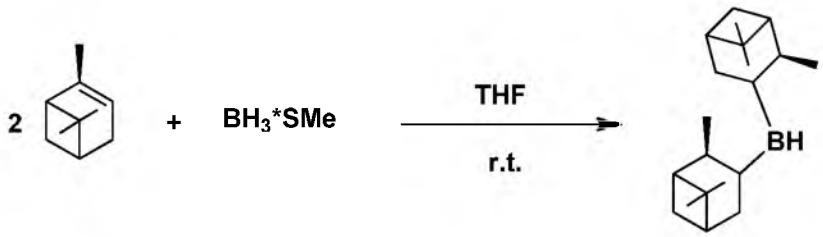

Scheme A.2: Preparation of α-pinene borohydride.

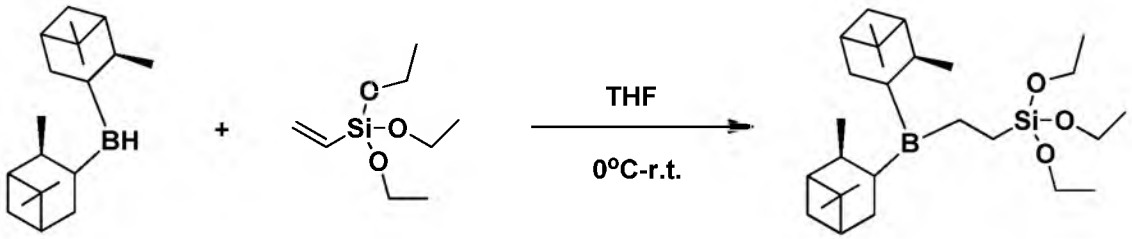

Scheme A.3: Hydroboration of vinyltriethoxysilane with α-pinene borohydride.

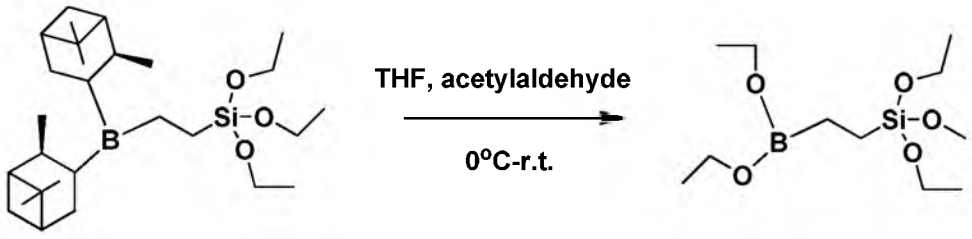

Scheme A.4: Oxidation of 2-(dipineneboro)ethyltriethoxysilane with acetaldehyde.

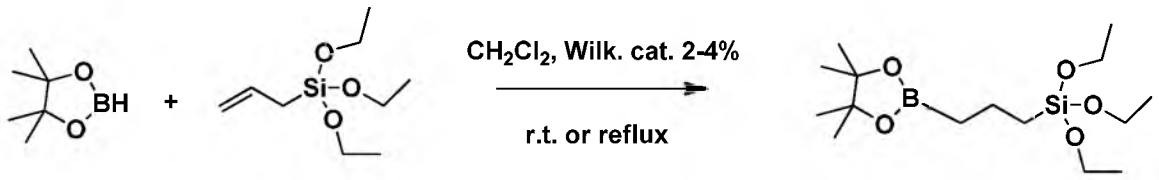

Scheme A.5: Catalytic hydroboration of allyltriethoxysilane with pinacolborane

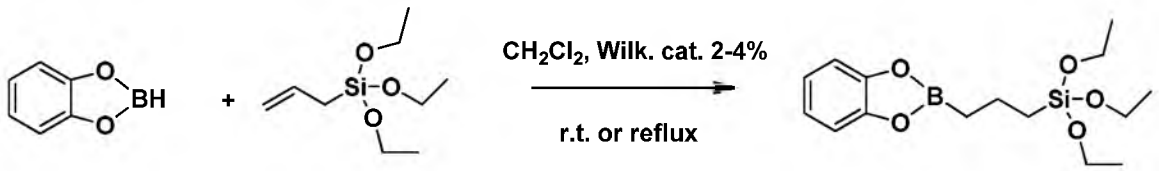

Scheme A.6: Catalytic hydroboration of allyltriethoxysilane with catecholborane

Scheme A.7: Catalytic hydrosilation of allylboronic acid pinacol ester

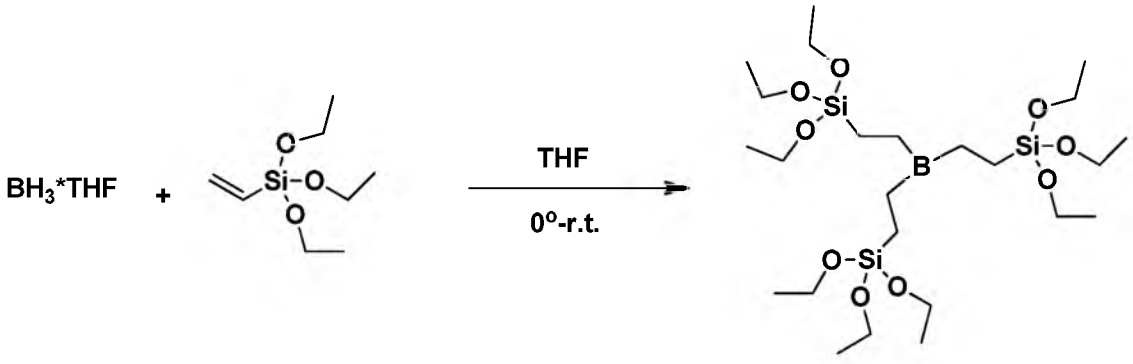

Scheme A.8: Attempted hydroboration of vinyltriethoxysilane.

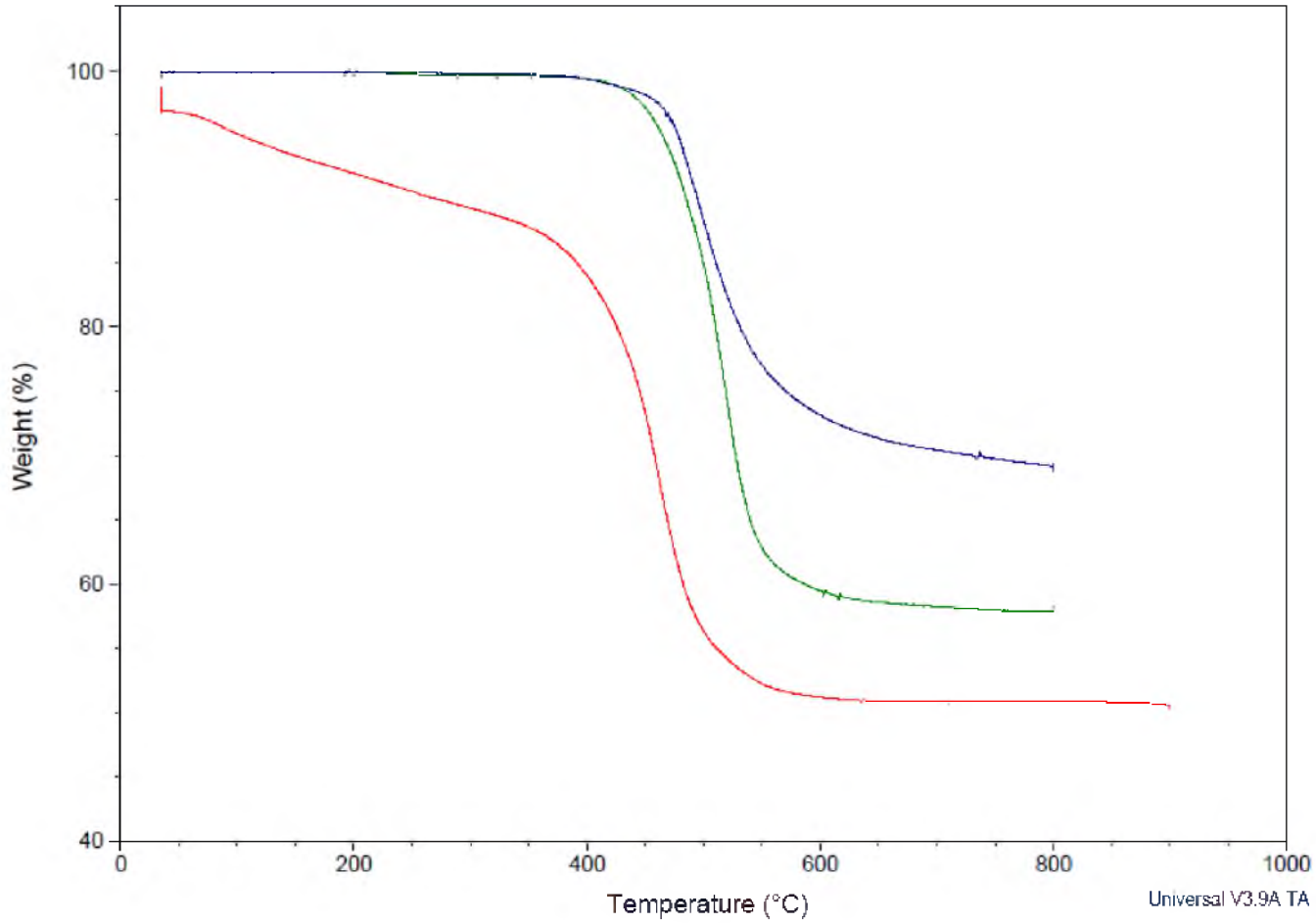

Figure A.1: TGA of ethyl-cyano (blue), propyl-cyano (green), and isocyanato-containing (red) ORMOSILS

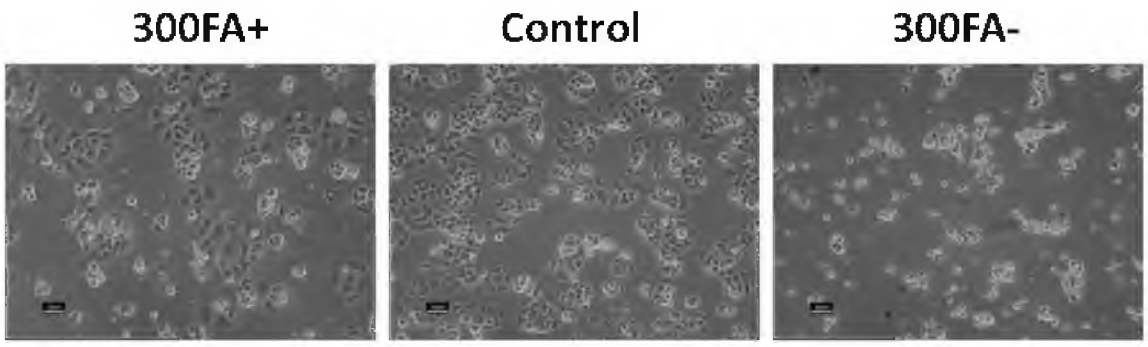

Figure A.2: Phase contrast images of (left) FA-modified particles, (middle) control, and (right) particles not FA-modified.

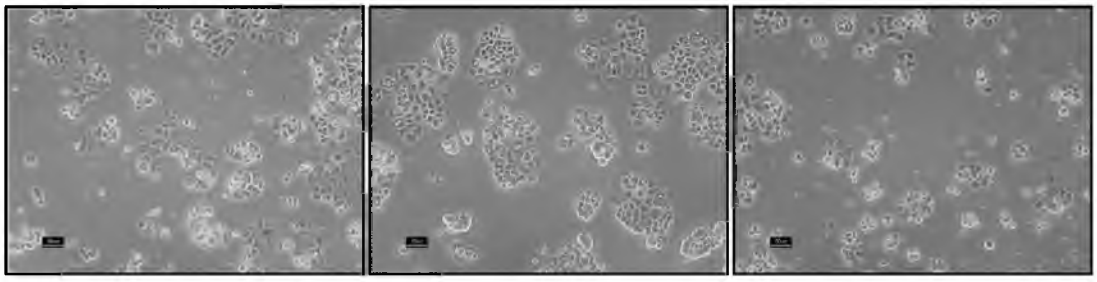

Figure A.3: Phase contrast images of (left) FA-modified particles, (middle) control, and (right) no FA modification

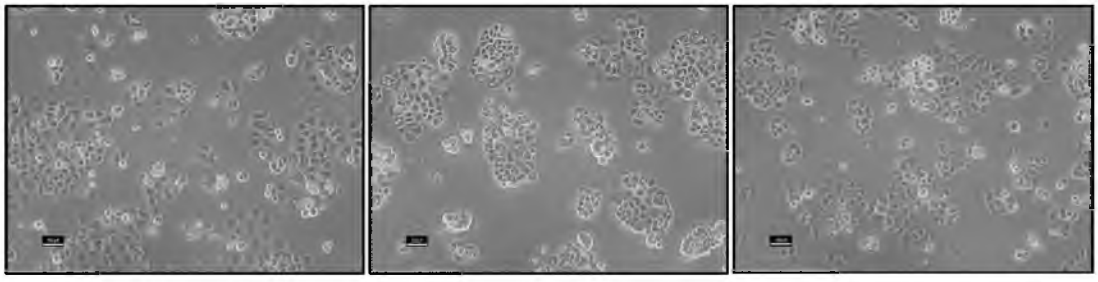

Figure A.4: Phase contrast images with aliquot additions of (left) FA-modified particles, (middle) control, and (right) no FA modification

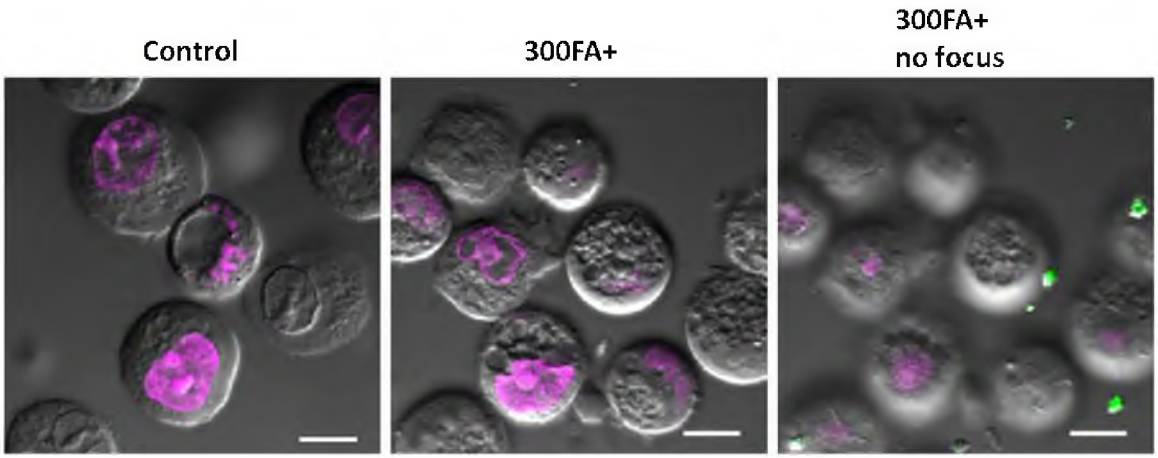

Figure A.5: Confocal image of (left) control, (middle) FA-modified particles focused, and (right) FA-modified particles w/out focus.

Appendix References

[1] Blaaderen, A.; Vrij, A. *Langmuir,* **1992,** *8,* 2921-2931.

[2] Brown, H. C.; Ramachandran, P. V. *Journal of Organometallic Chemistry* **1995,** *500,* 1-19

[3] Pereira, S.; Srebnik, M. *Tetrahedron,* **1996,** 3283-3286.

[4] Polarz, S.; Kuschel, A. *Adv. Mater.* **2006,** *18,* 1206-1209.

[5] Lukevics, E.; Pudova, O.; Sturkovich, R.; Gaukhman, A. *Journal of Organometallic Chemistry* **1988,** *346,* 293-303.